

DOCUMENT PUBLIC

*Review of kinetic data on carbonate  
mineral precipitation*

september 1996  
R 39062



Research funded in part by the COMMISSION OF THE EUROPEAN COMMUNITIES  
in the framework of the Non Nuclear Energy Programme JOULE III  
Sub-programme: Energy from Fossil Sources - Hydrocarbons  
Project : QC-SCALE

DOCUMENT PUBLIC

*Review of kinetic data on carbonate  
mineral precipitation*

B. Sanjuan  
J.P. Girard

september 1996  
R 39062



Keywords : Carbonate, Calcite, Aragonite, Dolomite, Witherite, Kinetics, Thermodynamics, Pitzer, Solid Solutions, High Salinity Solutions.

In bibliography, this report should be cited as follows:

Sanjuan B., Girard J.P. (1996) - Review of Kinetic Data on Carbonate Mineral Precipitation. BRGM Report R39062, 91 p., 15 tables, 1 figure, 1 App.

## Abstract

The technical report is a review of the main data available in the literature on kinetics of carbonate mineral precipitation. A summary of a prior survey of thermodynamic data and of numerical models for calculating ionic activity coefficients is provided in the appendix.

Particular emphasis is placed on calcite because it constitutes (with aragonite) the most commonly studied carbonate mineral. Kinetics of dolomite precipitation/dissolution has also been investigated experimentally with limited success, because of the relatively low reactivity of this carbonate (dissolution rates are  $\approx 100$  times lower than calcite).

At temperatures  $< 150^\circ\text{C}$  and  $\text{pH} > 4.5$ , surface controlled precipitation rates seem to be predominant for calcium carbonates but molecular diffusion can have some influence on these rates. In both laboratory and field studies, a certain critical degree of oversaturation ( $\Omega > 5-10$ ) has to be achieved to allow to start the nucleation of calcite at relatively low temperatures ( $< 60^\circ\text{C}$ ). However, laboratory experiments have shown that adding seed crystals in solutions can induce immediate crystal growth. In order to obtain reliable kinetic data, most of calcite precipitation experiments have been performed with the presence of seed crystals and consequently, describe crystal growth.

As precipitation rate depends on many factors such as temperature,  $\text{pCO}_2$ , pH, solution ionic composition, saturation state, reacting surface area, presence of inhibiting substances, solution hydrodynamics, many kinetic laws have been developed. Most of these laws are only applicable in very specific conditions. Equations and conditions of applicability are given in this review. A survey of the main inhibitors (magnesium, sulphate, phosphate and manganese) and their effects on precipitation rates is also presented.

The mechanistic model of Plummer *et al.* (1978), tested and refined by several other investigators, appears to be the only model that applies over a wide range of values for the factors mentioned above. It has been used with success for calculating calcite precipitation rates in natural systems at fast flow, low salinity, and low temperature conditions, after outgasing of  $\text{CO}_2$  in spring-fed streams. However, this model cannot describe accurately calcite precipitation in seawater or in deep-sea sediments where precipitation rates are much slower. This model does not take into account the influence of complex solutions (high salinity, presence of inhibitor species) and cannot predict accurate crystal growth rates at very near equilibrium conditions. Moreover, its use at  $100^\circ\text{C}$  and 100 bar, seems to be limited.

No reliable kinetic data were found for calcite precipitation in the conditions of oil field formation waters, i.e., low pH, high salinity, high  $\text{pCO}_2$  and high temperature ( $100-150^\circ\text{C}$ ). An adapted model of Plummer *et al.* (1978) or a specific law similar to those found in this review, will have to be selected for the geochemical modelling of carbonate scales in oil field wells.

# Contents

<b>Introduction .....</b>	<b>7</b>
<b>1. Kinetics of calcium carbonate precipitation.....</b>	<b>9</b>
1.1. Influence of the degree of saturation of a solution on precipitation .....	10
1.2. Experimental data.....	12
1.2.1. General considerations.....	12
1.2.2. Calcium carbonate growth processes .....	12
1.2.3. Main rate laws of calcium carbonate growth .....	12
1.3. Field data for calcite precipitation rates.....	28
1.3.1. Spring-fed streams .....	29
1.3.2. Deep-sea sediments.....	29
<b>2. Kinetics of precipitation of other carbonates.....</b>	<b>31</b>
2.1. Kinetics of dolomite .....	31
2.1.1. Kinetics of dolomite dissolution .....	31
2.1.2. Dolomite growth: rate-limiting steps .....	34
2.1.3. Kinetics of experimental dolomitization of CaCO <sub>3</sub> at high temperature.....	34
2.2. Kinetics of magnesite and witherite.....	35
<b>3. Chemical inhibition of calcium carbonate growth .....</b>	<b>37</b>
3.1. Some basic aspects of inhibition processes .....	37
3.2. Influence of specific inhibitors .....	38
3.2.1. Magnesium.....	38
3.2.2. Sulphate.....	40
3.2.3. Phosphate .....	40
3.2.4. Manganese and iron .....	44
3.2.5. Organic acids.....	46
<b>Conclusions .....</b>	<b>47</b>
<b>References .....</b>	<b>49</b>
<b>Appendix .....</b>	<b>69</b>

## Tables

Table 1a - Kinetics of calcite precipitation .....	59
Table 1b - Kinetics of calcite dissolution .....	61
Table 2a - Kinetics of calcite precipitation .....	62
Table 2b - Kinetics of calcite precipitation .....	63
Table 2c - Kinetics of aragonite precipitation .....	64
Table 2d - Kinetics of calcite precipitation .....	65
Table 3 - Mechanistic rate equations assuming multiple elementary reactions .....	66
Table 4a - Values of a and b constants needed to calculate the temperature dependence between 0 and 45°C of the dissolution rate constants .....	67
Table 4b - Kinetics of dissolution and backward reaction of dolomite .....	67
Table 5 - Kinetics of magnesite and witherite dissolution and precipitation .....	67
Table 6 - Main experimental data and results from calcite kinetic experiments of Busenberg and Plummer (1985) .....	68
Table 7 - Reaction orders and calcite precipitation rate constants calculated from experimental results obtained by Busenberg and Plummer .....	68
Table 8 - Reaction orders and calcite precipitation rate constants calculated from experimental results obtained by Dromgoole and Walter .....	68

## Appendix

Figure 1 - Calculations of saturation index (SI) for oil field brines from the North Sea with respect to calcite, aragonite, dolomite and magnesite at 25°C using the extended Debye-Hückel equation (B-dot equation) and the Pitzer model developed by Harvie <i>et al.</i> (1984) .....	74
Table 1a - Compilation of standard partial molal thermodynamic data (Gibbs free energy of formation $\Delta G^\circ_f$ , enthalpy of formation $\Delta H^\circ_f$ , entropy $S^\circ$ , heat capacity $C_p^\circ$ at constant pressure, volume $V^\circ$ and compressibility $\kappa^\circ$ ) in the Na, K, Ca, Mg, H, Cl, OH, CO <sub>2</sub> , HCO <sub>3</sub> , CO <sub>3</sub> , H <sub>2</sub> O system: Inorganic neutral species .....	76
Table 1b - Compilation of standard partial molal thermodynamic data in the Na, K, Ca, Mg, H, Cl, OH, CO <sub>2</sub> , HCO <sub>3</sub> , CO <sub>3</sub> , H <sub>2</sub> O system: Ions .....	77
Table 1c - Compilation of standard partial molal thermodynamic data in the Na, K, Ca, Mg, H, Cl, OH, CO <sub>2</sub> , HCO <sub>3</sub> , CO <sub>3</sub> , H <sub>2</sub> O system: Complexes .....	78
Table 1d - Compilation of standard partial molal thermodynamic data in the Na, K, Ca, Mg, H, Cl, OH, CO <sub>2</sub> , HCO <sub>3</sub> , CO <sub>3</sub> , H <sub>2</sub> O system: Minerals .....	79
Table 2 - Values commonly used for ionic equilibrium constants in the Na, K, Ca, Mg, H, Cl, OH, CO <sub>2</sub> , HCO <sub>3</sub> , CO <sub>3</sub> , H <sub>2</sub> O system .....	80
Table 3 - Values commonly used for the equilibrium constants of mineral dissolution-precipitation reaction in the Na, K, Ca, Mg, H, Cl, OH, CO <sub>2</sub> , HCO <sub>3</sub> , CO <sub>3</sub> , H <sub>2</sub> O system .....	82
Table 4 - Chemical composition of oil field brines from the North Sea (Warren and Smalley, 1994; Ziegler and Coleman, 1995; Sanjuan <i>et al.</i> , 1995) .....	83

## **Introduction**

The work presented in this report was conducted as part of the research carried out in the framework of the QC-SCALE project (CEC-JOULE III programme, contract N° JOF3-CT95-0009). It compiles the results of a critical review of the most significant published data on kinetics of carbonate mineral precipitation. This task was undertaken in order to select the most adapted data for geochemical modelling of carbonate scaling tendencies in oil field wells. It followed a survey of relevant thermodynamic data and numerical models for calculating ionic activity coefficients, a summary of which is appended to this report.

Carbonate minerals, in particular calcite, are among the most common scale-forming minerals in oil field wells. The formation of carbonate scales is mainly due to pressure drops and can result in a significant decrease in oil production or even a complete stop. Successful control of oil field scale depends on accurate prediction of scaling regimes. Presently, most of the available models are equilibrium models which can predict precipitation potential of carbonate scales on the basis of saturation indices under specific conditions. However, these models fall short of predicting the amount, the timing and the duration of carbonate deposition. In addition, they are blind to the possible formation of thermodynamically metastable carbonate phases. Consequently, reliable and useful predictions of amounts of precipitated carbonate require a precise knowledge of precipitation/dissolution kinetics of carbonate minerals.

Although the reaction kinetics of several carbonate minerals have been investigated, most studies focused on calcite and aragonite. These two carbonate minerals are among the most common carbonates in recent sediments and soils. In addition, their rates of dissolution-precipitation are relatively high. In contrast, dolomite, a common carbonate mineral in older sedimentary rocks, is relatively unreactive. Attempts to study its precipitation kinetics have been largely unsuccessful. Finally, a number of studies have investigated the inhibitory effect of dissolved components, such as magnesium, phosphate, sulphate, manganese or organic acid on carbonate mineral growth and dissolution.

## 1. Kinetics of calcium carbonate precipitation

Of all calcium carbonate minerals, calcite is the most studied (Morse, 1983). Limited data are also available for aragonite reaction kinetics in simple solutions (Busenberg and Plummer, 1986; Chou *et al.*, 1989) and in seawater solutions at different salinities (Burton and Walter, 1987; Zhong and Mucci, 1989). A major problem in synthesis experiments with aragonite is that it is metastable relative to calcite under surface conditions (Morse, 1983). However, it can be synthesized at elevated temperatures ( $\sim 70^\circ\text{C}$ ) from highly supersaturated solutions (Katz *et al.*, 1972).

Numerous experimental studies on the kinetics of calcite dissolution and precipitation have been performed at ambient surface conditions (low temperatures and relatively dilute solutions or seawater). These studies have revealed the importance of pH and  $\text{pCO}_2$  in calcite dissolution and precipitation up to  $60^\circ\text{C}$ . Particularly, they have shown that calcite dissolution in acid solutions ( $\text{pH} < 4$ ) is diffusion-controlled. The mechanism of calcite dissolution becomes surface-reaction controlled above pH4. Above pH5.5, the reaction rate becomes pH-independent (Plummer *et al.*, 1978; Sjöberg and Rickard, 1983, 1984).

The kinetics of calcium carbonate precipitation has been experimentally investigated mainly at high pH and low  $\text{pCO}_2$  (Wollast, 1990) and has received less attention than dissolution reactions. This perhaps reflects the fact that most sedimentary carbonates are initially formed biogenically. Consequently that the primary interest in carbonate precipitation reactions has been directed at reaction inhibitors and coprecipitation reactions (Morse, 1983). However, it must be pointed out that the study of precipitation reactions is more complicated than that of dissolution reactions. Because of the sensitivity of surface properties, the presence of impurities absorbed on the interface and the inclusions of foreign ions and molecules in the precipitated phase, the experimental results of precipitation reactions are often inconsistent (Wollast, 1990). Using the relation between the kinetic rate constants, according to which, near equilibrium, the rates of forward and reverse microscopic processes must be equal for every elementary reaction, many data obtained from dissolution reactions can be used for describing precipitation reactions. In doing so, it is very important to accurately determine the effective reactive surface area which is a critical parameter to heterogeneous kinetics. This variable depends on surface morphology (grain size, etch pit distribution representing highly localized dissolution), surface roughness (smooth geometric grains, irregularities) and internal structure (dislocation density, impurities, point defect clusters) of the mineral (MacInnis and Brantley, 1991; 1993). Besides, reactive surface area is difficult to estimate when applying experimental dissolution rates to natural systems.

Only very limited data are available for calcite-water reaction rates at elevated temperatures (Hirano and Kikuta, 1985, 1987; Higuchi *et al.*, 1988; Talman *et al.*,



1990; Beck *et al.*, 1992; Shiraki and Brantley, 1995). Only a small part of the available data is applicable to reservoir conditions, i.e., low pH (as low as 5), high temperature (>100°C) and high salinity (>1 M).

### 1.1. INFLUENCE OF THE DEGREE OF SATURATION OF A SOLUTION ON PRECIPITATION

According to Wiechers *et al.* (1975), crystallization can be categorized into two processes: nucleation and growth. Nucleation is the generation ("birth") of crystals from solution. Growth is the process whereby solute is transported to the crystal surface and is then oriented into the crystal lattice. Growth is the dominant process if the precipitant or crystal concentration is high and is thereby referred to as heterogeneous crystallization. When there are no or only small concentrations of crystals present both nucleation and growth takes place simultaneously, and is then referred to as spontaneous or homogeneous crystallization.

Calcite will precipitate from a supersaturated solution. However, both laboratory and field studies have shown that calcite precipitation at relatively low temperatures (<60°C) is kinetically inhibited (Herman and Lorah, 1988). A critical degree of supersaturation must be achieved to overcome the energy barrier which allows to start the nucleation of calcite (Berner, 1980). Laboratory studies of calcite crystallization kinetics indicate that the necessary ion activity product can be as much as ten times the equilibrium calcite solubility value at low temperatures (Reddy, 1983). According to Reddy (1983), the metastable region where the supersaturated solutions yield no precipitate over extended periods of time and where the nucleation rate is very low or zero can extend to supersaturation values of ten, while the labile region where solutions spontaneously precipitate a crystalline or amorphous material through nucleation and subsequent crystal growth lies above supersaturation values of twenty.

In field studies of travertine-depositing streams where the formation of calcite is due to the loss of CO<sub>2</sub> to the atmosphere (increase of pH and of CO<sub>3</sub><sup>2-</sup>), it was shown that solutions reach five to ten times supersaturation before precipitation (Jacobson and Udowski, 1975; Dandurand *et al.*, 1982).

Laboratory experiments have shown that adding seed crystals in solutions can induce immediate crystal growth. The technique of calcium carbonate seed inoculation (crystal or powder added to solution), suggested by Reddy and Nanchollas (1971), causes a brief initial surge in reaction rate, which was interpreted as representing both nucleation and surface roughening, and is immediately followed by a crystalline growth process. This technique was used in all subsequent experiments of calcium carbonate precipitation because the spontaneous crystallization technique does not permit reliable kinetic analysis to be made (Nanchollas and Purdie, 1968). The assumption that homogeneous nucleation takes place is of doubtful validity: nucleation is likely to occur on impurity particles which offer available sites for crystal growth and during

spontaneous crystallization, both the total number and size distribution of the particles vary (Wiechers *et al.*, 1975).

Reddy and Gaillard (1981) had already suggested that when the degree of saturation  $\Omega$  was greater than 7, surface nucleation at the start of an experiment using seed crystals could yield faster rate constants. Results obtained by Dove and Hochella (1993), using Scanning Force Microscopy (SFM), supported these interpretations and showed that calcite growth initiated with the formation of surface nuclei in every case where  $\Omega$  was greater than 2. At conditions very near equilibrium ( $\Omega$  of approximately 1.2), they also observed calcite growth but they concluded that the rate of growth at these conditions was very slow or zero. This is consistent with surface nucleation theory which indicates that surface nucleation is extremely slow near equilibrium (Nielsen, 1964).

Beck *et al.* (1992) reported rates of calcite recrystallization under conditions of near-neutral pH, low  $p\text{CO}_2$ , high temperature and pressure and close to equilibrium. These rates were much lower than those determined by Busenberg and Plummer (1986) at 25°C under similar conditions of pH and  $p\text{CO}_2$  but far from equilibrium. These findings were consistent with those of Busenberg and Plummer (1986) who recorded significantly slower overall reaction rates as calcite saturation was approached. Exceptionally slow calcite recrystallization rates for near-equilibrium conditions were also observed by Lorens (1981). Beck *et al.* (1992) suggested that a change in the reaction mechanism could occur for conditions very close to equilibrium. This near-equilibrium rate-controlling mechanism is extremely slow, even at high temperatures, and is apparently unrelated to the dissolution and precipitation mechanisms which have been measured under conditions relatively far from equilibrium. Under their experimental conditions (table 1a), at high stirring speeds and when the activity of aqueous  $\text{H}_2\text{CO}_3$  ( $a_{\text{H}_2\text{CO}_3}$ ) was smaller than  $2.33 \cdot 10^{-3}$ , Shiraki and Brantley (1995) found a rate law showing a parabolic dependance and suggesting a spiral growth regime when  $\Omega < 1.72$ . When  $\Omega > 1.72$ , the precipitation rate increased exponentially following a law based upon a surface nucleation mechanism.

According to Wollast (1990), very high degrees of supersaturation favor a rapid growth of the precipitated layer (low surface area and high rate of precipitation), which has not the chance to age during a sufficient time in contact with the aqueous solution and thus to recrystallize to the stable phase. In such conditions, precipitated solids are rather disordered or have not been completely dehydrated and have larger values of solubility than the stable phase. The influence of the crystal growth rate on the stability of the precipitated calcium carbonates has been described by Weyl (1965), Wollast *et al.* (1980) and Shoonmaker (1981).

## 1.2. EXPERIMENTAL DATA

### 1.2.1. General considerations

As the spontaneous crystallization time for calcium carbonate formation in the oil field wells is short relative to the time necessary for the precipitating mineral to grow, experimental data on the kinetics of calcite growth obtained using the seed technique (crystal growth) may be considered as applicable to conditions prevailing in wellbores.

Reddy and Gaillard (1981) made an extensive study of the influence of the solid to solution ratio on calcite precipitation rate. They showed that at low solid/solution ratio, the rate constant slightly increased with decreasing seed concentration. This can be explained by the fact that the nucleation process becomes more significant: small crystals and surface roughening characteristic of nucleation are observed. Above a seed concentration of around 300 mg/l, the calcite precipitation rate seem to be almost independent of seed concentration. The crystal growth process predominates. Mucci and Morse (1983) also concluded that the solid to solution ratio did not affect the precipitation rates.

In many studies, rate constants are normalized to the reactive surface area and are given in  $\text{mol cm}^{-2} \text{s}^{-1}$ . Uncertainties on rate constants may be due to the determination of the reactive surface area because it is not necessarily equal to the total surface area measured by gas adsorption techniques. This is particularly true for biogenic carbonates having irregular external surfaces and complex internal microstructures, but not as much for synthetic calcite or spar rhombs with relatively smooth crystalline surfaces. In studies in which constants were not normalized to surface area (apparent kinetic constant), the initial measured surface area of the seed crystals was used in our calculations. This introduces an additional uncertainty on the calculation of precipitation rate because precipitation causes the surface area of the crystals to increase. In most of the experiments, the measured total surface areas for calcite and aragonite seed crystals ranged from 0.004 to 0.9  $\text{m}^2/\text{g}$  and from 2.04 to 3.4  $\text{m}^2/\text{g}$ , respectively. Some workers estimated the surface areas from the geometry and the mean dimension of the particles (Chou *et al.*, 1989). Shiraki and Brantley (1995) found a linear relation between the measured surface area of the starting crystal ( $A_{\text{init.}}$ ) and its run products ( $A_{\text{final}}$ ), which could be used to obtain the surface area of calcite for each run. This relation was given by:

$$A_{\text{final}} (\text{m}^2/\text{g}) = 0.034 (\text{mppt}/\text{minit. seed}) + A_{\text{init.}} (\text{m}^2/\text{g})$$

where mppt was the calcite mass precipitated during a run and minit. seed the mass of seed crystal used in the experiments.

### **1.2.2. Calcium carbonate growth processes**

Crystal growth involves (Berner, 1980):

- various surface reactions (adsorption, surface nucleation, surface diffusion, dehydration, ion exchange, etc.) that result in incorporation of the ions into the crystal lattice;
- transport of ions to the surface of a crystal (diffusion);
- removal of products of the reaction from the crystal.

Ignoring product removal, the rate of growth may be limited either by transport, by surface chemical reaction, or by a combination of both processes.

Surface-reaction controlled growth results when attachment via surface reactions is so slow that concentrations adjacent to the surface build up to values essentially the same as in the surrounding solution. Rate of growth is limited by surface reactions and is not affected by increased flow velocities or increased stirring in the external solution. The transport properties of the surrounding solution have no influence. Instead the problem reduces to one of trying to formulate the slowest or rate controlling step at the surface. This is not a simple problem (Berner, 1980) and, as a result, many theories of surface-reaction controlled growth have been developed. Nielsen (1983) summarizes three general precipitation rate laws, based on physical models of surface-controlled crystallization limited by :

- adsorption (linear law with respect to the free energy change of the overall reaction  $\Delta G$ );
- spiral growth at screw dislocations (parabolic law with respect to  $\Delta G$ );
- two-dimensional nucleation on crystal surfaces (exponential law with respect to  $\Delta G$ ).

In transport-controlled growth, ions are attached so rapidly to the surface of the crystal that the concentration in solution immediately adjacent to the crystal is lowered to essentially the equilibrium or saturation level. Growth is then limited by the rate at which ions can migrate to the surface via diffusion and advection. The rate of growth, consequently, depends upon hydrodynamic conditions in the solution, with faster growth resulting from increased flow velocities or increased stirring. Situations can arise where surface reactions are sufficiently fast that ion depletion occurs adjacent to the crystal surface but transport prevents the concentration from being lowered to the saturation value.

### 1.2.3. Main rate laws of calcium carbonate growth

#### a) Laws linear with respect to $\Delta G$ : the model of adsorption-controlled growth

Linear rate laws for crystallization have been attributed to adsorption-controlled growth (Nielsen, 1983). All these models are examples of rate laws of the simplified form derived from transition state theory by Aagaard and Helgeson (1982) and Lasaga (1981, 1984):

$$v_{\text{net}} = -k_+ [1 - \exp(p \Delta G/RT)] = -k_+ (1 - \Omega^p)$$

where  $v_{\text{net}}$  is the net rate of the reaction (forward +; backward -) normalized to the reacting surface area,  $k_+$  is the rate constant of the forward (dissolution) reaction (with  $k_+ / k_- = K$ ),  $R$  is the gas constant,  $T$  is absolute temperature,  $\Omega (= Q/K)$  is the degree of saturation,  $Q$  is the ionic activity product,  $K$  is the constant of mass action law and  $p$  is a constant.

The following equation:

$$v_{\text{net}} = v_p - v_d = k_p [\text{Ca}^{2+}] [\text{CO}_3^{2-}] - k_d = k_d (\Omega - 1)$$

corresponding to the rate of the reaction:  $\text{Ca}^{2+} + \text{CO}_3^{2-} = \text{CaCO}_3$  is equivalent to that used for adsorption-controlled growth ( $v_{\text{ads}} = k_{\text{ads}} (\Omega - 1)$ ).  $v_p$  and  $v_d$  are the calcite precipitation and dissolution rates normalized to the reacting surface area,  $[\text{Ca}^{2+}]$  and  $[\text{CO}_3^{2-}]$  refer to the concentrations of  $\text{Ca}^{2+}$  and  $\text{CO}_3^{2-}$  in solution,  $k_p$  and  $k_d$  are the precipitation and dissolution rate constants (with  $k_d / k_p = K_{\text{sp}}$ ) and  $K_{\text{sp}}$  is the constant of calcite solubility.

This equation has been used by Reddy and Nancollas (1971), Nanchollas and Reddy (1971) and Wiechers *et al.* (1975). Reddy and Nancollas (1971) made the first major systematic study of calcite precipitation kinetics in simple solutions. They used the free drift method with calcite seeds and followed the reaction by monitoring the calcium change using either  $^{45}\text{Ca}$  or atomic absorption spectroscopy. The pH range of their solutions was 8.53-8.80 and  $p\text{CO}_2$  was atmospheric. The precipitation rate was independent of stirring rate. This pointed against diffusion as the rate-controlling mechanism.

An equation derived from the general form with  $p = 1/2$  has been used to fit the dissolution rate data of calcite obtained by Sjöberg (1976), Sjöberg and Rickard (1983) and Sjöberg and Rickard (1984). According to Sjöberg and Rickard (1983), this relation results from a mixed kinetic regime: the interaction of a transport process and a first-order surface chemical reaction. In the experiments performed using a rotating disc method (Sjöberg and Rickard, 1983, 1984), a relationship between the observed rate of dissolution and the rotational velocity of the disc was obtained, which shows that transport processes are relatively important in controlling the dissolution rate. The

chemical rate constant was found to be dependent on the crystallochemical nature of the reactant calcite.

Examination of later studies on calcite growth kinetics suggests that models with a linear rate law were partly abandoned in favor of the "parabolic law" (Dove and Hochella, 1993). However, Inskeep and Bloom (1985) tested several precipitation rate equations and concluded that the Nancollas and Reddy (1971) model appeared to be the most successful model to describe calcite precipitation at 25°C, pH>8 and pCO<sub>2</sub><0.01 atm. In their comparative study, different experiments using a seeded growth technique with a pH-stat were performed at initial Ca and HCO<sub>3</sub> ranging from 0.7-2 and 4-7 mmol l<sup>-1</sup>, pH values ranging from 8.25 to 8.70, pCO<sub>2</sub> values ranging from 6 10<sup>-4</sup> to 0.01 atm, and ionic strengths ranging from 0.015 to 0.10 mol l<sup>-1</sup>. Nagy (1988) used a kinetic linear law to estimate the temperature dependence of the rate of precipitation of calcite from data obtained in initially undersaturated 2m NaCl solutions at 25, 60 and 90°C. These solutions immediately became supersaturated due to rapid dissolution of fine particles. From their experimental results in CaCl<sub>2</sub>-NaHCO<sub>3</sub> solutions at 10, 25 and 50°C and at different pCO<sub>2</sub> (0.097, 0.099, 0.88, 0.97 atm), Dromgoole and Walter (1990) found linear rate laws. The rate constant increased with increasing temperature. At 25°C, it decreased with decreasing pCO<sub>2</sub>. Shiraki and Brantley (1995) also found a rate showing a linear dependence upon exp(ΔG/RT) and suggesting growth by a simple surface adsorption mechanism, when α<sub>H2CO3</sub> was greater than 5.07 10<sup>-3</sup>.

A summary of the main experiments and results using a linear rate law is given in tables 1a and 1b. If the rate constant found by Nagy (1988) at 25°C in NaCl solution is compared to those obtained by Dromgoole and Walter (1990b), it appears that high NaCl concentrations in solution result in a slightly higher precipitation rate constant. From Sjöberg and Rickard (1984) experiments, it is shown that high KCl concentrations have a similar effect on the dissolution rate constant.

The value for the apparent Arrhenius activation energy *E<sub>a</sub>* of the calcite precipitation reaction calculated by Nancollas and Reddy (1971) was 11.0 kcal mol<sup>-1</sup>, which is in good agreement with the values of 10.3±0.9 kcal mol<sup>-1</sup> of Wiechers *et al.* (1975), 9.4±0.9 kcal mol<sup>-1</sup> of Kazmierczak *et al.* (1982), 11.5 kcal mol<sup>-1</sup> of Inskeep and Bloom (1985) and 8.9 and 10.7 kcal mol<sup>-1</sup> of Dromgoole and Walter (1990b). All these investigators interpreted the value of the apparent Arrhenius activation energy for the reaction to be indicative of a surface controlled process rather than a diffusion controlled precipitation (*E<sub>a</sub>* ≈ 4-5 kcal mol<sup>-1</sup>). Nagy (1988) found a value of 15.8 kcal mol<sup>-1</sup> for *E<sub>a</sub>* in the temperature range from 25 to 89°C. Between 25 and 60°C, *E<sub>a</sub>* was estimated to be 11.2 kcal mol<sup>-1</sup>, which was in excellent agreement with the previous published values, obtained in the temperature range from 10 to 40°C. The data reported by Nagy (1988) suggest a temperature dependence of the activation energy of calcite precipitation. This dependence has also been mentioned by Beck *et al.* (1992). All these values are slightly higher than those found by Sjöberg (1976) and Sjöberg and Rickard (1984) for pure calcite and Carrara marble dissolution reaction (8.4 kcal mol<sup>-1</sup> and 7.4-8.6 kcal mol<sup>-1</sup>, respectively) or similar to that calculated by Inskeep and Bloom (1985)

for calcite dissolution ( $9.1 \text{ kcal mol}^{-1}$ ). On the other hand, they are smaller than the activation energy of  $25.5 \text{ kcal mol}^{-1}$  reported by Beck *et al.* (1992) for calcite precipitation under near equilibrium conditions at high temperatures.

When activation energy is calculated from the results of Dromgoole and Walter (1990b) and Shiraki and Brantley (1995), at  $25^\circ\text{C}$  and  $100^\circ\text{C}$  respectively, using the relation derived from the Arrhenius equation:

$$E_a = R \cdot \ln(k_{25^\circ\text{C}}/k_{100^\circ\text{C}})/(1/373.15 - 1/298.15)$$

where  $R$  is the gas constant,  $E_a$  is found to be  $7.0 - 11.1 \text{ kcal mol}^{-1}$ , which is very close to the previous values.

**b) Laws non linear with respect to  $\Delta G$ : the mechanistic model of Davies and Jones (1955)**

A rate law based on the model developed by Davies and Jones (1955) for crystal growth from experiments investigating the precipitation of silver chloride at  $25^\circ\text{C}$ , was selected by Reddy and Nanchollas (1973), Reddy (1977) and Reddy and Gaillard (1981) for calcite precipitation experiments at  $25^\circ\text{C}$  (table 2a). The observation that the relation between growth rate and degree of supersaturation was non-linear meant that the equations previously described (linear with respect to  $\Delta G$ ) could not be applied. The equation used is the following:

$$v_p = k (C_A - C_{A,eq}) (C_B - C_{B,eq})$$

where  $C_A$  and  $C_B$  are concentrations of species A and B,  $C_{A,eq}$  and  $C_{B,eq}$  are concentrations of these species at equilibrium and  $k$  is the rate constant. When  $C_A$  and  $C_B$  are equal, it can be written:

$$v_p = k (C - C_{eq})^2 = k (\Omega - 1)^2$$

Burton and Walter (1987) also used a similar rate law for calcite and aragonite precipitation in seawater at  $25^\circ\text{C}$  (table 2b and 2c) but the rate constant for calcite was much lower than those obtained in dilute solutions by the previous workers. As we shall see later, calcite precipitation from seawater is a complex mechanism where several inhibitors such as magnesium, sulphate slaken the reaction. In their near-equilibrium experiments at  $100^\circ\text{C}$  and 100 bar, Shiraki and Brantley (1995) found that the rate followed this same law at high stirring speeds, when  $\alpha_{\text{H}_2\text{CO}_3}$  was smaller than  $2.33 \cdot 10^{-3}$  and  $\Omega < 1.72$ .

This parabolic kinetics was popularized by the BCF (Burton, Cabrera and Frank, 1951) theory of crystal growth at screw dislocations, also known as the spiral growth mechanism. The validity of the BCF growth theory and the accompanying parabolic

rate law for describing near-equilibrium crystal growth has been demonstrated (Bennema and Gilmer, 1973; Berner and Morse, 1974; Gratz *et al.*, 1990). Unfortunately, it has been used to explain a great deal of crystal growth data outside the range of conditions for which the model was originally intended. Though the parabolic rate law is a popular explanation of calcite growth kinetics, it should be applied cautiously for two reasons. First, this rate law gives a good fit to almost any initial rate experiment (Rimstidt and Dove, 1986). Virtually any set of initial rate data can be fit to a parabolic function if a sufficiently short initial time interval is chosen. Second, Inskeep and Bloom (1985) demonstrate that the fit of data to a particular model is not a good criteria for choosing a reaction mechanism by showing that calcite precipitation data fit eight different kinetic models with  $r^2$  values greater than 0.96. These observations suggest that published studies may overlook other explanations for the measured crystallization kinetics, particularly without mechanistic evidence from in-situ methods.

While the non-linear behavior of growth rate with increasing saturation state is frequently described by the parabolic rate law, the observations performed by Dove and Hochella (1993) suggest that much of this behavior can be attributed to the non-linear rates associated with early-stage surface nucleation. For examples, at saturation states of  $\Omega > 2$ , observations show that precipitation invariably begins with the formation of surface nuclei. These nuclei "roughen" the surface which makes available a higher reactive area for rapid initial growth rates. With continued precipitation, the nuclei coalesce to form a new smoother surface that grows by the spreading of monolayer steps. A mechanism resembling spiral growth appears to become the dominant reaction process only after longer reaction times (after nearly two hours). This implies that rates of mononuclear growth by spiral mechanisms must be obtained from data collected at later stages of an experiment when growth processes are no longer dominated by surface nucleation. Otherwise, calculated rates of spiral growth will be too high. Taken together, results obtained by Dove and Hochella (1993) suggest that rates of stable layer calcite in natural system may be slower than experimentally determined values have predicted, because the latter values sometimes include initially rapid rates associated with the nucleation phase.

Using in situ, real time Atomic Force Microscope (AFM) measurements of calcite surface kinetics, a technique similar to that of Dove and Hochella (1993), very different results were obtained by Gratz *et al.* (1993). These workers indicate that calcite growth is by advance of monomolecular steps nucleating primarily at screw dislocation, and that the rate-controlling step is rotation of the spiral core. They observed no spontaneous surface nucleation. It is conceivable that the change in the mechanisms of calcite growth is related to the difference in pH in the two experiments (around 6 for Dove and Hochella's experiments and around 8 for Gratz *et al.*'s experiments).

In the constant composition experiments performed by Mucci and Morse (1983) and Mucci (1986) in natural and artificial seawater ( $\Omega$  from 1.8 to 141) at 25°C, calcite



precipitation kinetics is shown to follow third and higher order rate laws following the equation:

$$v_p = k (\Omega - 1)^n$$

where  $v_p$  is the precipitation rate normalized to the reacting surface area and  $k$  is the rate constant. These high reaction orders (3, 3.7) bear a resemblance to reaction orders found in calcite nucleation studies (Möller and Rajagopalan, 1975) and may suggest that the Mucci and Morse (1983) growth experiments are dominated by an extended surface nucleation stage. Similar relations were found by Morse (1978) for calcite dissolution experiments in seawater and deep-sea sediment porewater at 25°C.

In order to investigate the influence of seawater salinity on the precipitation rates of calcite and aragonite, Zhong and Mucci (1989) performed experiments of calcite and aragonite overgrowths from seawater solutions of various salinities (5, 15, 25, 35 and 44 ‰) at 25°C and  $p\text{CO}_2 = 10^{-2.5}$  atm, using a constant disequilibrium seeded technique. The precipitation reactions of aragonite and calcite in seawater could be satisfactorily described by the same kind of empirical rate law. High reaction orders (from 2.53 to 3.27 for calcite and 1.8 to 2.36 for aragonite) were also found. Salinity had no noticeable effect on the precipitation rate of calcite and only a small effect on the reaction rate of aragonite as the salinity of the solution was increased from 25 to 35 ‰ under the experimental conditions. Three condensed empirical equations and coefficients describing the precipitation rate of calcite and aragonite from seawater at various salinities were given (table 2b and 2c). These results did not support the hypothesis developed from field studies, which suggested that salinity might influence the kinetics of carbonate-solution interactions. Also these results are not in agreement with those of Badiozamani *et al.* (1977), who studied the influence of ionic strength on carbonate cementation and concluded that an increase in salinity inhibited nucleation but enhanced the crystallization rate of both calcite and aragonite. On the other hand, they concurred with the conclusions of previous studies of Chen *et al.* (1979), Kazmierczak *et al.* (1982) and Walter (1986) in solutions other than seawater. These studies indicated that calcite growth rates did not change significantly when NaCl or  $\text{CaCl}_2$  was added to the medium up to a ionic strength of the solution of 0.7 m (for NaCl addition) and 0.2 m (for  $\text{CaCl}_2$  addition). The results found for calcite precipitation experiments seem to be different from those obtained by Busenberg and Plummer (1986) in dissolution experiments, where the addition of single salts of KOH,  $\text{KHCO}_3$ ,  $\text{K}_2\text{CO}_3$  or  $\text{CaCl}_2$  far from equilibrium decreased the rate of dissolution. This change in rate was accounted for by Langmuir isotherm for  $\text{OH}^-$ ,  $\text{HCO}_3^-$ ,  $\text{CO}_3^{2-}$  and  $\text{Ca}^{2+}$  on the calcite or aragonite surface. The decrease in rate was attributed to backward reactions between adsorbed species and surface species.

The study of Zhong and Mucci (1989) also confirmed previously published findings (Burton and Walter, 1987) that above a given saturation state ( $\Omega \geq 2.6$ ), aragonite precipitated more rapidly than calcite at 25°C in seawater. Burton and Walter (1987) carried out laboratory experiments to investigate the relative growth of calcite, Mg

calcite, and aragonite in seawater as functions of both temperature (5, 25 and 37°C) and of carbonate ion concentration (2.5 to 15 times supersaturated with respect to calcite). The rate equations (table 2b and 2c) obtained were similar to those of Zhong and Mucci (1989, 1993). The reaction order  $n$  ( $\approx 2$  at 25°C) for calcite precipitation was lower than the values closer to 3 reported by Mucci and Morse (1983) and Mucci (1986). The precipitation rates of aragonite relative to those of calcite increased strongly with increasing temperature (at 5°C, the precipitation rates of both minerals are nearly equivalent) and were not affected greatly by changes in saturation state. Calcite compositions varied from less than 5 mol%  $\text{MgCO}_3$  at 5°C to 14 mol%  $\text{MgCO}_3$  at 37°C.

All the rate equations based on parabolic rate law mentioned so far are examples of the general equation suggested by Lasaga (1981) for interpreting most dissolution and precipitation rates which are controlled by crystal defects:

$$v_{\text{net}} = -k^+ (1 - \exp(\Delta G/RT))^n = -k^+ (1 - \Omega)^n$$

For small  $\Delta G$  (near equilibrium), this equation simplifies to the following form:

$$v = \pm k^+ (|\Delta G|/RT)^n$$

where  $|\Delta G|$  is the absolute value of  $\Delta G$ .  $-k^+$  applies when  $\Delta G$  is negative and  $k^+$  when  $\Delta G$  is positive.

When  $n = 2$ , Blum and Lasaga (1987) showed that mineral growth is controlled by spiral growth at screw dislocations while when  $2 < n \leq 3$ , growth is controlled by both screw and edge dislocations.

Another form of the mechanistic model of Davies and Jones (1955) can be derived for the case when  $C_A$  in solution is not equal to  $C_B$ . The resulting equation can be written as follows:

$$v_p = k (\Omega^{1/2} - 1)^2$$

House (1981) showed that this model led to good agreement with experimental data when the extent of precipitation was between 0.1 and 0.45 (table 2d). Kazmierczak *et al.* (1982) used this equation to fit the precipitation rate data of calcite obtained over a pH range from 8.25 to 10.0 and between 15 and 35°C. Inskeep and Bloom (1985) tested this model to describe calcite precipitation at values of  $p\text{CO}_2$  less than 0.01 atm and values of pH greater than 8 at 25°C. They concluded that this model was consistent with the experimental data but was based on an erroneous explanation of surface potentials. This model probably fitted the data because it was mathematically similar to the Nancollas and Reddy (1971) model which describes elementary reactions at the crystal surface and was more successful at predicting calcite precipitation rates than parabolic models based on disequilibrium driving force processes.

Tables 2a, 2b, 2c and 2d summarize the main experiments and results.

**c) Laws non-linear with respect to  $\Delta G$ : the surface nucleation limited rate law**

At high values of supersaturation, nucleation and growth occur not only at screw dislocation outcrops, but also at two-dimensional nuclei on the crystal surface. Two-dimensional nucleation can occur as one nuclei per crystal face (mononuclear growth) or as several nuclei per crystal face (polynuclear growth).

In polynuclear growth where many nuclei form on a crystal surface before the face grows a complete new layer of crystal, the growth rate is rate-limited by nucleation following the equation (Nielsen, 1983):

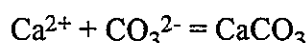
$$v_p = A \exp (- K/(\Delta G/RT))$$

where A and K are constants.

In their near-equilibrium experiments at 100°C and 100 bar, Shiraki and Brantley (1995) found a growth rate described by this model at high stirring speeds, when  $\alpha_{\text{H}_2\text{CO}_3} < 2.33 \cdot 10^{-3}$  and  $\exp (\Delta G/RT) > 1.72$ . Values for A and K constants were  $10^{-7.28}$  and 2.36 respectively.

**d) Complex reaction rate law (for seawater and relatively high salinity solutions)**

Experiments of calcite precipitation in phosphate-free seawater at 25°C, using a constant addition technique, led Zhong and Mucci (1993) to propose a complex reaction rate model. Their results consistent with those of Mucci (1986) and Burton and Walter (1990) showed that calcite precipitation rate was not affected significantly by variations of  $p\text{CO}_2$  in seawater solutions. Similar observations had been made by Berner in calcite and aragonite precipitation experiments (1975). Zhong and Mucci (1993) concluded that the influence of dissolved carbonates on precipitation rate was dominant. Consequently, their model was based upon the fastest and therefore the rate determining precipitation reaction, which involves interaction of the carbonate and calcium ions:



The measured precipitation rate,  $v_{\text{net}}$ , was adequately described by the equation:

$$v_{\text{net}} = v_f - v_b = k_{f1}(a_{\text{Ca}})^{n1}(a_{\text{CO}_3})^{n2} - k_{b1}$$

where  $v_f$ ,  $v_b$  and  $k_{f1}$ ,  $k_{b1}$  are the forward and backward reaction rates and rate constants respectively and  $n1$  and  $n2$  is the partial reaction rate order for each species involved in the reaction.

When  $[\text{Ca}^{2+}]$  was held constant through the precipitation experiments, the above equation was reduced to:

$$v_{\text{net}} = K_{f1}[\text{CO}_3^{2-}]^{n2} - k_{b1}$$

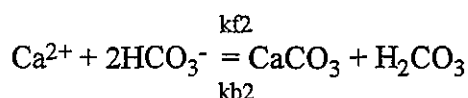
Over a wide range of saturation states and extending to near saturation conditions at 25°C, the least-squares fit to this expression yielded values of  $K_{f1} = 10^{3.5} \mu\text{mol}(\text{kg})^3/\text{m}^2\text{h}(\text{mmol})^3$ ,  $n2 = 3$  and  $k_{b1} = 0.29 \mu\text{mol}/\text{m}^2\text{h}$ , when  $p\text{CO}_2 = 0.0031 \text{ atm}$  and  $[\text{Ca}^{2+}] \approx 10.5 \text{ mmol/kg sw}$  ( $v_{\text{net}}$  was given in  $\mu\text{mol}/\text{m}^2\text{h}$ ).

The partial reaction order of 3 for the carbonate species confirmed that calcite precipitation in seawater proceeded through a complex mechanism, as suggested by previous calcite-seawater interaction studies. The consequence is that mechanistic kinetic expressions derived from an elementary reaction to describe calcite precipitation in dilute solutions cannot be applied directly to seawater. The interaction of seawater solutes in solution as well as at the surface of the precipitating solid are most likely responsible for the different reaction mechanisms in dilute and complex electrolyte solutions (Zhong and Mucci, 1993). The calcite dissolution rate constant derived from this study ( $10^{-14.09} \text{ mol cm}^{-2} \text{ s}^{-1}$ ) was significantly lower than values obtained in dilute solutions ( $k_3$  value in Plummer *et al.*, 1978 or in Chou *et al.*, 1989). As we will see later (section 1.3.), this observation is in agreement with the results of others studies indicating that calcite dissolution is much faster in dilute solutions than in seawater under identical saturation conditions.

The experimental data obtained by Zhong and Mucci (1993) were also very well fitted over a wide range of calcite supersaturation ( $\Omega$  from 1.2 to 8) by the empirical law:  $v = k(\Omega - 1)^n$  where  $k = 10^{-13.35} \text{ mol cm}^{-2} \text{ s}^{-1}$  and  $n = 2.22$  (table 2b). These values are in agreement with those of previous studies.

In another kinetic study using a similar technique, Zuddas and Mucci (1994) carried out experiments in  $\text{NaCl-CaCl}_2$  solutions at 25°C, at total ionic strength of 0.7 m and at four different  $p\text{CO}_2$  ( $3.04 \cdot 10^{-4}$ ,  $3.14 \cdot 10^{-3}$ ,  $2.04 \cdot 10^{-2}$  and 0.305 bar) in order to characterize the influence of solution composition and specific dissolved components on the complex mechanism of calcite precipitation in seawater. Calcite precipitation was dominated by the same reaction as in seawater solutions and the same rate law equation was applied.  $n2$  was also found to be equal to 3. However, unlike experiments performed with seawater precipitation rates were affected by variations in  $p\text{CO}_2$ . This

was interpreted as a contribution of the bicarbonate ion to the precipitation reaction. This contribution can be represented by the reaction:



Under their experimental conditions ( $1.1 < \Omega < 8.3$ ), the calcite precipitation rate  $v_{\text{net}}$  was described by the following equation:

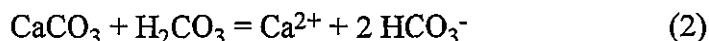
$$v_{\text{net}} = K_{f1}[\text{CO}_3^{2-}]^3 - k_{b1} + K_{f2}[\text{HCO}_3^-]^2 - k_{b2} (\gamma_{\text{H}_2\text{CO}_3}) \propto p\text{CO}_2$$

where  $K_{f2} = k_{f2} (\alpha_{\text{Ca}^{2+}})^n (\gamma_{\text{HCO}_3^-})^2$ ,  $\alpha$  is the solubility of  $\text{CO}_2$  in the experimental solution and  $\gamma_i$ ,  $n$  are activity coefficients, partial reaction rate order respectively, for each species involved in the reaction.

The experimental data obtained by these workers were also well fitted by the empirical law equation:  $v = k (\Omega - 1)^n$  but the values of the constants  $k$  and  $n$  were different for different  $p\text{CO}_2$  values (table 2b). The lack of dependence of  $p\text{CO}_2$  reported by Zhong and Mucci (1993) for calcite precipitation rates measured in seawater was interpreted by Zuddas and Mucci (1994) as a differential inhibition of the reactions participating in the overall growth process.

#### e) Mechanistic rate equations assuming multiple elementary reactions

The first comprehensive study of the influence of the concentration of the reactants on the rate of dissolution of calcite has been performed by Plummer *et al.* (1978). These workers carried out systematic experiments on calcite dissolution in  $\text{CO}_2$ - $\text{H}_2\text{O}$  solutions using pH-stat and free-drift methods. The ranges of values of pH,  $p\text{CO}_2$  and temperature were 2-7, 0.0003-0.97 atm, and 5-60°C, respectively. Plummer *et al.* (1978) found that their results could be interpreted following three regions of pH and suggested that calcite dissolution was controlled by the following three reactions:



They presented a rate law for net calcite dissolution rate given by the following equation:

$$v_{\text{net}} = k_1 a_{\text{H}^+} + k_2 a_{\text{H}_2\text{CO}_3} + k_3 a_{\text{H}_2\text{O}} - k_4 a_{\text{Ca}^{2+}} a_{\text{HCO}_3^-}$$

where  $v_{\text{net}}$  is the rate of dissolution normalized to surface area.  $k_1$ ,  $k_2$  and  $k_3$  (moles  $\text{cm}^{-2} \text{s}^{-1}$ ) are rate constants for dissolution which are dependent upon temperature.  $k_4$  is a rate constant for the backward reaction of equations (1) through (3) and is dependent on temperature and  $p\text{CO}_2$ .  $a_{\text{H}_2\text{O}}$  was always close to unity.  $k_4$  was determined from the slope of the line obtained when  $(v_{\text{net}} - k_1 a_{\text{H}^+})$  is plotted against the product  $a_{\text{Ca}^{2+}} a_{\text{HCO}_3^-}$  at constant  $p\text{CO}_2$ .

In region I ( $\text{pH} < 4$ ) dissolution rate was described by the term  $k_1$ , which is dependent on the stirring rate but independent of  $p\text{CO}_2$ . In this region, rate was limited primarily by  $\text{H}^+$  transport through the diffusional boundary layer adjacent to the calcite surface and was directly proportional to the bulk-fluid hydrogen ion activity. In region II ( $4.0 < \text{pH} < 5.5$ ) dissolution rate depended on both  $\text{pH}$  and  $p\text{CO}_2$  and was described by the  $k_1$  and  $k_2$  terms. The rate above  $\text{pH} 5.5$  was described by  $k_2$ ,  $k_3$  and the precipitation rate  $k_4$  (dependent on  $p\text{CO}_2$ ) and was independent of  $\text{pH}$  for  $\text{CO}_2$ -free solutions far from calcite equilibrium.

The expressions of  $k_1$ ,  $k_2$  and  $k_3$  as a function of temperature ( $T$  in  $^\circ\text{K}$ ) were as follows:

$$\begin{aligned}\log k_1 &= 0.198 - 444/T - 3 \\ \log k_2 &= 2.84 - 2177/T - 3 \\ \log k_3 &= -1.10 - 1737/T - 3\end{aligned}$$

The Arrhenius activation energies were found to be about 2, 10 and 7.9  $\text{kcal mol}^{-1}$  for  $k_1$ ,  $k_2$  and  $k_3$ , respectively. The  $k_1$  value is similar to that of the activation energy for transport control under turbulent conditions. The  $k_2$  value indicates control by a heterogeneous reaction. The  $k_3$  value is close to that found by Sjöberg (1976) and Sjöberg and Rickard (1984) for dissolution reaction of pure calcite and Carrara marble (8.4  $\text{kcal mol}^{-1}$  and 7.4-8.6  $\text{kcal mol}^{-1}$ , respectively) and is not far from those commonly given for calcite precipitation rates (around 10  $\text{kcal mol}^{-1}$ ).

Plummer *et al.* (1978) also derived the same rate equation using an extension of the adsorption heterogeneous reaction model of Mullin (1972) and showed that the rate constant  $k_4$  could be written:

$$k_4 = k'_4 + k''_4 a_{\text{HCO}_3^-}(\text{s}) + k'''_4 a_{\text{OH}^-}(\text{s})$$

where  $k'_4$ ,  $k''_4$  and  $k'''_4$  are the constants for the backward reactions of equations (1) through (3) and the subscript  $s$  denotes surface (adsorption layer) values. From the principle of microscopic reversibility, forward and backward rates of all reactions must

balance at equilibrium. Consequently,  $k_4$  relation became:

$$k_4 = K_2/K_c (k'_1 + 1 / \alpha_{H^+}(s)) (k_2 \alpha_{H_2CO_3}(s) + k_3 \alpha_{H_2O}(s))$$

where  $K_2$  is the second dissociation constant of carbonic acid,  $K_c$  is the equilibrium constant for  $CaCO_3 = Ca^{2+} + CO_3^{2-}$ ,  $k'_1$  is the forward rate constant of reaction (1) ( $k'_1$  being some 10 to 20 times larger than the transport constant  $k_1$  derived in the pH-stat experiments).

Plummer *et al.* (1978) assumed that  $\alpha_{H_2CO_3}(s)$  was equal to  $\alpha_{H_2CO_3}$  of the bulk solution and  $\alpha_{H^+}(s)$  could be approximated by the equilibrium value of  $\alpha_{H^+}$ . They adopted the experimentally determined value of  $k_1$  for  $k'_1$ . Because  $k'_1 > k_1$ , the calculated value of  $k_4$  should be smaller than the experimentally determined value. They observed this systematic bias and considered it as evidence of validity of their model.

Plummer *et al.* (1978) tested their model using only dissolution experiments and did not run experiments to observe net precipitation of calcite. Plummer *et al.* (1979) noted the similarity of the equation described by Nancollas and Reddy (1971) for precipitation to the results obtained for dissolution at low  $pCO_2$  values. Reddy *et al.* (1981) measured calcite precipitation rate at 25°C, and  $pCO_2$  between 0.03 and 0.3 atm. They showed that the Plummer *et al.* (1978) model was applicable in these conditions. It was usually possible to predict the reaction rate to within a factor of 3 over a several order of magnitude change in reaction rate. The agreement was generally poorest near equilibrium. The model was found to be not as good a predictor of reaction rate at high  $pCO_2$  values as at low values. However, the Plummer *et al.* (1978) model remains the only model which attempts to describe calcite dissolution and precipitation at all solution pH and  $pCO_2$  values.

House (1981) carried out a complex test of different models for calcite precipitation using a seeding technique and found that the experimental data were adequately described by the Plummer *et al.* (1978) model. Most of others models (Nancollas and Reddy, 1971; parabolic law models) were not in agreement with the data. In their comparative study, Inskeep and Bloom (1985) found that most of their experimental data were consistent with the model of Plummer *et al.* (1978). However, this rate model which is first order in  $OH^-(s)$  (calcite saturation value) underestimated precipitation rates when initial ratio  $[Ca]/[CO_3]$  varied. At  $pH > 8$  and  $pCO_2 < 0.01$  atm, Inskeep and Bloom (1985) suggested the formation of a surface activated complex.

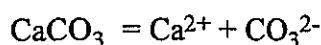
Busenberg and Plummer (1986) indicated that the Plummer *et al.* (1978) model failed to predict accurately calcite and aragonite dissolution rates very far from equilibrium and particularly very near equilibrium in  $Ca(HCO_3)_2$  solutions. In addition, the model could not predict reasonably accurate crystal growth rates near equilibrium. Therefore, they investigated the dissolution and growth of calcite and aragonite in supersaturated  $Ca(HCO_3)_2$  solutions at 25°C over a wide range of saturation states (up to 100) and  $CO_2$  partial pressures (from  $10^{-3.5}$  to 1 atm). They used and refined the model of Plummer *et*

*al.* (1978). For experimental data of calcite and aragonite dissolution near equilibrium, they proposed the empirical rate law:  $v_d = k_5 (1-\Omega)^n$ . They obtained:  $k_5 = 10^{-9.19} \text{ mol cm}^{-2} \text{ s}^{-1}$  and  $n = 0.9$  for calcite and  $k_5 = 10^{-9.44} \text{ mol cm}^{-2} \text{ s}^{-1}$  and  $n = 1.16$  for aragonite. In general, these constants are expected to depend on composition of the solution. At  $\Omega > 1.5$  for calcite and  $> 2$  for aragonite and over the range of  $p\text{CO}_2$  investigated, they found a rate of crystal growth given by:

$$v_p = k_4 (cE - a_{\text{Ca}^{2+}} a_{\text{HCO}_3^-})$$

where  $c$  is a constant (1.45 for calcite and 2.0 for aragonite),  $E$  is the equilibrium product of  $\text{Ca}^{2+}$  and  $\text{HCO}_3^-$  for the appropriate  $\text{CaCO}_3$  polymorph. Near equilibrium, the rate of calcite growth might be described following a similar empirical relation to that used for the dissolution near equilibrium:  $v_p = k_5 (1-\Omega)^n$ . However, Busenberg and Plummer (1986) could not determine the  $k_5$  constant because of the extremely slow rates of precipitation and because of the metastable nature of the supersaturated solutions. Results showed the existence of a change in reaction mechanism at  $\Omega \approx 1.5$  for calcite and  $\Omega \approx 2.0$  for aragonite. The latter mineral was found to grow at significantly slower rates than calcite in supersaturated calcium bicarbonate solutions. Consequently, kinetic factors were considered to account for the absence of aragonite in fresh-water environments.

Talman *et al.* (1990) showed the applicability of the Plummer *et al.* (1978) model to calcite dissolution in dilute solutions at 100, 150, and 210°C. Chou *et al.* (1989) carried out dissolution experiments for calcite, aragonite, dolomite, magnesite and witherite using a continuous fluidized bed reactor at 25°C. The dependence of reaction rate on pH observed for calcite and aragonite was similar and in agreement with the results obtained by Plummer *et al.* (1978). Chou *et al.* (1989) confirmed that calcite and aragonite dissolution/precipitation was controlled by the three same reactions as those used by Plummer *et al.* (1978) but proposed to express reaction (3) as:



This expression was not consistent with the experimental observations of Plummer *et al.* (1978). According to the stoichiometry of the three reaction steps and following thermodynamic constraints, the total forward and backward rates could be expressed as:

$$v_d = k_1 a_{\text{H}^+} + k_2 a_{\text{H}_2\text{CO}_3} + k_3$$

and

$$v_p = k_{-1} a_{\text{Ca}^{2+}} a_{\text{HCO}_3^-} + k_{-2} a_{\text{Ca}^{2+}} (a_{\text{HCO}_3^-})^2 + k_{-3} a_{\text{Ca}^{2+}} a_{\text{CO}_3^{2-}}$$



For each of the elementary reactions, the equilibrium conditions implies that:  $K_i = k_i/k_{-i}$  ( $K_i$  is the equilibrium constant of reaction) and thus the values of the backward rate constant  $k_{-i}$  can be calculated from its corresponding equilibrium and forward rate constants. Chou *et al.* (1989) noticed that the decrease in the rate of calcite dissolution observed at high pH clearly showed that the rate of the backward reaction of calcite precipitation close to saturation became important above pH 8. They showed the relative contribution of the three backward rates at pH > 6, indicating that the third backward equation was the prevailing step in their experiments. Consequently, they interpreted calcite and aragonite dissolution/precipitation reactions with the following rate law:

$$v_{\text{net}} = k_1 a_{\text{H}^+} + k_2 a_{\text{H}_2\text{CO}_3} + k_3 - k_{-3} a_{\text{Ca}^{2+}} a_{\text{CO}_3^{2-}}$$

which they argued describe calcite and aragonite growth and dissolution under varying  $p\text{CO}_2$ .  $k_{-3} = k_3 / K_{\text{sp}}$  and  $K_{\text{sp}}$  is the solubility product of the corresponding calcium carbonate. Their observations as well as those of Inskeep and Bloom (1985) suggested that it was not necessary to evoke the existence of a difference in composition between the bulk solution and the surface layer (model of Plummer *et al.*, 1978).

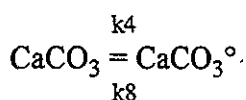
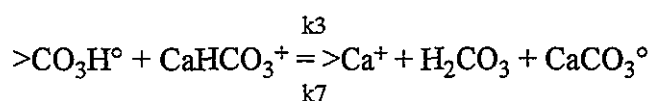
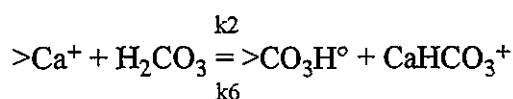
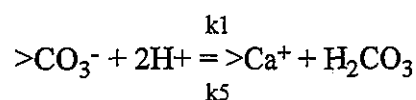
In their experiments of calcite dissolution in 0.5 M KCl solutions at pH > 7 and at 25°C, Compton and Pritchard (1990) found a rate equation derived from the model of Plummer *et al.* (1978) to be the one that best described the rate of dissolution in terms of surface speciation:

$$v_{\text{net}} = k - k' [\text{Ca}^{2+}]_s [\text{CO}_3^{2-}]_s$$

where  $k' = k / K_{\text{sp}}$ .  $k$  is dependent upon surface morphology. The subscript  $s$  denotes the surface values of concentration. The values found for the rate constants  $k$  and  $k'$  (corresponding to  $k_3$  and  $k_{-3}$  in the modified Plummer *et al.* (1978) model) were  $10^{-10.02}$  and  $10^{-2.15} \text{ mol cm}^{-2} \text{ s}^{-1}$ , respectively.

The mechanistic model of Plummer *et al.* (1978) adequately described the precipitation rate when growth followed the spiral growth equation in the near-equilibrium experiments at 100°C and 100 bar performed by Shiraki and Brantley (1995). The rate constant  $k_4$  ranged between  $7.08 \cdot 10^{-4}$  to  $1.01 \cdot 10^{-3} \text{ mol cm}^{-2} \text{ s}^{-1}$  in the  $a_{\text{H}_2\text{CO}_3}$  range studied. Outside of the regime of spiral growth, Plummer's model failed, suggesting that different elementary reactions controlled growth in the adsorption or two-dimensional nucleation regimes. Shiraki and Brantley (1995) concluded that no one model covered dissolution and precipitation under all values of  $\Delta G$  for calcite growth. Tests of the affinity-based models for calcite growth revealed that none of these models accurately predicted dissolution. Therefore, although affinity-based models may yield insights concerning the physical mechanism of growth, they may not be as useful in modelling dissolution and growth over the full range of  $\Delta G$ .

Araki and Mucci (1995) measured calcite dissolution rates in deionized water at 25°C and fixed pCO<sub>2</sub> (1 atm, 30%, 2%, 0.3%) using a free-drift technique. The data were corrected for gas phase disequilibrium and combined to corrected dissolution and precipitation rate measurements from previous investigations. These results were fitted to a kinetic expression derived by coupling the mechanistic models of Plummer *et al.* (1978) and Chou *et al.* (1989) to the surface complexation model of Van Cappellen *et al.* (1983). Araki and Mucci (1995) found that the following reactions adequately described calcite dissolution and precipitation mechanism in dilute solutions over a wide range pCO<sub>2</sub>, pH and state saturation:



The reaction rate  $v_{\text{net}}$  was given by:

$$v_{\text{net}} = k1 >\text{CO}_3^- (a_{\text{H}^+})^2 + (k2-k5) >\text{Ca}^+ a_{\text{H}_2\text{CO}_3} + k4 - (k6-k3) >\text{CO}_3\text{H}^\circ a_{\text{CaHCO}_3^+} - k7 >\text{Ca}^+ a_{\text{H}_2\text{CO}_3} a_{\text{CaCO}_3^\circ} - k8 a_{\text{CaCO}_3^\circ}$$

where  $> i$  are the densities of surface complexes (mol/m<sup>2</sup>),  $a_i$  are the activities of dissolved species and  $k_i$  are the constants corresponding to the above reactions. The calculations and values obtained for  $k_i$  and densities of surface complexes are not reported in this review due to their complexity.

The rate constants obtained from fitting the data set to this equation were compatible with values reported by Plummer *et al.* (1978) and Chou *et al.* (1989). However, Araki and Mucci (1995) concluded that their model provided a much better representation of calcite reaction kinetics in distilled water than the previously proposed models, particularly for the precipitation component. According to Araki and Mucci (1995) the model of Plummer *et al.* (1978) adequately described calcite dissolution rate but overestimated precipitation rates particularly at high pH and low pCO<sub>2</sub>. The model of Chou *et al.* (1989) overestimated dissolution rates and underestimated precipitation rates at low pH or high pCO<sub>2</sub>. Araki and Mucci (1995) announced that the validity of their model would be demonstrated for the same reactions in strong electrolytic solutions, including seawater, in a forthcoming paper.

A summary of the main experiments and results is given in table 3.

#### **f) Diffusion-limited crystal growth law**

At the surface of crystals growing from solution, transport of species occurs only by diffusion (Mullin, 1972) in a thin stagnant layer, the diffusion boundary layer (DBL). If precipitation is very fast, a gradient of concentration of solute  $(C_{\text{bulk}} - C_{\text{eq}}) / \Delta x$  is observed in the DBL ( $\Delta x$  is the thickness of the DBL) and provides the driving force for diffusion. If crystal growth is entirely controlled by diffusion, the precipitation rate  $v_p$  normalized to the specific surface area is proportional to this gradient following the relation:

$$v_p = D / \Delta x (C_{\text{bulk}} - C_{\text{eq}})$$

where  $D$  is the diffusion coefficient of solute in the DBL. This equation predicts that the precipitation rate is considerably affected by the stirring speed because the thickness of the DBL is itself a function of the stirring speed. For diffusion-controlled reactions, the rates are higher than those of surface reactions and the activation energies are lower.

As indicated by several workers (Berner and Morse, 1974; Plummer and Wigley, 1976; Plummer *et al.*, 1978; Sjöberg and Rickard, 1983, 1984), diffusion-controlled reactions are dominant for calcite dissolution below pH 4 at low temperature. In their near-equilibrium experiments of calcite precipitation at 100°C and 100 bar, Shiraki and Brantley (1995) observed that the precipitation rate was entirely controlled by diffusion only at low stirring speeds (400 rpm), but also:

- at low values of  $\Omega$  when  $\alpha_{\text{H}_2\text{CO}_3}$  was smaller than  $3.53 \cdot 10^{-4}$ ;
- at high  $\alpha_{\text{H}_2\text{CO}_3}$  and higher  $\Omega$ .

Very little information about diffusion-controlled precipitation of calcite is available in the literature because most studies conducted at low temperature were performed at relatively high pH and studies carried out at high temperature, where diffusional processes are more likely to be rate limiting (Murphy *et al.*, 1988), are very rare. For example, Talman *et al.* (1989) found that the rate of calcite dissolution was dependent on  $p\text{CO}_2$  and stirring rate in their experiments in  $\text{CO}_2$ - $\text{H}_2\text{O}$  system at 210°C.

### **1.3. FIELD DATA FOR CALCITE PRECIPITATION RATES**

If many laboratory experiments have been performed to investigate the reaction kinetics of calcite in  $\text{H}_2\text{O}$ - $\text{CO}_2$  systems and in seawater at 25°C, few researchers have attempted to quantify calcite dissolution or precipitation rates on the basis of field data (Herman

and Lorah, 1988). Field measurements of precipitation rates were done for two kinds of natural systems: spring-fed streams and deep-sea carbonate sediments.

### 1.3.1. Spring-fed streams

Herman and Lorah (1988) determined rates of calcite precipitation in a travertine-depositing stream by measuring changes in stream composition between consecutive sampling points. Rates were calculated from a combination of mass transfer modelling and hydrologic measurements and ranged from 0.02 to  $3.0 \cdot 10^{-9}$  mol cm<sup>-2</sup> s<sup>-1</sup>. These values compare well with the range in precipitation rates observed in laboratory crystal growth experiments. Herman and Lorah (1988) compared the values obtained in the field with rates predicted from the laboratory-derived rate law of Plummer *et al.* (1978). The agreement was generally within an order of magnitude and routinely within a factor of 3. Because of the fundamental differences between the two approaches, the agreement between mass transfer rates and the values calculated from the Plummer *et al.* rate law was considered to be good. The surface area estimated for stream bed appeared to be the dominant source of error when comparing the different approaches. Herman and Lorah (1988) pointed out that the assumption of uniform flow velocity might cause a large error if the rates were calculated in terms of reaction in a volume of solution per unit time.

Dreybrodt *et al.* (1992) and Zaihua *et al.* (1995) calculated deposition rates for calcite precipitated in spring-fed streams due to outgassing of CO<sub>2</sub>. They used a mass transfer model for calcite precipitation taking into account the reaction rates given by Plummer *et al.* (1978), the slow conversion of CO<sub>2</sub> into H<sup>+</sup> and HCO<sub>3</sub><sup>-</sup>, and the diffusional mass transport across the diffusion boundary layer (Buhmann and Dreybrodt, 1985; Dreybrodt and Buhmann, 1991). The calculated rates were in good agreement with the field data (values from 0.1 to  $6.5 \cdot 10^{-11}$  mol cm<sup>-2</sup> s<sup>-1</sup>). Using only the model of Plummer *et al.* (1978), the calculated rates turned out to be too high by one order of magnitude. These workers noticed that this result was not unexpected since these calculations neglected the diffusion boundary layer between the surface of the tablets and the turbulent flowing solution, which represented a diffusive resistance (the chemical composition measured in the bulk fluid was different from that at the calcite surface). They concluded that, at fast flow conditions, a reasonable prediction of calcite precipitation rates was possible by using the rate equation of Plummer *et al.* (1978) and correcting it for the influence of the boundary layer by reducing the obtained rates by a factor of ten. For still waters of identical chemical composition to that of fast flowing waters, Zaihua *et al.* (1995) measured lower calcite deposition rates, by a factor about 4. They deduced a clear evidence for the influence of hydrodynamic conditions on calcite deposition rates.

### 1.3.2. Deep-sea sediments

Baker *et al.* (1982) calculated rates of recrystallization of calcite in deep-sea carbonate sediments from the degree of equilibration between the carbonate sediments and their

pore fluids in Deep Sea Drilling Project drill cores. They found rate constants ranging from  $10^{-22}$  to  $10^{-19}$  mol cm<sup>-2</sup> s<sup>-1</sup>, at 5°C. They are much lower than those given by Lorens (1981), Mucci and Morse (1983) or Busenberg and Plummer (1986), which range from  $10^{-14.0}$  to  $10^{-9.5}$  mol cm<sup>-2</sup> s<sup>-1</sup> at 25°C.

On the other hand, these values are in agreement with the rate extrapolated to low temperatures from the results obtained by Beck *et al.* (1992), using an isotopic doping technique, in a 0.5 m NaCl fluid at 500 bar and at 250, 300, 350 and 400°C ( $10^{-12.7}$ ,  $10^{-12.33}$ ,  $10^{-11.55}$  and  $10^{-10.88}$  mol cm<sup>-2</sup> s<sup>-1</sup>, respectively). Beck *et al.* (1992) indicated that the rate-controlling mechanism is extremely slow at near-equilibrium conditions, even at high temperatures, and apparently unrelated to the dissolution/precipitation mechanism prevailing under conditions relatively far from equilibrium.

The rates of recrystallization for deep-sea carbonates determined by Baker *et al.* (1982) are also very different from the net CaCO<sub>3</sub> dissolution rate given for deep-sea sediments. Peterson (1966) estimated a dissolution rate of around  $10^{-13.10}$  mol cm<sup>-2</sup> s<sup>-1</sup> in the Central Pacific. Dymond and Lyle (1985) in the Guatemala Basin (eastern equatorial Pacific) and Berelson *et al.* (1990) in the central equatorial north Pacific found an approximate value of  $10^{-12.33}$  mol cm<sup>-2</sup> s<sup>-1</sup>. For Berelson *et al.* (1990) the degree of undersaturation ( $1 - \Omega$ ) used in the study was 0.16. This dissolution rate is already 20% of previous estimates but is consistent with dissolution rate constants predicted from laboratory experiments with deep-sea and shallow sediments (Morse, 1978; Keir, 1980; Walter and Morse, 1985). The experiments of Morse (1978) were carried out near equilibrium conditions ( $\Omega$  from 0.54 to 0.91) for calcium carbonate rich deep-sea sediments collected in the Indian, Pacific and Atlantic oceans. All these values are closer to those found by Lorens (1981) or Mucci and Morse (1983) and Zhong and Mucci (1993) in calcite precipitation experiments. Even if the reactive surface area, which is related to grain size and the structure of calcite, is highly variable (a factor of about 100), especially for biogenic calcites (Walter and Morse, 1984; Walter and Morse, 1985), the large difference observed between the rates obtained by Baker *et al.* (1982) and Berelson *et al.* (1990) cannot be explained by variation in this parameter only.

## 2. Kinetics of precipitation of other carbonates

Kinetic studies of dissolution-precipitation reaction for carbonate minerals other than calcium carbonate are not as abundant as for calcite. Numerous experimental studies and field studies investigated the mechanism of dolomite formation (Hardie, 1987) but attempts to study the reaction kinetics of dolomite have been largely unsuccessful (Morse, 1983). Only a few most significant studies of the kinetics of dolomite, magnesite and witherite dissolution (Lund *et al.*, 1973; Busenberg and Plummer, 1982; Herman and White, 1985; Faux *et al.*, 1986; Chou *et al.*, 1989; Talman and Gunter, 1992) are reported in this review. Most of the data obtained by these workers were described by an empirical mechanistic rate law, assuming elementary reactions and similar to that used by Plummer *et al.* (1978) for calcite. No kinetic data for dolomite precipitation were found in the laboratory syntheses of dolomite used to examine the controls on growth. To achieve discernible reaction in the laboratory, high temperatures and/or extreme supersaturation were required in these studies. Sibley *et al.* (1994) reviewed most of the data on dolomitization of  $\text{CaCO}_3$  at high temperatures (100-300°C) and presented new data but no value of dolomitization rate was given. Brady *et al.* (1996) considered the dolomite growth solely from an interfacial kinetics standpoint but did not report any kinetic data. They used surface adsorption measurements to test reaction pathways for dolomite growth as a continuum exists between metal sorption and growth of metal carbonate minerals. The measured total surface area for the dolomite used in their experiments was  $0.5 \text{ m}^2/\text{g}$ .

### 2.1. KINETICS OF DOLOMITE

#### 2.1.1. Kinetics of dolomite dissolution

Busenberg and Plummer (1982) studied the dissolution kinetics of eight different dolomites far from equilibrium in dilute solutions, from 1.5 to 65°C, at fixed pH values from 0 to 10 and at fixed  $\text{pCO}_2$  values (from 0 to 0.96 atm) using single crystals and a weight loss method. In their experiments, two stages were recognized in the dissolution of dolomites:

- a very brief non-stoichiometric dissolution stage from the fresh dolomite surface releases  $\text{CaCO}_3$  faster than  $\text{MgCO}_3$  and results in a  $\text{MgCO}_3$  enriched surface;
- in the next and most important stage, both  $\text{CaCO}_3$  and  $\text{MgCO}_3$  are released stoichiometrically.

These workers showed that when samples with a small surface area were dissolved for long periods of time, the dissolution appeared congruent. Samples with a very large surface area dissolved for short periods of time showed non-stoichiometric dissolution.

There was a strong evidence for backward reaction in many of their experiments even far from equilibrium, but no evidence for the formation of dolomite. The most important backward rate observed below pH 7.0 resulted from the reaction of positively charged surface sites with adsorbed  $\text{HCO}_3^-$  from the bulk solution. It was apparent that the presence of  $\text{HCO}_3^-$  caused a decrease in the net rate of dolomite dissolution.

The overall rate of dissolution of dolomite was described by the following mechanistic rate equation:

$$v_{\text{net}} = k_1 a_{\text{H}^+}^n + k_2 a_{\text{H}_2\text{CO}_3}^n + k_3 a_{\text{H}_2\text{O}}^n - k_4 a_{\text{HCO}_3^-}$$

where  $k_1$ ,  $k_2$ ,  $k_3$  are forward rate constants and  $k_4$  is the backward rate constant. The exponent  $n$  is equal to 0.5 at temperatures below 45°C, and for hydrogen ion rate dependence,  $n$  equals 0.6, 0.7, and 0.85 at 55, 65 and 100°C, respectively. This equation could be used to predict dissolution rate of dolomite in a variety of aqueous solutions provided the calculated rate was greater than  $10^{-13} \text{ mol cm}^{-2} \text{ s}^{-1}$ .

Because of the lack of microscopic reversibility between the forward and backward reaction mechanisms, Busenberg and Plummer (1982) emphasized that this equation was not complete and did not account for all backward reaction mechanisms. It was clearly showed that equilibrium took an extremely long time to be achieved. It was noticed that dissolution rates of dolomite were 100 times slower than calcite, and the backward reactions reduced these rates even further to the point where weeks or months were necessary to dissolve detectable amounts of solid ( $\sim 5 \mu\text{g}$ ) at pH values greater than 6.0. Relatively low concentrations of  $\text{HCO}_3^-$  could almost completely stop the dissolution of dolomite far from equilibrium. Results suggested that reversible dolomite-solution equilibrium could not be achieved in the laboratory at less than 45°C. Backward reactions were demonstrated that can form calcite and aragonite in calcium bicarbonate solutions.

The observed rates varied from sample to sample. There were very significant differences between dissolution rates of sedimentary dolomites and of hydrothermal dolomites. The hydrothermal dolomite dissolved significantly slower at 5°C; however, the rates of dissolution were comparable at 45°C and above. Dissolution reaction rates were significantly more dependent on crystallographic order than they were on compositional variations. Solids with the highest crystallographic ordering dissolved the slowest and might be more stable. The backward rate constant  $k_4$  was independent of the mode of origin of the dolomite but dependent on the mole percent  $\text{FeCO}_3$  in the dolomites.

Experimentally determined values of  $k_1$ ,  $k_2$ ,  $k_3$  and  $k_4$  between 5 and 65°C were reported for the eight dolomite samples. Below 45°C, all the forward reaction rates were controlled by heterogeneous surface reactions, had large Arrhenius activation energies, and were independent of stirring speed. The Arrhenius activation energies of  $k_1$ ,  $k_2$  and  $k_3$  for hydrothermal dolomites (12.4-21.4, 12.2-18.5 and 16.2-38.0 kcal

mol<sup>-1</sup>, respectively) were higher than those for sedimentary dolomites (7.3, 7.0 and 9.5-13.1 kcal mol<sup>-1</sup>, respectively). A temperature dependence of the rate constants between 0 and 45°C for typical sedimentary and typical hydrothermal dolomites was given by Busenberg and Plummer (1982).

This dependence was described by the equation:

$$\log k_i = a(1/T) + b$$

where a and b are constants,  $k_i$  and T are given in mol cm<sup>-2</sup> s<sup>-1</sup> and °K, respectively.

The values of a and b constants are shown in table 4a. The corresponding calculated values of  $k_i$  at 25°C and 45°C are reported in table 4b. Above 45°C, a change in the dissolution mechanism probably occurred. The H<sup>+</sup> dependence of the forward rate was at least in part controlled by the hydrodynamic transport of reactants and products between the surface and the bulk solution. These results were consistent with those of Lund *et al.* (1973), who investigated the kinetics of dolomite dissolution as a function of HCl concentration between 25 and 100°C, and found significant stirring dependence at 100°C in 1M HCl solution under 41 atm N<sub>2</sub> pressure but not at temperatures below 50°C. The values of  $k_1$  and n (10<sup>-7.2</sup> mol cm<sup>-2</sup> s<sup>-1</sup> and 0.48 respectively) calculated from the original data of Lund *et al.* (1973) at 25°C were in good agreement with the values obtained by the study of Busenberg and Plummer (1982) for similar sedimentary dolomites.

In their dissolution experiments of various carbonate minerals using a continuous fluidized bed reactor at 25°C, Chou *et al.* (1989) obtained results similar to those of Busenberg and Plummer (1982) and used the same rate equation to describe their experimental data for the forward dissolution rate of dolomite (table 4b). They found, however, that n was equal to 0.75 (instead of 0.5). Chou *et al.* (1989) pointed out that the two-step reaction mechanism proposed by Busenberg and Plummer (1982) did not explain the fractional reaction order observed (< 1), which might be due to a more complex surface reaction. They did not give any value for the backward rate constant.

Talman and Gunter (1992) studied the rates of dolomite dissolution in CO<sub>2</sub> and HCl bearing solutions from 100-200°C. The results of this study supported the observation of Busenberg and Plummer (1982) that the rate of dolomite dissolution above about 50°C became progressively more dependent on diffusional processes as temperature was increased (shift from a surface reaction controlled reaction to a transport controlled reaction). It was found that the rate constants of the rate equation proposed by Busenberg and Plummer (1982) were more sensitive to stirring speed as temperature increased. At 200°C, experimental data were inconsistent with the rate expression.



### 2.1.2. Dolomite growth: rate-limiting steps

According to Brady *et al.* (1996), exchange and/or adsorption of metals onto carbonate mineral surfaces causes an initial rapid uptake of metals from solution. This is followed by incorporation of metals with the formation of surface precipitates and/or solid solutions. To construct a unit cell of dolomite from a dolomite seed crystal or nucleus requires the stoichiometric adsorption of Ca and Mg onto their respective planes followed by the dehydration and carbonation of each ion. Because Ca and Mg adsorption is stoichiometric, metal dehydration and carbonation must be a slow, rate-determining step for dolomite growth. As calcite grows rapidly at low temperature, dehydration and carbonation of adsorbed Ca is rapid relative to Mg (magnesite is notoriously difficult to grow in the laboratory at low temperature). The rate-limiting steps for dolomite growth are therefore thought to be the dehydration and carbonation of the adsorbed Mg ion. At alkaline pH (pH > 9), CO<sub>3</sub> levels are high, the MgCO<sub>3</sub> complex is abundant in solution and the adsorption and incorporation of the latter into a growing dolomite structure is easily envisioned. Nevertheless, the pH values of natural waters rarely exceed pH 9 and MgCO<sub>3</sub> is generally a minor constituent. In sulphate-rich solutions, Ca and Mg absorb as metal sulfate complexes.

Brady *et al.* (1996) proposed that one path for dolomite growth from low temperature natural waters was through the initial adsorption of Mg-sulphate complexes onto either growing dolomite crystals or rate-limiting dolomite nuclei. They presented two interfacial pathways for dolomite growth, one for sulphate-poor solutions (< 0.005 M), the other for sulphate-rich solutions (> 0.005 M). Inhibition of dolomite growth by trace amounts of sulphate in sulphate-poor solutions but acceleration by sulphate in sulphate-rich solutions were consistent with experimental and geologic observations (Siegel, 1961; Baker and Kastner, 1981; Morrow and Ricketts, 1988). Massive dolostone sequences would be formed from evaporatively modified seawater due, in part, to the high sulphate levels that would favor dolomite growth.

### 2.1.3. Kinetics of experimental dolomitization of CaCO<sub>3</sub> at high temperature

Sibley *et al.* (1994) indicated that at high temperature (100-300°C), the rate of dolomitization of CaCO<sub>3</sub> increased with temperature, reactant surface area, reactant solubility, ionic strength, HCO<sub>3</sub><sup>-</sup> concentration and Mg<sup>2+</sup>/Ca<sup>2+</sup> of the solution. The high activation energies found by Katz and Matthews (1977) for Very High-Mg Calcite (VHMC) and dolomite (48 and 49-50 kcal mol<sup>-1</sup>, respectively), compared to the approximately 10 kcal mol<sup>-1</sup> activation energy for calcite precipitation, explain the relatively high temperature dependence of the rate of dolomitization. Sibley *et al.* (1994) also noticed that the mineralogy of the initial reactant affected dolomitization rates. For example, aragonite was dolomitized faster than low-Mg calcite. From their experiments at high temperature (150-300°C), they divided the dolomitization reaction in three steps:

- nucleation: nucleation of VHMC (35-40 mole %  $\text{MgCO}_3$ ) or nonstoichiometric dolomite is followed by nucleation of more stoichiometric dolomite on  $\text{CaCO}_3$ . The composition of the VHMC or nonstoichiometric dolomite is a function of  $\text{Mg}^{2+}/\text{Ca}^{2+}$  of the solution. Other variables such as dissolved Fe can affect the composition of the nuclei;
- long induction period: this longer period corresponds to post-nucleation growth of VHMC, of nonstoichiometric and of stoichiometric dolomite nuclei. Changes in the solution and substrate surface area affect the duration of this period. The rate of growth is slow during most of this period but there is a marked and rapid increase in crystal growth rate towards the end, which is probably due to a change in crystal growth mechanism;
- replacement period: a)  $\text{CaCO}_3$  is replaced by VHMC or nonstoichiometric dolomite. VHMC nucleates faster than stoichiometric dolomite and therefore begins to replace the reactant first. b)  $\text{CaCO}_3$  and VHMC and/or nonstoichiometric dolomite are rapidly replaced by stoichiometric dolomite. This phase of the reaction is sensitive to solution variables such as  $\text{Mg}^{2+}/\text{Ca}^{2+}$  and ionic strength.

Sibley *et al.* (1994) suggested that the three-phase model was consistent with eight characteristics of natural dolomites. They concluded that laboratory experiments provided an accurate qualitative model for dolomitization at low temperature in natural settings because of the similarity of kinetics effects, in the composition of reaction products and in textures. The most significant characteristic of the dolomite reaction model was the long induction period, which offered a phenomenological explanation for the lack of dolomite at low temperature in many solutions that were supersaturated with respect to dolomite. In these solutions, dolomite might have nucleated but the reaction might still be in the induction period and therefore no products were detected. Therefore, the formation of massive dolomite was favored by long residence times in dolomitizing solutions. Sibley *et al.* (1994) argued that it was the combination of several variables, not a single variable, that determined the reaction kinetics. The kinetically most favorable natural low-temperature setting for dolomitization was the tidal flat, where elevated temperature,  $\text{Mg}^{2+}/\text{Ca}^{2+}$  and ionic strength might occur. However, this could be contravened by rapid sea-level fluctuations, which made the residence time in dolomitizing solutions less than the induction period.

## 2.2. KINETICS OF MAGNESITE AND WITHERITE

There are very few data existing on the dissolution rate of magnesite at room temperature and over a wide range in pH because of its extremely low dissolution rate. The kinetics of magnesite dissolution far from equilibrium from 25 to 85°C and pH's from 1 to 10 at atmospheric  $\text{pCO}_2$  was investigated by Faux *et al.* (1986), using the single crystal weight loss method. Very few details on the experimental results and interpretation are given. For example, rate law equations were described but the values of the corresponding rate constants  $k_1$ ,  $k_2$ ,  $k_3$  and  $k_4$  were not reported. However, it can be pointed out that below 55°C, the dissolution rate was dependent on pH at values

lower than 6 and independent of pH at values greater than 6. At 55°C and above, the dissolution rate was pH dependent at pH values less than 2.0 and between 4.5 and 6.0. It was pH independent at values ranging from 2.0 to 4.5 and above 6.0. The large calculated activation energies of reactions ( $E_a = 15.8-21.2 \text{ kcal mol}^{-1}$ ) and the partial order of the dissolution rate ( $n$  often between 0.25 and 0.5) were generally indicative of surface controlled reactions.

Chou *et al.* (1989) indicated that dissolution of magnesite and witherite at 25°C followed similar mechanisms than that of calcite and aragonite. Consequently, they used the rate equation they proposed the latter minerals. The rate of dissolution of whiterite was comparable to that of calcite and aragonite. In contrast, the rate of magnesite dissolution was approximately four orders of magnitude lower than that of calcite. In addition the influence of  $p\text{CO}_2$  appeared to be more pronounced for magnesite than for the other carbonates studied. Because of the low dissolution rate of magnesite, the system remained constantly far from equilibrium and no backward reaction was observed. The backward rate constant was therefore calculated according to the relation obtained at equilibrium conditions:

$$k_3 / k_{-3} = K_{sp} \text{ (solubility product of magnesite).}$$

For witherite, the  $k_3/k_{-3}$  ratio could be measured experimentally. The solubility product  $K_{sp}$  calculated on the basis of measured data was in good agreement with the thermodynamic value, suggesting that the dissolution mechanism was coherent.

The main experiments and results are summarized in table 5.

### **3. Chemical inhibition of calcium carbonate growth**

#### **3.1. SOME BASIC ASPECTS OF INHIBITION PROCESSES**

The presence of various constituents and their interaction with the surface of carbonate grains have been used to account for the lack of reactivity of calcite in seawater (Mucci, 1986). This has most often been associated with the existence of the disequilibrium state of the  $\text{CaCO}_3$  system in near-surface seawater and the persistence of aragonite and high magnesium calcites which are unstable with respect to calcite. Experimental studies have shown that many dissolved components in natural waters inhibit calcite precipitation rates (Berner, 1975; Morse, 1983; Mucci and Morse, 1983; Busenberg and Plummer, 1985; Mucci, 1986, 1988; Walter, 1986; Burton and Walter, 1990). It is beyond the scope of this section to review all the papers dealing with these effects. Many of them are largely phenomenological or relate to a very specific system. The primary goal is to summarize the main quantitative results relative to the most important inhibitors.

Seawater and seawater-like solutions have been used in much experimental work, and  $\text{Mg}^{2+}$ ,  $\text{SO}_4^{2-}$  and  $\text{PO}_4^{3-}$  were shown to be the main inhibitors of calcite growth. However, in burial diagenetic waters, where  $\text{Mg}^{2+}$  and  $\text{SO}_4^{2-}$  concentrations are often lower, other ions such as  $\text{Mn}^{2+}$  and  $\text{Fe}^{2+}$  or organic compounds at relatively high concentrations can be major inhibitors. Experimental studies indicate that incorporation of many of these cations in calcite is strongly dependent on growth kinetics. Furthermore, there is a feedback relationship between these two processes, and the presence of the incorporated ion in solution affects the rate of calcite growth. Additionally, incorporation of an apparent inhibitor species can result in formation of a solid solution that is more soluble than pure calcite. For such solid solutions, the fluid will be at a lower degree of supersaturation leading to lower precipitation rates (Berner, 1975; Busenberg and Plummer, 1985). This effect may be very important for cations that can form extensive solid solutions with calcite, such as  $\text{Mg}^{2+}$  and  $\text{Mn}^{2+}$ . However, only the precipitation kinetics of Mg-calcites has been investigated in any detail (Berner, 1975; Mucci and Morse, 1983; Burton, 1988).

Before proceeding to specific systems, it is worth pointing out that there are two primary ways in which inhibitor species can influence reaction rates. The first is in the solution where they can form complexes with the reaction ions. This can alter both activity coefficients, and hence the saturation state of the solution, and the rate at which transformation reactions occur. The second is that inhibitor species can adsorb on the surface of the reacting solid and be preferentially incorporated at higher energy sites, which are also favored for crystal growth. The adsorption processes have a significant role in both the precipitation inhibition and the incorporation of species. However, other

processes also may influence inhibition or incorporation. For example, differences in solubility with pure calcite may in part explain lower precipitation rates if solid solutions are precipitated.

In order to quantify the degree of inhibition, many investigators have used the relation:  $(v_0 - v)/v_0$  where  $v$  is the measured precipitation rate in solutions containing the inhibitor ion, and  $v_0$  is the rate in the absence of the inhibitor. The effect of varying the concentration of inhibitor ions, at a given calcium concentration, degree of saturation and temperature, may be described using the relation (from Meyer, 1984):

$$(v_0 - v)/v_0 = a C_{\text{inh}}$$

where  $C_{\text{inh}}$  is the concentration (or activity) of inhibitor ion in solution and  $a$  is a constant which is different for each ion. This expression is derived from a Langmuir-type adsorption isotherm (Adamson, 1967). The degree of inhibition is assumed to be proportional to the fraction of adsorption sites on the calcite crystals occupied by the inhibitor ions, which is a function of inhibitor concentration. Such a relation has been used successfully to model calcite growth inhibition by various ions (Reddy and Nanchollas, 1973; Reddy, 1977; Reddy and Wang, 1980; Meyer, 1984; Dromgoole and Walter, 1990b). A similar relation which links the rate constant to the inhibitor concentration was also used by Mucci and Morse (1983).

## **3.2. INFLUENCE OF SPECIFIC INHIBITORS**

### **3.2.1. Magnesium**

Magnesium has received by far the most attention because of its common occurrence in natural waters and large influence on calcite. No area of carbonate reaction kinetics has been more controversial than the precipitation of calcite from solutions containing magnesium (Morse, 1983). This is due to the complexity of the process because  $\text{MgCO}_3$  may coprecipitate with the calcite causing major alterations in its properties.

Weyl (1965) made the first serious attempt to evaluate the influence of magnesium on calcium carbonate reaction kinetics. The results were generally qualitative in nature, but clearly pointed to the general inhibitory nature of magnesium. His work indicated that  $\text{Mg}^{2+}$  was the most important cationic coprecipitate in calcite formed in the marine environment. The inhibition effect of magnesium on calcite growth was explained as being due to the adsorption of Mg onto calcite nuclei surfaces (Bischoff, 1968; Pytkowicz, 1973; Katz, 1973; Lippmann, 1973). This Mg layer prevented growth by either raising the surface free energy or by causing the formation of Mg-calcite, a carbonate of substantially higher solubility. It was also well established that the presence of dissolved magnesium favored the precipitation of  $\text{CaCO}_3$  as aragonite rather than calcite in supersaturated seawater and other magnesium-rich aqueous solutions (Kitano, 1962; Lippmann, 1973).

Berner (1975) made the first detailed study of the inhibition of seeded calcite and aragonite precipitation by  $\text{Mg}^{2+}$  in seawater, Mg-depleted seawater and Mg-free seawater at 25°C and at different  $p\text{CO}_2$  ( $10^{-3.5}$ ,  $10^{-2.54}$ ,  $10^{-2.01}$  and  $10^{-1.51}$  atm). Dissolved magnesium at seawater level appeared to have no effects on the rate of crystal growth of aragonite (no adsorption of Mg on the surface of this mineral), but a strong retarding effect on that of calcite. At a same degree of solution saturation with respect to calcite, rates obtained from normal seawater could decrease by a factor greater than 20 relative to Mg-free seawater solutions. However, at low concentrations of Mg (less than 5% that of normal seawater), no retardation of growth rate occurred. Extended crystal growth on pure calcite seeds in seawater of normal Mg content resulted in the crystallization of magnesium calcite overgrowths, containing 7 to 10 mole %  $\text{MgCO}_3$ . This suggested that the rate inhibition by Mg was due to its incorporation within the calcite crystal structure during growth, which caused the resulting magnesian calcite to be significantly more soluble than pure calcite but more stable than aragonite. Direct reversible equilibrium measurements of the solubility of calcite in seawater solutions at different Mg concentrations (Mucci and Morse, 1983) indicated that at seawater  $\text{Mg}^{2+}$  to  $\text{Ca}^{2+}$  ratios, the change in solubility was less than 10%.

More recent studies have generally favored an interpretation of the inhibiting influence of  $\text{Mg}^{2+}$  which results from difficulties in rapidly dehydrating it after adsorption and before incorporation (Lahann, 1978; Mucci and Morse, 1983), or crystal poisoning by adsorption of  $\text{Mg}^{2+}$  at reactive sites (Reddy and Wang, 1980; Reddy, 1983). It was considered that the process of inhibition was likely to be a consequence of the smaller size, higher charge density and resultant stronger hydration of  $\text{Mg}^{2+}$  in comparison to  $\text{Ca}^{2+}$  ions. The growth inhibition could then be attributed to the impingement of hydrated  $\text{Mg}^{2+}$  ions ( $\text{Mg}(\text{H}_2\text{O})_6^{2+}$ ) on the crystal lattice of the seed material on active growth sites, such as kinks.

Reddy and Wang (1980) and Reddy (1983) observed in dilute solutions ( $[\text{Ca}]_t = 2.5 \cdot 10^{-4}$  M,  $\text{pH} = 8.9$ ), at 25°C and ambient  $p\text{CO}_2$ , a decrease in the seeded precipitation rate constant by a factor more than 20 when magnesium ion concentrations varied from 0 to  $13 \cdot 10^{-4}$  M (see figure 5 in Reddy, 1983). These workers showed that such decrease was consistent with the hypothesis of inhibition by adsorbed  $\text{Mg}^{2+}$  at calcite growth sites on the crystal surface if a Langmuir type adsorption isotherm was assumed. A curious finding of their research was that no coprecipitation of  $\text{MgCO}_3$  occurred at  $\text{Mg}^{2+}$  concentrations of less than  $2 \cdot 10^{-4}$  M. No attempt was made to characterize the formation of Mg-calcites at higher  $\text{Mg}^{2+}$  concentrations, although significant changes in solution  $\text{Mg}^{2+}$  content were interpreted as indicating the formation of Mg-calcites.

Mucci and Morse (1983) found no influence of growth rate on the magnesium content of calcite in experiments performed in seawater at 25°C and at supersaturation levels ( $\Omega$ ) of 3 to 17. They showed that the amount of  $\text{Mg}^{2+}$  incorporated in the overgrowths was not directly proportional to  $\text{Mg}^{2+}/\text{Ca}^{2+}$  in solution over the entire range (1-20) of ratios

studied. Below a ratio of 7.5, the composition of the calcite overgrowths was not only influenced by the  $\text{Mg}^{2+}/\text{Ca}^{2+}$  concentration ratio in the solution but also by the presence of an adsorbed Mg layer. In solutions where  $\text{Mg}^{2+}/\text{Ca}^{2+}$  ratios were low ( $< 1$ ),  $\text{Mg}^{2+}$  incorporation was small ( $< 3$  mol%) and  $\text{Mg}^{2+}$  had little effect on calcite growth kinetic. Using the empirical law:  $v_{\text{net}} = k (\Omega - 1)^n$ , they found that the computed reaction orders  $n$  for the precipitation of Mg-calcite in each one of the seawater solutions used in their experiments were similar, ranging from 3.07 to 3.70. Also the growth rate constant  $k$  decreased by a factor about 500 as the  $[\text{Mg}^{2+}]$  to  $[\text{Ca}^{2+}]$  concentration ratio increased from 1 to 10.3 (with  $[\text{Ca}^{2+}]$  always equal to  $10.28 \cdot 10^{-3}$  mol  $\text{kg}^{-1}$  solution). Their experimental results yielded the following relation could be obtained:

$$\log k (\text{mol cm}^{-2} \text{s}^{-1}) = -12.567 - 0.27275 ([\text{Mg}^{2+}]/[\text{Ca}^{2+}])$$

with a correlation coefficient  $r = -0.99$ . This relation shows the strong influence of  $\text{Mg}^{2+}$  on the growth rate constant  $k$ . For instance,  $k$  is 20 times greater in Mg-free seawater than in normal seawater.

### 3.2.2. Sulphate

Many studies on calcium carbonate reaction kinetics were done in seawater because of the many significant geochemical problems in this natural system. The only major seawater component in addition to  $\text{Mg}^{2+}$  which was identified as a dissolution and precipitation inhibitor was  $\text{SO}_4^{2-}$  (Morse, 1983). This species may be incorporated in significant amounts in solid-solution in calcites precipitated from seawater or synthetic seawater and form solid solutions. Biogenic high Mg-calcites average about 1 mole %  $\text{SO}_4^{2-}$ . Aragonites and biogenic low Mg-calcites generally contain smaller amounts of  $\text{SO}_4^{2-}$ . Kitano *et al.* (1975) indicated that  $\text{SO}_4^{2-}$  was more easily incorporated into calcite than into aragonite and that with increasing concentrations of NaCl in solution, the  $\text{SO}_4^{2-}$  content of calcites decreased significantly.

In the presence of dissolved  $\text{SO}_4^{2-}$ , Busenberg and Plummer (1985) showed that the substitution of  $\text{SO}_4^{2-}$  in place of the smaller  $\text{CO}_3^{2-}$  ions increased the unit cell dimensions of calcite and significantly reduced the rate of crystal growth at  $25^\circ\text{C}$  in 0.50 molal NaCl and 0.01 molal  $\text{CaCl}_2$  solutions (table 6). For experiments at  $\Omega = 2.5$  and 10, where several rate values were obtained, the decrease in crystal growth rate was proportional to the log of the concentration of  $\text{SO}_4^{2-}$  in solution. Using the empirical rate law  $v_{\text{net}} = k(\Omega-1)^n$ , we calculated the reaction order  $n$  and the rate constant  $k$  for the precipitation of calcite in each one of the solutions with different  $\text{SO}_4$  concentrations (table 7). The values of  $n$  were similar and close to 1 whereas the growth constant was decreased by a factor of about 10, as the total dissolved sulphate concentration  $[\text{SO}_4^{2-}]_t$  increased from 0.003 to 0.05 m. From these calculations, a similar relation to that obtained by Mucci and Morse (1983) could be found:

$$\log k \text{ (mg min}^{-1} \text{ g}^{-1} \text{ seed)} = 0.9475 - 0.22785 ([\text{SO}_4^{2-}]_t / [\text{Ca}^{2+}]_t)$$

with a correlation coefficient  $r = -0.98$ . Moreover, Busenberg and Plummer (1985) showed that the amount of  $\text{SO}_4^{2-}$  in solid-solution in calcites at 25°C varied as a function of the rate of crystal growth.

The  $\text{SO}_4^{2-}$  distribution coefficient  $D$  in calcite was kinetically controlled and proportional to the rate of crystal growth of calcite  $v$  following the equation:

$$D = a + b v$$

where  $a$  and  $b$  are constants equal to  $6.16 \cdot 10^{-6}$  and  $3.941 \cdot 10^{-6}$ , respectively, and  $v$  is given in  $\text{mg min}^{-1} \text{ g}^{-1}$  of seed. These workers pointed out also that  $\text{SO}_4^{2-}$  in solid solutions significantly affected the solubility of calcite. The solid-solution showed a solubility minimum at about 0.5 mole %  $\text{SO}_4^{2-}$ . The solubility then rapidly increased and was the same as that of aragonite at 3 mole %  $\text{SO}_4^{2-}$ .

### 3.2.3. Phosphate

This trace component has been found to be an extremely strong inhibitor of carbonate reaction kinetics, even at micromolar concentrations (Morse, 1983). Brooks *et al.* (1950) showed that the growth of calcium carbonate spherulitic seed crystals from highly supersaturated solutions in the presence of sodium phosphate (consisting of a mixture of polymetaphosphate and polyphosphate) at a concentration of 25 ppm was completely inhibited. Measurement of the phosphate concentration revealed that a large percentage of the additive originally in solution had adsorbed onto the seed crystals. Miura *et al.* (1963) examined the effect of several phosphate anions on the rate of spontaneous precipitation of calcium carbonate from supersaturated solutions and found that a phosphate concentration equal to only 1/1000 that of calcium in solution prevented the spontaneous precipitation of calcium carbonate. They concluded that surface adsorption was the major factor in the mechanism of phosphate inhibition of calcium carbonate crystal growth.

Griffin and Jurinak (1973) found that the processes of adsorption and heterogeneous nucleation were inseparable when describing phosphate interaction with calcite in  $\text{H}_2\text{O}-\text{CO}_2$  system. They showed that adsorption isotherms of phosphate on calcite (at 0, 22 and 31 °C and at pH 8.4) could be described by a two-region Langmuir isotherm equation. The break in the slope of the Langmuir plot, at a P concentration value around 0.6 ppm, was found to correspond closely to the division between hydroxylapatite and octocalcium phosphate stability. At high Ca/P ratios, the formation of hydroxylapatite nuclei was encouraged while at lower ratios, octocalcium phosphate was nucleated. Comparison of monolayer capacities with the total surface area of the calcite indicated that only approximately 5% of the total surface was covered with phosphate ions. In brief, the process could be visualized by an initial adsorption of phosphate on a limited



number of specific surface sites. As adsorption proceeded, site coverage increased to the extent that lateral interaction occurred between the adsorbed ions. Lateral interaction produced doublets, triplets, and eventually surface clusters of phosphate ions. These clusters served as centers (heteronuclei) from which spontaneous calcium phosphate crystal growth could occur.

Reddy and Nanchollas (1973) found that the addition of several phosphonic acid derivatives to a supersaturated calcium carbonate solution at 25°C greatly reduced the rate of growth of calcite seed crystals at 25°C. The rate constant of the parabolic law used by the authors was decreased by a factor close to 200 (values from  $10^{-10.12}$  to  $10^{-12.42}$  mol s<sup>-1</sup> cm<sup>-2</sup>) when phosphonate concentrations varied from 0 to  $5.8 \cdot 10^{-6}$  M in NaHCO<sub>3</sub> solutions with a total calcium concentration value of about  $10^{-4}$  M and pH<sub>initial</sub> > 9. It was seen that a Langmuir isotherm satisfactorily described the marked inhibiting effect of the phosphonates in terms of a monomolecular blocking layer of foreign ions at the growth sites on the crystal surface. Reddy (1977) studied the influence of phosphate and glycerophosphate on calcite seeded growth at 25°C. Crystallization rate constants were reduced to half of their value in pure solutions by a glycerophosphate concentration of  $1.6 \cdot 10^{-5}$  M or an orthophosphate concentration of  $2 \cdot 10^{-6}$  M. The relation between the additive ion concentration and rate was consistent with Langmuir adsorption of phosphate and a site blocking nuclei.

Berner *et al.* (1978) demonstrated that dissolved orthophosphate inhibited the seeded precipitation of aragonite from artificial seawater at 25°C. The  $v/v_0$  rate ratio was reduced from 0.6 to 0.04 when phosphate concentrations varied from  $1.7$  to  $6.7 \cdot 10^{-6}$  M. DeKanel and Morse (1978) made an extensive study of the interaction of phosphate with calcite, aragonite and biogenic Mg-calcite surfaces. The results indicated that at low phosphate concentrations, the rate of phosphate uptake on the mineral surfaces could be described by the Elovich equation. This model was based on the uptake of phosphate at sites of increasing activation energy for chemisorption as the extent of surface coverage increased. These workers also proposed that either the HPO<sub>4</sub><sup>2-</sup> or PO<sub>4</sub><sup>3-</sup> ion was the reacting species.

House and Donaldson (1985) reported the adsorption of inorganic phosphate (concentrations <  $20 \cdot 10^{-6}$  M) from dilute aqueous solutions in equilibrium with two crystalline samples of calcite over a range of temperatures from 5 to 35°C and pH of 7 to 9.5. A simple two-component model of adsorption involving PO<sub>4</sub><sup>3-</sup> or CaPO<sub>4</sub><sup>-</sup> and HPO<sub>4</sub><sup>2-</sup> or CaHPO<sub>4</sub><sup>0</sup> described the isotherms and their pH dependence. This model was applied to the coprecipitation of phosphate with calcite at various precipitation rates and in a temperature range of 5 to 25°C. The results indicated that only a fraction of the total adsorbed phosphorus was incorporated into the growing crystals and that the adsorption of this fraction was rapid enough that the amount of phosphorus coprecipitated was independent of the adsorption rate. It was postulated that active surface sites (kink sites) were able to allow the incorporation of phosphorus into the

solid lattice. There was no evidence for a control of the solution composition by the formation of a distinct calcium phosphate phase.

Mucci (1986) determined the quantitative influence of orthophosphate ions on the growth kinetics and composition of magnesian calcite overgrowths, precipitated from artificial seawater ( $S = 35\%$ ). Experimental conditions were:  $T=25^\circ\text{C}$ ,  $p\text{CO}_2 = 0.032\%$  and  $0.31\%$ ,  $\text{pH} = 7.5\text{--}8.6$ ,  $\Omega$  ranging from 1.8 to 141, and concentrations of  $\text{Na}_2\text{HPO}_4$  ranging from 0 to  $500 \cdot 10^{-6}$  M. Mucci (1986) did not examine the amount of phosphate incorporated in the magnesian calcites but found that the amount of phosphate removed from the solution was approximately proportional to the amount of carbonate precipitated. No distinct phosphate mineral phase could be detected in the X-ray diffraction spectra.

The observed influence of  $p\text{CO}_2$  on the precipitation-inhibition effectiveness of orthophosphate ions led to the finding that the  $\text{PO}_4^{3-}$  ion concentration, rather than the reactive concentration, was the governing factor in determining the rate of magnesian calcite precipitation at a given  $\Omega$ . The precipitation rate data were fitted to an empirical law similar to that used by Mucci and Morse (1983). It was found that the calculated reaction orders  $n$  for the precipitation of calcite in each one of the seawater solutions were close to 3.40 (instead of 2.8 in phosphate-free seawater) and that the growth rate constant  $k$  was decreased by a factor around 200, when  $[\text{PO}_4^{3-}]$  concentrations increased from 1.8 to  $47.9 \cdot 10^{-6}$  M. A regression analysis of the data indicated that the precipitation-inhibition effectiveness of orthophosphate was a function of the  $\text{PO}_4^{3-}$  concentration and increased as  $\Omega$  approached unity. A linear log-log relationship between the rate constant and the  $\text{PO}_4^{3-}$  concentration suggested a strong interaction between the  $\text{PO}_4^{3-}$  and the energetically heterogeneous surface of the growing magnesian calcite (holes, kinks and steps). All the precipitation rate data measured in the presence of orthophosphate ions were fitted to an appropriate mathematical expression, expressed as follows:

$$\log v = -23.32 - 1.45 \log ([\text{PO}_4^{3-}]) + 3.17 \log (\Omega - 1)$$

where  $v$  was expressed in  $\text{mole cm}^{-2} \text{s}^{-1}$  and  $[\text{PO}_4^{3-}]$  is in  $\text{mole l}^{-1}$ . This expression was valid in seawater ( $S = 35\%$ ) for at least the following set of conditions:  $10^{-6} \text{ M} < [\text{PO}_4^{3-}] < 10^{-4} \text{ M}$ ,  $0.032\% < p\text{CO}_2 < 0.31\%$  and  $1.8 < \Omega < \text{onset of spontaneous nucleation}$ .

These results were consistent with those of DeKanel and Morse (1978), who showed that their data could only be fitted by the Elovichian chemisorption theory but not with those of Reddy (1977), who observed that a Langmuir isotherm satisfactorily described the inhibitory effect of phosphate ions on calcite growth from a  $\text{CaCl}_2\text{--NaHCO}_3\text{--Na}_2\text{CO}_3$  low ionic strength solution. This discrepancy could reflect the different adsorption behavior of phosphate ions on the surface of calcite in seawater and in low ionic strength magnesium-free solutions.

Using a Scanning Force Microscopy technique, Dove and Hochella (1993) described two inhibition mechanisms on calcite precipitation by orthophosphate ions at 25°C, 0.96 atm pCO<sub>2</sub> and pH 6.0. Phosphate (0.6 and 1 10<sup>-5</sup> M PO<sub>4</sub>) introduced during the nucleation stage (initial stage) resulted in the formation of nuclei with amorphous shapes. Phosphate introduced during layer growth (later stage) disrupted the relatively straight steps produced during PO<sub>4</sub>-free growth to form jagged steps. Both of the phosphate-calcite surface interactions were consistent with mechanisms proposed in previous studies:

- surface nucleation of amorphous calcium phosphate phases or specific sorption of phosphate which blocks growth of the calcium carbonate nuclei;
- sorption of phosphate ions at surface heterogeneities such as kinks, steps or holes. Although rates of calcite precipitation by SFM were not measured, it was again observed that kink-type inhibitors were most effective at conditions near equilibrium calcite growth.

### **3.2.4. Manganese and iron**

The influence of heavy metals on calcium carbonate reaction rates has not been extensively studied (Morse, 1983). However, substitution of Mn<sup>2+</sup> and Fe<sup>2+</sup> for Ca<sup>2+</sup> in diagenetic calcite cements plays an important role in the chemical environment of cementation. Relatively high concentrations of these cations in some diagenetic fluids is reflected in Mn<sup>2+</sup> and Fe<sup>2+</sup> substitution that can exceed several mol %. Experimental studies (Dromgoole and Walter, 1990a) have indicated that incorporation of these cations was strongly dependent on calcite growth kinetics and that the presence of these ions affected the rate of calcite growth.

Experimental data of Meyer (1984) and Mucci (1988) indicated that Mn<sup>2+</sup> influenced calcite growth rates, but both inhibition and catalysis were observed. Meyer (1984) investigated the effect of Mn<sup>2+</sup> over a limited concentration range on seeded calcite growth rates in low ionic strength CaCl<sub>2</sub>-NaHCO<sub>3</sub> solutions (~ 0.001 M CaCl<sub>2</sub>). Mn<sup>2+</sup> inhibited calcite growth, and the degree of inhibition increased with increasing Mn<sup>2+</sup> concentration. A factor of 5-10 decrease in calcite precipitation rate occurred at 10<sup>-5</sup> M (~ 0.5 ppm), the highest solution Mn<sup>2+</sup> concentration investigated. These experiments suggested that Mn<sup>2+</sup>, and also other metals such as Fe<sup>2+</sup>, significantly reduced calcite precipitation rates even at < 1 ppm levels. This level is well below the concentration of Mg<sup>2+</sup>, SO<sub>4</sub><sup>2-</sup> or PO<sub>4</sub><sup>3-</sup> required to produce an equivalent degree of inhibition.

Mucci (1988) examined the effects of varying Mn<sup>2+</sup> concentration and the degree of calcite supersaturation on seeded calcite growth rate in artificial seawater and obtained results significantly different from those of Meyer (1984). Although the used Mn<sup>2+</sup> concentrations (1-28 ppm) were much higher, growth rates for Ca-Mg-Mn-calcite solid solutions increased rather than decreased. Moreover, for a given degree of solution supersaturation with respect to calcite, growth rates increased with increasing Mn<sup>2+</sup>

concentration. Mucci (1988) also observed proportionally larger increases in growth rate for a given  $\text{Mn}^{2+}$  concentration at lower saturation states while decreasing the degree of solution supersaturation usually results in lower precipitation rates and more pronounced effects of calcite growth inhibitors.

Direct comparison of results from these investigations is complicated by differences in experimental conditions and solution compositions. Although the cumulative effect of multiple inhibitors on calcite growth are generally additive (Mucci, 1986; Burton, 1988), adsorption of  $\text{Mn}^{2+}$  onto calcite was reduced, probably as a result of site competition between  $\text{Mg}^{2+}$  and  $\text{Mn}^{2+}$  in seawater and solutions with similar  $\text{Mg}^{2+}/\text{Ca}^{2+}$  ratios ( $\sim 5$ ), lacking other components such as  $\text{SO}_4^{2-}$ ,  $\text{PO}_4^{3-}$  (Franklin and Morse, 1983). In order to explain the results from the experiments of Mucci (1988), Dromgoole and Walter (1990b) suggested an interaction between  $\text{Mn}^{2+}$  and  $\text{Mg}^{2+}$  which, because of the high  $\text{Mg}^{2+}/\text{Ca}^{2+}$  ratio, is a stronger inhibitor of calcite growth in seawater. Perhaps the competition by  $\text{Mn}^{2+}$  for adsorption on the active crystal growth sites displaced  $\text{Mg}^{2+}$ , reducing the otherwise stronger effect that  $\text{Mg}^{2+}$  could have on calcite growth. These workers concluded that the strongest inhibition effects of calcite growth by  $\text{Mn}^{2+}$  occurred in solutions where  $\text{Mg}^{2+}/\text{Ca}^{2+}$  ratios were low ( $< 1$ ) and  $\text{Mg}^{2+}$  had little effect on calcite precipitation rate. They pointed out that fluids with low  $\text{Mg}^{2+}/\text{Ca}^{2+}$  ratios were often encountered in sedimentary basin formation waters.

Dromgoole and Walter (1990b) reported similar degrees of calcite precipitation inhibition in  $\text{CaCl}_2$  solutions as those obtained in the experiments of Meyer (1984) but using much higher  $\text{Mn}^{2+}$  concentrations in solution. The strong dependence of inhibition on  $\text{Mn}^{2+}/\text{Ca}^{2+}$  ratio rather than absolute metal concentration accounted for most of the discrepancy. These workers noticed that variations in temperature (10, 25 and  $50^\circ\text{C}$ ),  $\text{pCO}_2$  (0.097, 0.099, 0.88, 0.97 atm) or  $\text{Mn}^{2+}$  and  $\text{Ca}^{2+}$  concentrations, at a fixed  $\text{Mn}^{2+}/\text{Ca}^{2+}$  ratio (0.01), had little effect on the degree of inhibition observed in comparison to the influence of the  $\text{Mn}^{2+}/\text{Ca}^{2+}$  ratio and the calcite saturation state. Using an empirical law similar to that of Mucci and Morse (1983), they found that the calculated reaction orders  $n$  for the precipitation of calcite varied from 1.34 to 2.05 instead of 1.1-1.3 in manganese-free solutions. When the  $[\text{Mn}^{2+}]/[\text{Ca}^{2+}]$  was increased from 0.001 to 0.05, the growth rate constant  $k$  at  $25^\circ\text{C}$  was decreased by a factor of about 30. Results obtained by Dromgoole and Walter (1990b) are reported in table 8.

In this study, rhodochrosite was not detected by X-ray diffraction. Only  $\text{CaCO}_3$ - $\text{MnCO}_3$  solid solutions were found. The degree of inhibition was related to the mol %  $\text{MnCO}_3$  in the calcite overgrowth suggesting that the inhibitory effects of  $\text{Mn}^{2+}$  on calcite growth kinetics depended on  $\text{Mn}^{2+}$  adsorption and uptake in the calcite crystal lattice. It was also deduced that calcites containing more than 2 mol %  $\text{MnCO}_3$  likely experienced significant inhibition during precipitation. At a calcite saturation state of 3, Dromgoole and Walter (1990b) found a linear relationship between  $\log ((v_0-v)/v_0)$  vs.  $\log ([\text{Mn}^{2+}]/[\text{Ca}^{2+}])$ , derived from a Langmuir-type adsorption isotherm. As for phosphate ions, inhibition by  $\text{Mn}^{2+}$  appeared greater at lower calcite saturation state. A qualitative explanation for this behavior, considering kinetic vs. equilibrium controls on

the adsorption of inhibitor ions at active growth sites, was that slower precipitation rates allowed the inhibitor ion to occupy a greater proportion of the energetically favorable growth sites. The adsorption processes seemed to be predominant but other processes also might influence inhibition or incorporation of  $\text{Mn}^{2+}$ . Differences in solubility could in part explain the lower precipitation rates if Mn-calcite solid solutions were more soluble than calcite. Probably of minor importance when the extent of solid solution was less than 1 mol %, this effect might be significant for more Mn-rich solids precipitated from higher  $[\text{Mn}^{2+}]/[\text{Ca}^{2+}]$  solutions but could not be accurately evaluated because the solubility of Mn-calcites was unknown.

### **3.2.5. Organic acids**

Considerable work has been done on the influence of organic acids on carbonate precipitation, and important effects have been observed (Morse, 1983). The analysis of a large number of formation waters from oil reservoirs has shown that carboxylic acids are the major dissolved organic acids in the water, with acetic acid dominant (Barth, 1991). For this reason only studies concerned with the effect of acetic acids were considered in this review.

Kitano and Hood (1965) were among the first to investigate the influence of organic material on the polymorphic crystallization of calcium carbonate. They used an homogeneous precipitation procedure. The general trend observed was that the organic matter influence was roughly proportional to the association constant of the organic compound with  $\text{Ca}^{2+}$ . Three classes of organic inhibitors were determined: strong (citrate, malate, pyruvate, glycylglycerine, glycogen), moderate (arginine, glutamate, glycine, glycoprotein, succinate, taurine and chondroitin sulphate), and weak (galactose, dextrose, alanine and acetate).

The most complete study of inhibition of calcium carbonate precipitation by organic matter was the carried out by Berner *et al.* (1978) in artificial seawater at 25°C and 1 atm. Their primary concern was lack of carbonate precipitation from supersaturated seawater. Among the organic acids studied, they found no aliphatic polycarboxylic acid as strong inhibitors.

## Conclusions

Determination of kinetic data for carbonate mineral growth is a very laborious work because of the many factors involved, including temperature,  $p\text{CO}_2$ , pH, solution ionic composition, saturation state, reacting surface area, presence of inhibiting substances and solution hydrodynamics. At temperatures  $< 150\text{-}200^\circ\text{C}$  and  $\text{pH} > 4\text{-}5$ , surface-controlled precipitation seems to be predominant in experimental studies. However, in natural systems, mass transport by molecular diffusion from the solid into the bulk solution and vice versa can have some influence on precipitation rate.

Calcite is by far the most studied carbonate mineral from a kinetic standpoint. Very little kinetic data are available for the other carbonate minerals. This is not a major limitation to the QC-SCALE project because carbonate scales in oil field wells are mostly calcite. In both laboratory and field studies, it was shown that a certain critical degree of super-saturation ( $\Omega > 5\text{-}10$ ) had to be achieved to allow calcite nucleation at relatively low temperatures ( $< 60^\circ\text{C}$ ). Assuming that the spontaneous crystallization time for calcium carbonate formation in the oil field wells is short relative to the time necessary for the precipitating mineral to grow, the kinetic data obtained from calcite seeded precipitation experiments, which describe crystal growth and are the most reliable experiments, are also the most adapted for modelling such systems.

Many kinetic laws have been developed to describe calcite precipitation rate in experimental studies but most of these laws are only applicable in very specific conditions of temperature,  $p\text{CO}_2$ , solution ionic compositions, calcite saturation state. Tests of the affinity-based models carried out by Shiraki and Brantley (1995) revealed that none of these models accurately predicted dissolution and growth over the full range of the degree of saturation.

Practically, the mechanistic model presented by Plummer *et al.* (1978) and modified by several investigators (Busenberg and Plummer, 1986; Chou *et al.*, 1989; Talman *et al.*, 1990) for calcite dissolution-precipitation in dilute solutions is the only model that applies over a wide range of solution pH values,  $p\text{CO}_2$  and temperatures. However, its use at high temperature and pressure ( $100^\circ\text{C}$  and 100 bar) may be limited (Shiraki and Brantley, 1995). Moreover, this model does not take into account the influence of complex solutions (high salinity, presence of inhibitor species, etc.). Applying the model of Plummer *et al.* (1978) for calculating calcite precipitation rates in natural systems at fast flow, low salinity and low temperature conditions, after outgassing of  $\text{CO}_2$  in spring-fed streams, reasonable rate values are estimated in reducing the rates calculated by a factor about ten (Dreybrodt *et al.*, 1992; Zaihua *et al.*, 1995). This factor is introduced to correct the influence of molecular diffusion (diffusion boundary layer model). The precipitation rates obtained for deep-sea sediments are much lower than those calculated using the model of Plummer *et al.* (1978). This difference can be partly explained by the fact that calcite precipitation in deep-sea sediments occurs at near

equilibrium conditions. Under such conditions, the rate-controlling mechanism seems to be very slow, even at high temperature, and is apparently different from the precipitation mechanisms occurring under conditions far from equilibrium. At this point calcite precipitation rates obtained from deep-sea sediments remain uncertain and need to be confirmed. The precipitation rates obtained from spring-fed streams may be more readily applicable to oil field conditions, which are typically far from equilibrium.

Oil field formation waters commonly have low pH, high salinity ( $> 0.5$  m), high  $p\text{CO}_2$  and high temperature (100-150°C). Under such conditions there is no reliable and general kinetic law available in literature to estimate calcite scaling rate. In fact, very few studies have been carried out in these experimental conditions. Two possibilities are recommended for modelling:

- use of an adapted model of Plummer *et al.* (1978);
- use of specific laws similar to those presented in this work. The selection will have to be made by choosing the rate law obtained from the closest experimental conditions to those required by the study, such as temperature,  $p\text{CO}_2$  value, water composition (similar to seawater, low Mg and  $\text{SO}_4$  concentrations, presence of an inhibitor etc.). In many cases, extrapolations will have to be performed.

We will be able to compare the results obtained from these models. However, these results would be more accurate if they might be fitted to field calcite precipitation rate measurements.

## References

- Adamson, A.W., 1967. Physical Chemistry of Surfaces. Interscience Publishers, New York, 747p.
- Arakaki, T., and Mucci, A., 1995. A continuous and mechanistic representation of calcite reaction-controlled kinetics in dilute solutions at 25°C and 1 atm total pressure. *Aquatic Geochem.*, 1, 105-130.
- Aagaard, P., and Helgeson, H.C., 1982. Thermodynamic and kinetic constraints on reaction rates among minerals and aqueous solutions. I. Theoretical considerations. *Amer. J. Sci.*, 282, 237-285.
- Badiozamani, K., Mackenzie, F.T., and Thorstenson, D.C., 1977. Experimental carbonate cementation: salinity, temperature and vadose-phreatic effects. *J. Sediment. Petrol.*, 47, 529-542.
- Baker, P.A., and Kastner, M., 1981. Constraints on the formation of sedimentary dolomite. *Science*, 213, 214-216.
- Baker, P.A., Gieskes, J.M., and Elderfield, H., 1982. Diagenesis of carbonates in deep-sea sediments - evidence from Sr/Ca ratios and interstitial dissolved  $\text{Sr}^{2+}$  data. *J. Sediment. Petrol.*, 52, 71-82.
- Barth, T., 1991. Organic acids and inorganic ions in waters from petroleum reservoirs, norwegian continental shelf: A multivariate statistical analysis and comparison with American reservoir formation waters. *Appl. Geochem.*, 6, 1-15.
- Beck, J.W., Berndt, M.E., and Seyfried W.E., Jr, 1992. Application of isotopic doping techniques to evaluation of reaction kinetics and fluid/mineral distribution coefficients: An experimental study of calcite at elevated temperatures and pressures. *Chem. Geol.*, 97, 125-144.
- Bennema, P., and Gilmer, G.H., 1973. Kinetics of crystal growth. In "Crystal Growth: An Introduction" (Ed. P. Hartman), 263-327. North-Holland Publishing.
- Berelson, W.M., Hammond, D.E., and Cutter, G.A., 1990. *In situ* measurements of calcium carbonate dissolution rates in deep-sea sediments. *Geochim. Cosmochim. Acta*, 54, 3013-3020.
- Berner, R.A., 1975. The role of magnesium in the crystal growth of calcite and aragonite from seawater. *Geochim. Cosmochim. Acta*, 39, 489-504.
- Berner, R.A., 1980. Early Diagenesis. Princeton Univ. Press, Princeton, New Jersey, 241 p.
- Berner, R.A., and Morse, J.W., 1974. Dissolution kinetics of calcium carbonate in sea water: IV. Theory of calcite dissolution. *Amer. J. Sci.*, 274, 108-134.



- Berner, R.A., Westrich, J.T., Graber, R., Smith, J., and Martens, C., 1978. Inhibition of aragonite precipitation from supersaturated seawater: A laboratory and field study. *Am. J. Sci.*, 278, 816-837.
- Bischoff, J.L., 1968. Kinetics of calcite nucleation: Magnesium ion inhibition and ionic strength catalysis. *J. Geophys. Res.*, 73, 3313-3322.
- Blum, A.E., and Lasaga, A.C., 1987. Monte Carlo simulations of surface reaction rate laws. In "Aquatic Surface Chemistry" (ed. W. Stumm), 255-292.
- Brady, P.V., Krumhansl, J.L., and Papenguth, H.W., 1996. Surface complexation clues to dolomite growth. *Geochim. Cosmochim. Acta*, 60, 727-731.
- Brooks, R., Clark, L.M., and Thurston, E.F., 1950. Calcium carbonate and its hydrates. *Phil. Trans. Roy. Soc. London*, A243, 145-167.
- Buhmann, D., and Dreybrodt, W., 1985. The kinetics of calcite dissolution and precipitation in geologically relevant situations of karst areas. 2. Closed system. *Chem. Geol.*, 53, 109-124.
- Burton, E.A., 1988. Laboratory investigation of the effects of seawater chemistry on carbonate mineralogy. Ph.D. dissertation, Washington University, St Louis Mo.
- Burton, E.A., and Walter, L.M., 1987. Relative precipitation rates of aragonite and Mg calcite from seawater: temperature or carbonate ion control? *Geology*, 15, 111-114.
- Burton, E.A., and Walter, L.M., 1990. The role of pH in phosphate inhibition of calcite and aragonite precipitation rates in seawater. *Geochim. Cosmochim. Acta*, 54, 797-808.
- Burton, W.K., Cabrera, N., and Frank, F.C., 1951. The growth of crystals and the equilibrium structure of their surfaces. *Phil. Trans. Roy. Soc. London*, 243, 299-358.
- Busenberg, E., and Plummer, L.N., 1982. The kinetics of dissolution of dolomite in CO<sub>2</sub>-H<sub>2</sub>O systems at 1.5 to 65°C and 0 to 1 atm P<sub>CO2</sub>. *Amer. J. Sci.*, 282, 45-78.
- Busenberg, E., and Plummer, L.N., 1985. Kinetic and thermodynamic factors controlling the distribution of SO<sub>4</sub><sup>2-</sup> and Na<sup>+</sup> in calcites and aragonites. *Geochim. Cosmochim. Acta*, 49, 713-725.
- Busenberg, E., and Plummer, L.N., 1986. A comparative study of the dissolution and crystal growth kinetics of calcite and aragonite. *USGS Bull.*, 1578, 139-168.
- Chen, Y., Wang, X., Sha, Q., and Zhang, N., 1979. Experimental studies on the system of Ca<sup>2+</sup> - Mg<sup>2+</sup> - HCO<sub>3</sub><sup>-</sup> - H<sub>2</sub>O at room temperatures and pressure. *Sci. Geol. Sin.*, 1, 22-36 (in chinese, with english abstract)
- Chou, L., Garrels, R.M., and Wollast, R., 1989. Comparative study of the kinetics and mechanisms of dissolution of carbonate minerals. *Chem. Geol.*, 78, 269-282.
- Compton, R.G., and Pritchard, K.L., 1990. The dissolution of calcite at pH > 7: Kinetics and mechanism. *Phil. Trans. Roy. Soc. London*, A330, 47-70.

- Dandurand, J.L., Gout, R., Hoefs, J., Menschel, G., Shott, J., and Usdowski, E., 1982. Kinetically controlled variations of major components and carbon and oxygen isotopes in a calcite-precipitating spring. *Chem. Geol.*, 36, 299-315.
- Davies, C.W., and Jones, A.L., 1955. The precipitation of silver chloride from aqueous solutions. Part 2, Kinetics of growth of seed crystals. *Trans. Faraday Soc.*, 51, 812-817.
- DeKanel, J., and Morse, J.W., 1978. The chemistry of orthophosphate uptake from seawater onto calcite and aragonite. *Geochim. Cosmochim. Acta*, 42, 1334-1340.
- Dove, P.M., and Hochella, M.F., 1993. Calcite precipitation mechanisms and inhibition by orthophosphate: In situ observations by Scanning Force Microscopy. *Geochim. Cosmochim. Acta*, 57, 705-714.
- Dreybrodt, W., and Buhmann, D., 1991. A mass transfer model for dissolution and precipitation of calcite from solutions in turbulent motion. *Chem. Geol.*, 90, 107-122.
- Dreybrodt, W., Buhmann, D., Michaelis, J., and Usdowski, E., 1992. Geochemically controlled calcite precipitation by CO<sub>2</sub> outgassing: Field measurements of precipitation rates in comparison to theoretical predictions. *Chem. Geol.*, 97, 285-294.
- Dromgoole, E.L., and Walter, L.M., 1990a. Iron and manganese incorporation into calcite: Effects of precipitation rate, temperature, and solution composition. *Chem. Geol.*, 81, 311-336.
- Dromgoole, E.L., and Walter, L.M., 1990b. Inhibition of calcite growth rates by Mn<sup>2+</sup> in CaCl<sub>2</sub> solutions at 10, 25, and 50°C. *Geochim. Cosmochim. Acta*, 54, 2991-3000.
- Dymond, J., and Lyle, M., 1985. Flux comparisons between sediments and sediments traps in the eastern tropical Pacific: Implications for atmospheric CO<sub>2</sub> variations during the Pleistocene. *Limnol. Oceanogr.*, 30, 699-712.
- Faux, R.F., Busenberg, E., and Plummer, L.N., 1986. The dissolution kinetics of magnesite from 25°-85°C and pH's of 0 to 10 at atmospheric P<sub>CO2</sub>. *Geol. Soc. Am., Abstr. Prog.*, 18 (6), 599.
- Franklin, M.L., and Morse, J.W., 1983. The interaction of manganese (II) with the surface of calcite in dilute solutions and seawater. *Mar. Chem.*, 12, 241-254.
- Gratz, A.J., Manne, S., and Hansma, P., 1990. Atomic force microscopy of atomic-scale ledges and etch pits formed during dissolution of quartz. *Science*, 251, 1343-1346.
- Gratz, A.J., Hillner, P.E., and Hansma, P.K., 1993. Step dynamics and spiral growth on calcite. *Geochim. Cosmochim. Acta*, 57, 491-495.
- Griffin, R.A., and Jurinak, J.J., 1973. The interaction of phosphate with calcite. *Soil Sci. Soc. Amer. Proc.*, 37, 847-850.

- Hardie, L.A., 1987. Dolomitization. A critical review of some current views. *J. Sediment. Petrol.*, 57, 166-183.
- Herman, J.S., and Lorah, M.M., 1988. Calcite precipitation rates in the field: Measurement and prediction for a travertine-depositing stream. *Geochim. Cosmochim. Acta*, 52, 2347-2355.
- Herman, J.S., and White, W.B., 1985. Dissolution kinetics of dolomite: Effects of lithology and fluid flow velocity. *Geochim. Cosmochim. Acta*, 49, 2017-2026.
- Higuchi, M., Takeuchi, A., and Kodaira, K., 1988. Hydrothermal growth of calcite single crystals from  $\text{H}_2\text{O}-\text{CO}_2-\text{CaCO}_3$  system. *J. Cryst. Growth*, 92, 341-343.
- Hirano, S., and Kikuta, K., 1985. Hydrothermal crystal growth of calcite in NaCl and KCl solutions. *Chem. Lett.*, 1613-1616.
- Hirano, S., and Kikuta, K., 1987. Hydrothermal growth of calcite in NaCl solution. *Bull. Chem. Soc. Japan*, 60, 1109-1112.
- House, W.A., 1981. Kinetics of crystallisation of calcite from calcium bicarbonate solutions. *J. Chem. Soc. Faraday Transp.*, 77, 341-359.
- House, W.A., and Donaldson, L., 1986. Adsorption and coprecipitation of phosphate on calcite. *J. Colloid Interface Sci.*, 112, 309-324.
- Inskeep, W.P., and Bloom, P.R., 1985. An evaluation of rate equations for calcite precipitation kinetics at  $P_{\text{CO}_2}$  less than 0.01 atm and pH greater than 8. *Geochim. Cosmochim. Acta*, 49, 2165-2180.
- Jacobson, R.L., and Usdowski, E., 1975. Geochemical controls on a calcite precipitating spring. *Contrib. Mineral. Petrol.*, 51, 65-74.
- Kazmierczak, T.F., Tomson, M.B., and Nanchollas, G.H., 1982. Crystal growth of calcium carbonate: A controlled composition kinetic study. *J. Phys. Chem.*, 86, 103-107.
- Katz, A., 1973. The interaction of magnesium with calcite during crystal growth at 25-90°C and one atmosphere. *Geochim. Cosmochim. Acta*, 37, 1563-1586.
- Katz, A., Sass, E., Starinsky, A., and Holland, H.D., 1972. Strontium behavior in the aragonite-calcite transformation: An experimental study at 40-98°C. *Geochim. Cosmochim. Acta*, 36, 481-496.
- Katz, A., and Matthews, A., 1977. The dolomitization of  $\text{CaCO}_3$ : an experimental study at 252-295°C. *Geochim. Cosmochim. Acta*, 41, 297-308.
- Keir, R.S., 1980. The dissolution kinetics of biogenic calcium carbonates in seawater. *Geochim. Cosmochim. Acta*, 44, 241-252.
- Kitano, Y., 1962. The behavior of various inorganic ions in the separation of calcium carbonate from a bicarbonate solution. *Bull. Chem. Soc. Jap.*, 35, 1973-1980.
- Kitano, Y., and Hood, D.W., 1965. The influence of organic material on the polymorphic crystallization of calcium carbonate. *Geochim. Cosmochim. Acta*, 29, 29-41.

- Kitano, Y., Okumura, M., and Idogaki, M., 1975. Incorporation of sodium, chloride and sulfate with calcium carbonate. *Geochem. J.*, 84, 75-84.
- Lasaga, A.C., 1981. Transition state theory. In "Kinetics of Geochemical Processes" (ed. A.C. Lasaga and R.J. Kirkpatrick). *Rev. Mineral.*, 135-169.
- Lasaga, A.C., 1984. Chemical kinetics of water-rock interaction. *Geophys. J.*, 89, 4009-4025.
- Lippmann, F., 1973. *Sedimentary carbonate minerals*. Springer-Verlag, New York, 229p.
- Lorens, R.N., 1981. Sr, Cd, Mn, and Co distribution coefficients in calcite as a function of calcite precipitation rate. *Geochim. Cosmochim. Acta*, 45, 553-561.
- Lund, K., Fogler, H.S., and McCune, C.C., 1973. Acidization. I. The dissolution of dolomite in hydrochloric acid. *Chem. Eng. Sci.*, 28, 691-700.
- MacInnis, I.N., and Brantley, S.L., 1991. The role of dislocations and surface morphology in calcite dissolution. *Geochim. Cosmochim. Acta*, 56, 1113-1126.
- MacInnis, I.N., and Brantley, S.L., 1993. Development of etch pit size distributions on dissolving minerals. *Chem. Geol.*, 105, 31-49.
- Meyer, H.J., 1984. The influence of impurities on the growth rate of calcite. *J. Crystal Growth*, 66, 639-646.
- Miura, M., Otani, S., Abe, Y., and Fukumara, C., 1963. *Bull. Chem. Soc. Japan*, 36, 1091.
- Morrow, D.W., and Ricketts, B.D., 1988. Experimental investigation of sulphate inhibition of dolomite and its mineral analogues. In "Sedimentology and Geochemistry of Dolostones" (Shukla, V., and Baker, P.A., Eds). *SEPM Special Publication*, 43, 5-38.
- Morse, J.W., 1978. Dissolution kinetics of calcium carbonate in sea water. VI. The near-equilibrium dissolution kinetic of calcium carbonate-rich deep sea sediments. *Amer. J. Sci.*, 278, 344-353.
- Morse, J.W., 1983. The kinetics of calcium carbonate dissolution and precipitation. In "Carbonates: Mineralogy and Chemistry" (ed. R.J. Reeder); *Rev. Mineral.*, 11, 227-264.
- Mucci, A., 1986. Growth kinetics and composition of magnesian calcite overgrowths precipitated from seawater: Quantitative influence of orthophosphate ions. *Geochim. Cosmochim. Acta*, 50, 2255-2265.
- Mucci, A., 1988. Manganese uptake during calcite precipitation from seawater conditions leading to the formation of pseudokutnahorite. *Geochim. Cosmochim. Acta*, 52, 1859-1868.
- Mucci, A., and Morse, J.W., 1983. The incorporation of  $Mg^{2+}$  and  $Sr^{2+}$  into calcite overgrowths: Influences of growth rate and solution composition. *Geochim. Cosmochim. Acta*, 47, 217-233.

- Mucci, A., Canuel, R., and Zhong, S., 1989. The solubility of calcite and aragonite in sulfate-free seawater and seeded growth kinetics and composition of precipitates at 25°C. *Chem. Geol.*, 74, 309-329.
- Mullin, J.W., 1972. *Crystallization*. CRC Press.
- Murphy, W.M., Oelkers, E.H., and Lichtner, P.C., 1988. Coupled surface reaction and diffusion of aqueous species in the control of mineral dissolution and growth rates in geochemical processes. *G.S.A. Abstracts with Programs* Fall 1988, p. A40.
- Nagy, K.L., 1988. The solubility of calcite in sodium-chloride and sodium-calcium-chloride brines. Ph-D Thesis, Graduate College Station of Texas A & M University, 232 p.
- Nanchollas, G.H., and Reddy, M.M., 1971. The crystallization of calcium carbonate, II. Calcite growth mechanism. *J. Colloid Interface Sci.*, 37, 824-830.
- Nielsen, A.E., 1964. *Kinetics of precipitation*. Pergamon.
- Nielsen, A.E., 1983. Precipitates: formation, coprecipitation, and aging. In "Treatise on Analytical Chemistry" (ed. I.M. Kolthoff and P.J. Elving), 269-347, Wiley.
- Plummer, L.N., and Wigley, T.M.L., 1976. The dissolution of calcite in CO<sub>2</sub>-saturated solutions 25°C and 1 atmosphere total pressure. *Geochim. Cosmochim. Acta*, 40, 191-202.
- Peterson, M.N., 1966. Calcite: Rates of dissolution in a vertical profile in the Central Pacific. *Science*, 154, 1542-1544.
- Plummer, L.N., Wigley, T.M.L., and Parkhurst, D.L., 1978. The kinetics of calcite dissolution in CO<sub>2</sub>-water systems at 5 to 60°C and 0.0 to 1 atm CO<sub>2</sub>. *Amer. J. Sci.*, 278, 179-216.
- Plummer, L.N., Wigley, T.M.L., and Parkhurst, D.L., 1979. Critical review of the kinetics of calcite dissolution and precipitation. In "Chemical Modeling in aqueous systems; Amer. Chem. Soc. Symp., Ser. n° 93, 537-573.
- Pytkowicz, R.M., 1973. Calcium carbonate retention in supersaturated seawater. *Amer. J. Sci.*, 273, 515-522.
- Reddy, M.M., 1977. Crystallization of calcium carbonate in the presence of trace concentrations of phosphorus-containing anions. I. Inhibition by phosphate and glycerophosphate ions at pH 8.8 and 25°C. *J. Cryst. Growth*, 41, 287-295.
- Reddy, M.M., 1983. Characterization of calcite dissolution and precipitation using an improved experimental technique. *Sci. Geol. Mem.*, 71, 109-117.
- Reddy, M.M., and Nanchollas, G.H., 1971. The crystallization of calcium carbonate. I. Isotopic exchange and kinetics. *J. Colloid Interface Sci.*, 36, 166-172.
- Reddy, M.M., and Nanchollas, G.H., 1973. Calcite crystal growth inhibition by phosphonates. *Desalination*, 12, 61-73.

- Reddy, M.M., and Wang, K.K., 1980. Crystallization of calcium carbonate in the presence of metal ions. I. Inhibition by magnesium ion at pH 8.8 and 25°C. *J. Crystal Growth*, 50, 470-480.
- Reddy, M.M., and Gaillard, W.D., 1981. Kinetics of calcium carbonate (calcite)-seeded crystallisation: Influence of solid/solution ratio on the reaction rate constant. *J. Colloid Interface Sci.*, 80, 171-178.
- Reddy, M.M., Plummer, L.N., and Busenberg, E., 1981. Crystal growth of calcite from calcium bicarbonate solutions at constant PCO<sub>2</sub> and 25°C: A test of a calcite dissolution model. *Geochim. Cosmochim. Acta*, 45, 1281-1289.
- Rimstidt, J.D., and Dove, P.M., 1986. Mineral/solution reaction rates in a mixed flow reactor: wollastonite hydrolysis. *Geochim. Cosmochim. Acta*, 50, 2509-2516.
- Shiraki, R., and Brantley, S.L., 1995. Kinetics of near-equilibrium calcite precipitation at 100°C: An evaluation of elementary reaction-based and affinity-based rate laws. *Geochim. Cosmochim. Acta*, 59, 1457-1471.
- Sibley, D.F., Nordeng, S.H., and Borkowski, M.L., 1994. Dolomitization kinetics in hydrothermal bombs and natural settings. *J. Sediment. Research*, A64, n°3, 630-637.
- Schoonmaker, J.E., 1981. Magnesian calcite-seawater reactions: solubility and recrystallization behavior. Ph.D. dissertation, Northwestern University, Evanston, IL.
- Siegel, F.R., 1961. Factors influencing the precipitation of dolomite. *Kansas Geol. Survey Bull.*, 152, 127-158.
- Sjöberg, E.L., 1976. A fundamental equation for calcite dissolution kinetics. *Geochim. Cosmochim. Acta*, 40, 441-447.
- Sjöberg, E.L., and Rickard, D.T., 1983. Calcite dissolution kinetics: surface speciation and the origin of the variable pH dependence. *Chem. Geol.*, 42, 119-136.
- Sjöberg, E.L., and Rickard, D.T., 1984. Temperature dependence of calcite dissolution kinetics between 1 and 62°C at pH 2.7 to 8.4 in aqueous solution. *Geochim. Cosmochim. Acta*, 48, 485-493.
- Talman, S.J., Wiwchar, B., Gunter, W.D., and Scarfe, C.M., 1990. Dissolution kinetics of calcite in the H<sub>2</sub>O-CO<sub>2</sub> system along the steam saturation curve to 210°C. In "Fluid-Mineral Interactions (ed. R.J. Spencer and I.M. Chou). *Geochem. Soc. Spec. Issue* 2, 41-55.
- Talman, S.J., and Gunter, W.D., 1992. Rates of dolomite dissolution in CO<sub>2</sub> and HCl bearing solutions from 100-200°C. *Water-rock interaction, Kharaka and Maest Eds*, 1992 Balkema, 119-122.
- Van Cappellen, Ph., Charlet, L., Stumm, W., and Wersin, P., 1993. A surface complexation model of the carbonate mineral-aqueous solution interface. *Geochim. Cosmochim. Acta*, 57, 3505-3518.

- Walter, L.M., 1986. Relative efficiency of carbonate dissolution and precipitation during diagenesis: a progress report on the role of solution chemistry. In: D.L. Gauthier (Editor), "Roles of Organic Matter in Sediment Diagenesis". Soc. Econ. Paleontol. Mineral., Spec. publ., 38, 1-11.
- Walter, L.M., and Morse, J.W., 1984. Reactive surface area of skeletal carbonates during dissolution: Effect of grain size. *J. Sediment. Petrol.*, 54, 1081-1090.
- Walter, L.M., and Morse, J.W., 1985. The dissolution kinetics of shallow marine carbonates in seawater: a laboratory study. *Geochim. Cosmochim. Acta*, 49, 1503-1513.
- Wiechers, H.N.S., Sturrock, P., and Morais, G.V.R., 1975. Calcium carbonate crystallization kinetics. *Water Res.*, 9, 835-845.
- Weyl, P.K., 1965. The solution behavior of carbonate minerals in seawater. *Proc. Int. on Tropical Oceanogr.*, Miami, Fla., Univ. of Miami, 178-228.
- Wollast, R., 1990. Rate and mechanism of dissolution carbonates in the system  $\text{CaCO}_3\text{-MgCO}_3$ . In "Aquatic Chemical Kinetics" (ed. W. Stumm), Wiley & Sons, 431-445.
- Wollast, R., Garrels, R.M., and Mackenzie, F.T., 1980. Calcite-seawater reactions in ocean surface water. *Am. J. Sci.*, 280, 831-848.
- Zaihua, L., Svensson, U., Dreybrodt, W., Daoxian, Y., and Buhmann, D., 1995. Hydrodynamic control of inorganic calcite precipitation in Huanglong Ravine, China: Field measurements and theoretical prediction of deposition rates. *Geochim. Cosmochim. Acta*, 59, 3087-3097.
- Zhong, S., and Mucci, A., 1989. Calcite and aragonite precipitation from seawater solutions of various salinities: Precipitation rates and overgrowth compositions. *Chem. Geol.*, 78, 283-299.
- Zhong, S., and Mucci, A., 1993. Calcite precipitation in seawater using a constant addition technique: A new overall reaction kinetic expression. *Geochim. Cosmochim. Acta*, 57, 1409-1417.
- Zuddas, P., and Mucci, A., 1994. Kinetics of calcite precipitation from seawater: I. A classical chemical kinetics description for strong electrolytes solutions. *Geochim. Cosmochim. Acta*, 58, 4353-4362.

## **Tables**



Table 1a - Kinetics of calcite precipitation (linear laws:  $v = k (\Omega - 1)$ ).

References	Experimental conditions	Log k mol.cm <sup>-2</sup> .s <sup>-1</sup>	Ea kcal.mol <sup>-1</sup>
Reddy and Nancollas (1971) calcite precipitation calcite seed (0.315 g/l)	t = 25°C, pH = 8.53-8.80, atmospheric pCO <sub>2</sub> , 100 ml NaHCO <sub>3</sub> 0.02 M+100 ml CaCl <sub>2</sub> 8.10 <sup>-4</sup> M duration of 40-90 mn	-11.19	-
Nancollas and Reddy (1971) calcite precipitation calcite seed (0.42-2.3 g/l)	t = 10°C, pH = 8.46-8.80, atmospheric pCO <sub>2</sub> , 100 ml NaHCO <sub>3</sub> 0.02 M+100 ml CaCl <sub>2</sub> 8.10 <sup>-4</sup> M, stirring rate: 385-600 rpm, duration of 40-50 mn	-11.26	11.0
same workers and conditions	t = 25°C, same conditions	-11.09	11.0
same workers and conditions	t = 40°C, same conditions	-10.83	11.0
Wiechers <i>et al.</i> (1975) calcite precipitation calcite seed (0.1-1.0 g/l)	t = 11°C, pH = 8.0-10.0, NaHCO <sub>3</sub> -NaOH and CaCl <sub>2</sub> solutions, stirring rate: 300-800 rpm	< -9.99	10.3
same workers	t = 21°C, same conditions	< -9.89	10.3
same workers	t = 25°C, same conditions	< -9.79	10.3
same workers	t = 29°C, same conditions	< -9.75	10.3
same workers	t = 40°C, same conditions	< -9.62	10.3
Inskeep and Bloom (1985) calcite precipitation calcite seed (0.3 g/l)	t = 10°C, pH = 8.15, I = 0.016 M, pCO <sub>2</sub> = 0.0011 atm, CaCl <sub>2</sub> + KHCO <sub>3</sub> + KCl + KOH + HCl solutions	-10.81	11.5
Inskeep and Bloom (1985) calcite precipitation calcite seed (0.15-0.6 g/l)	t = 25°C, pH = 8.25-8.70, I = 0.015-0.1 M, pCO <sub>2</sub> = 6 10 <sup>-4</sup> -0.01 atm, CaCl <sub>2</sub> + KHCO <sub>3</sub> + KCl + KOH + HCl solutions	-10.41	11.5
Inskeep and Bloom (1985) calcite precipitation calcite seed (0.3 g/l)	t = 40°C, pH = 8.05-8.06, I = 0.016 M, pCO <sub>2</sub> = 0.0017 atm, CaCl <sub>2</sub> + KHCO <sub>3</sub> + KCl + KOH + HCl solutions	-10.11	11.5
Nagy (1988) undersaturated solutions immediately supersaturated by dissolution of fine particles	t = 25°C, NaCl 2 molal, duration of 30 days	-9.98	11.2 (25-60°C) 15.8 (25-89°C)
same worker	t = 60°C, NaCl 2 molal, duration of 30 days	-9.12	11.2-15.8
same worker	t = 89°C, NaCl 2 molal, duration of 30 days	-7.93	11.2-15.8

Table 1a - Continuation (linear laws:  $v = k (\Omega - 1)^n$  with  $n \approx 1$ ).

References	Experimental conditions	Log k mol.cm <sup>-2</sup> .s <sup>-1</sup>	n	Ea kcal.mol <sup>-1</sup>
Dromgoole and Walter (1990b) calcite precipitation calcite seed (0.07-0.8 g)	t = 10°C, 0.1 M CaCl <sub>2</sub> + NaHCO <sub>3</sub> solutions, pH 6.18-6.64, pCO <sub>2</sub> = 0.099 atm	-10.62	1.33	8.9
same workers calcite seed (0.02-0.1 g)	t = 25°C, 0.1 M CaCl <sub>2</sub> + NaHCO <sub>3</sub> solutions, pH 6.18-6.54, pCO <sub>2</sub> = 0.097 atm	-10.27	1.13	10.7
same workers calcite seed (0.05-0.3 g)	t = 25°C, 0.01 M CaCl <sub>2</sub> + NaHCO <sub>3</sub> solutions, pH 5.87-6.38, pCO <sub>2</sub> = 0.97 atm	-9.77	1.12	10.7
same workers calcite seed (0.07-0.5 g)	t = 25°C, 0.1 M CaCl <sub>2</sub> + NaHCO <sub>3</sub> solutions, pH 5.71-6.07, pCO <sub>2</sub> = 0.97 atm	-9.63	1.17	8.9
same workers calcite seed (0.02-0.1 g)	t = 50°C, 0.1 M CaCl <sub>2</sub> + NaHCO <sub>3</sub> solutions, pH 5.52-5.78, pCO <sub>2</sub> = 0.88 atm	-9.09	1.14	10.7
Shiraki and Brantley (1995) calcite precipitation calcite powder (seed crystal)	t = 100°C, NaOH-CaCl <sub>2</sub> -CO <sub>2</sub> -H <sub>2</sub> O solutions, P = 100 bar, pH = 6.38-6.98, duration of 0.72 h, stirring speeds > 1200 rpm, $\alpha_{\text{H}_2\text{CO}_3} > 5.07 \cdot 10^{-3}$	-8.64	1.09	-

Table 1b - Kinetics of calcite dissolution (linear laws:  $v = k (1 - \Omega^{0.5})$ ).

References	Experimental conditions	Log k mol.cm <sup>-2</sup> .s <sup>-1</sup>	Ea kcal.mol <sup>-1</sup>
Sjöberg (1976) pure calcite dissolution	0.7 M KCl - CaCl <sub>2</sub> - KCl - HCl solutions, t = 5-50°C, pH = 8.0-10.1, stirring rate = 276 rpm	-9.25 (25°C) -9.00 (50°C)	8.4
Sjöberg and Rickard (1984) Iceland spar dissolution	0.7 M KCl solutions far from equilibrium, t = 1-62°C, pH = 2.7-8.4	> -9.27 (25°C, pH 8.4, 400 rpm)	-
same workers	0.7 M KCl solutions far from equilibrium, t = 1-62°C, pH = 2.7-8.4	> -9.03 (25°C, pH 8.4, 4000 rpm)	-
same workers	0.7 M KCl solutions far from equilibrium, t = 1-62°C, pH = 2.7-8.4	> -8.82 (62°C, pH 8.4, 400 rpm)	-
same workers	0.7 M KCl solutions far from equilibrium, t = 1-62°C, pH = 2.7-8.4	> -8.46 (62°C, pH 8.4, 4000 rpm)	-
Sjöberg and Rickard (1984) Carrara marble dissolution	0.7 M KCl solutions far from equilibrium, t = 1-62°C, pH = 2.7-8.4	> -9.12 (25°C, pH 8.4, 400 rpm)	7.4
same workers	0.7 M KCl solutions far from equilibrium, t = 1-62°C, pH = 2.7-8.4	> -8.75 (25°C, pH 8.4, 4000 rpm)	8.6
same workers	0.1 M KCl solutions far from equilibrium, t = 1-62°C, pH = 2.7-8.4	> -9.34 (25°C, pH 8.4, 500 rpm)	7.4
same workers	0.1 M KCl solutions far from equilibrium, t = 1-62°C, pH = 2.7-8.4	> -9.00 (25°C, pH 8.4, 4000 rpm)	8.6
same workers	0.7 M KCl solutions far from equilibrium, t = 1-62°C, pH = 2.7-8.4	> -8.75 (62°C, pH 8.4, 400 rpm)	7.4
same workers	0.7 M KCl solutions far from equilibrium, t = 1-62°C, pH = 2.7-8.4	> -8.26 (62°C, pH 8.4, 4000 rpm)	8.6

Table 2a - Kinetics of calcite precipitation (non-linear laws:  $v_p = k (\Omega - 1)^n$ ).

References	Experimental conditions	Log k mol.cm <sup>-2</sup> .s <sup>-1</sup>	n
Reddy and Nancollas (1973) calcite precipitation pure calcite seed (0.458 g/l)	t = 25°C, pH = 9.06-9.16, ambient pCO <sub>2</sub> , NaHCO <sub>3</sub> 0.02 M + CaCl <sub>2</sub> 2.10 <sup>-4</sup> M solutions, stirring rate: 385 rpm, duration of 40 mn	-10.13	2
Reddy and Gaillard (1981) calcite precipitation calcite seed (0.28 -2.86 g/l)	t = 25°C, pH = 8.72-8.82, NaHCO <sub>3</sub> + CaCl <sub>2</sub> solutions, stirring rate: 200 rpm, duration of 105 mn	-10.62	2
same workers calcite seed (0.07 g/l)	same conditions	-10.32	2
same workers calcite seed (0.014 g/l)	same conditions	-10.28	2
Shiraki and Brantley (1995)	NaOH-CaCl <sub>2</sub> -CO <sub>2</sub> -H <sub>2</sub> O solutions, t = 100°C, P = 100 bar, pH = 6.38-6.98, stirring speeds > 400 rpm, duration of 0.72 h, $a_{\text{H}_2\text{CO}_3} < 2.33 \cdot 10^{-3}$ , exp ( $\Delta G/RT$ ) < 1.72	-9.00	1.93

Table 2b - Kinetics of calcite precipitation (non-linear laws:  $vp = k (\Omega - 1)^n$ ).

References	Experimental conditions	Log k mol.cm <sup>-2</sup> .s <sup>-1</sup>	n
Mucci and Morse (1983) calcite precipitation calcite seed	t = 25°C, pCO <sub>2</sub> = 3.2 10 <sup>-4</sup> -3.1 10 <sup>-3</sup> atm, pH = 7.83-7.98, aged Gulf Stream seawater far from calcite saturation ( $\Omega$ = 7.5-13.5)	-13.98	3.11
same workers	same conditions, synthetic seawater, pH = 7.83-7.95, $\Omega$ = 7.5-11.5	-14.09	3.13
Mucci (1986)	t = 25°C, pCO <sub>2</sub> = 3.2 10 <sup>-4</sup> -3.1 10 <sup>-3</sup> atm, pH = 7.53-8.38, aged artificial seawater far from calcite saturation ( $\Omega$ = 1.8-14.5)	-13.85	2.83
Burton and Walter (1987) calcite precipitation synthetic calcite seed	t = 5°C, pCO <sub>2</sub> = 10 <sup>-2</sup> atm, aged Gulf Stream seawater far from calcite saturation ( $\Omega$ = 2.5-17.0)	-12.41	0.6
same workers	same conditions, t = 25°C	-12.97	1.9
same workers	same conditions, t = 37°C	-12.99	2.3
Zhong and Mucci (1989) calcite precipitation synthetic calcite seed	t = 25°C, pCO <sub>2</sub> = 10 <sup>-2.5</sup> atm, pH = 7.53-8.38, aged artificial seawater solutions of various salinities (S = 5, 15, 25, 35, 44 ‰) and far from calcite saturation ( $\Omega$ = 1.8-16.1)	-13.66	2.87
same workers	same conditions, S = 5, 15 and 25 ‰, pH = 7.83-8.19, $\Omega$ = 2.8-13.0	-12.93	2.70
same workers	same conditions, S = 35 and 44 ‰, pH = 7.53-8.38, $\Omega$ = 1.8-16.1	-13.20	2.58
Zhong and Mucci (1993) calcite precipitation synthetic calcite seed (2.4 g/l)	t = 25°C, pCO <sub>2</sub> = 10 <sup>-2.5</sup> atm, aged artificial seawater with $\Omega$ = 1.2-8.0	-13.35	2.22
Zuddas and Mucci (1994) calcite precipitation synthetic calcite seed (0.1-0.5 g)	t = 25°C, pCO <sub>2</sub> = 10 <sup>-3.5</sup> atm, pH = 6-8, NaCl - CaCl <sub>2</sub> + NaHCO <sub>3</sub> - Na <sub>2</sub> CO <sub>3</sub> solutions at I = 0.7 m and $\Omega$ = 1.1-8.3	-12.54	2.35
same workers	same conditions, pCO <sub>2</sub> = 10 <sup>-2.5</sup> atm	-11.60	1.43
same workers	same conditions, pCO <sub>2</sub> = 10 <sup>-1.7</sup> atm	-10.53	1.42
same workers	same conditions, pCO <sub>2</sub> = 10 <sup>-0.5</sup> atm	-9.86	1.29

Table 2c - Kinetics of aragonite precipitation (non-linear laws:  $vp = k (\Omega - 1)^n$ ).

References	Experimental conditions	Log k mol.cm <sup>-2</sup> .s <sup>-1</sup>	n
Burton and Walter (1987) aragonite precipitation synthetic aragonite seed	t = 5°C, pCO <sub>2</sub> = 10 <sup>-2</sup> atm, aged Gulf Stream seawater far from aragonite saturation ( $\Omega$ = 2.5-17.0)	-12.22	0.4
same workers	same conditions, t = 25°C	-11.95	1.7
same workers	same conditions, t = 37°C	-11.90	2.4
Zhong and Mucci (1989) aragonite precipitation synthetic aragonite seed	t = 25°C, pCO <sub>2</sub> = 10 <sup>-2.5</sup> atm, pH = 7.58-8.03, aged artificial seawater solutions of various salinities (S = 5, 15, 25 ‰) and with $\Omega$ = 1.0-4.6	-12.03	2.33
same workers	t = 25°C, pCO <sub>2</sub> = 10 <sup>-2.5</sup> atm, pH = 7.48-7.67, aged artificial seawater solutions of various salinities (S = 35, 44 ‰) and with $\Omega$ = 1.1-6.2	-12.45	2.26

Table 2d - Kinetics of calcite precipitation (non-linear laws:  $vp = k (\Omega^{0.5} - 1)^2$ ).

References	Experimental conditions	Log k mol.cm <sup>-2</sup> .s <sup>-1</sup>	Ea kcal mol <sup>-1</sup>
House (1981) calcite precipitation calcite seed (0.2 g/l)	t = 25°C, pH = 7.5-8.5, dilute Ca(HCO <sub>3</sub> ) <sub>2</sub> solutions, stirring rate: 500 rpm, duration of 28-30 h	-9.95	-
same worker	same conditions, extent of precipitation $\alpha = 0-0.1$	-10.31	-
same worker	same conditions, extent of precipitation $\alpha = 0-0.1$	-9.93	-
same worker	same conditions, extent of precipitation $\alpha > 0.1$	-10.10	-
same worker	same conditions, extent of precipitation $\alpha > 0.1$	-9.73	-
Kazmierczak <i>et al.</i> (1982) calcite precipitation calcite seed (0.25-0.06 g/l)	t = 25°C, pH = 8.50, I = 2-5 10 <sup>-3</sup> M, 0.05 M CaCl <sub>2</sub> + 0.1 M NaHCO <sub>3</sub> + KOH solutions	-9.72	9.4
same workers calcite seed (0.1-0.2 g/l)	t = 25°C, pH = 8.50, I = 5-208 10 <sup>-3</sup> M, CaCl <sub>2</sub> + NaHCO <sub>3</sub> + Na <sub>2</sub> CO <sub>3</sub> + KCl solutions	-9.69	9.4
same workers calcite seed (0.2 g/l)	same conditions, I = 0.21 M	-9.63	9.4
same workers calcite seed (79.8 mg)	t = 25°C, pH = 8.25, I $\approx$ 0.1 M, CaCl <sub>2</sub> + NaHCO <sub>3</sub> + Na <sub>2</sub> CO <sub>3</sub> + KCl solutions	-9.86	9.4
same workers calcite seed (79.8 mg)	same conditions, pH = 8.50	-9.89	9.4
same workers calcite seed (79.8 mg)	same conditions, pH = 8.78	-9.85	9.4
same workers calcite seed (79.8 mg)	t = 15°C, pH = 8.52, I $\approx$ 0.1 M, CaCl <sub>2</sub> + NaHCO <sub>3</sub> + Na <sub>2</sub> CO <sub>3</sub> + KCl solutions	-9.86	9.4
same workers calcite seed (79.8 mg)	same conditions, t = 25°C, pH = 8.50	-9.83	9.4
same workers calcite seed (79.8 mg)	same conditions, t = 35°C, pH = 8.50	-9.68	9.4
Inskeep and Bloom (1985) calcite precipitation calcite seed (0.15-0.6 g/l)	t = 25°C, pH = 8.25-8.70, I = 0.015-0.1 M, pCO <sub>2</sub> = 6 10 <sup>-4</sup> -0.01 atm, CaCl <sub>2</sub> + KHCO <sub>3</sub> + KCl + KOH + HCl solutions	-10.14	11.5

Table 3 - Mechanistic rate equations assuming multiple elementary reactions.

## a) Calcite

References	Experimental conditions	Log k <sub>1</sub>	Log k <sub>2</sub>	Log k <sub>3</sub>	Log k <sub>-3</sub>
Plummer <i>et al.</i> (1978)	H <sub>2</sub> O-CO <sub>2</sub> system, t = 25°C, pCO <sub>2</sub> = 0.0003-0.97 atm, pH = 2-7, stirring speeds > 1800 rpm	-4.29	-7.46	-9.93	
same workers	H <sub>2</sub> O-CO <sub>2</sub> system, t = 60°C, pCO <sub>2</sub> = 0.0003-0.97 atm, pH = 2-7, stirring speeds > 1800 rpm	-4.13	-6.69	-9.31	
Busenberg and Plummer (1986)	H <sub>2</sub> O-CO <sub>2</sub> system, t = 25°C, pCO <sub>2</sub> = 10 <sup>-3.5</sup> -1 atm, pH = 2-7, stirring speeds = 250 rpm	-5.06	-7.32	-9.63	
Chou <i>et al.</i> (1989)	H <sub>2</sub> O-CO <sub>2</sub> system, t = 25°C, pH = 4-10, continuous fluidized bed reactor	-4.05	-7.30	-10.19	-1.73
Talman <i>et al.</i> (1990)	H <sub>2</sub> O-CO <sub>2</sub> system, t = 100°C, pH = 6.3-9.2, stirring speeds = 500 rpm	-4.8	-6.3	-9.0	
same workers	H <sub>2</sub> O-CO <sub>2</sub> system, t = 150°C, stirring speeds = 350-500 rpm	-4.1	-6.2	-8.6	
same workers	H <sub>2</sub> O-CO <sub>2</sub> system, t = 210°C, pH = 4.39-8.39, stirring speeds = 300-750 rpm	-3.3	-7.1	-8.2	
Arakaki and Mucci (1995)	H <sub>2</sub> O-CO <sub>2</sub> system, t = 25°C, pH = 4.8-6.0, pCO <sub>2</sub> = 0.003-0.97 atm stirring speeds = 305-620 rpm	-4.35	-7.30	-10.07	-1.46

log k<sub>i</sub> are given in mol.s<sup>-1</sup>.cm<sup>-2</sup>

## b) Aragonite

References	Experimental conditions	Log k <sub>1</sub>	Log k <sub>2</sub>	Log k <sub>3</sub>	Log k <sub>-3</sub>
Busenberg and Plummer (1986)	H <sub>2</sub> O-CO <sub>2</sub> system, t = 25°C, pCO <sub>2</sub> = 10 <sup>-3.5</sup> -1 atm, pH = 2-7, stirring speeds = 250 rpm	-5.06	-7.32	-9.46	
Chou <i>et al.</i> (1989)	H <sub>2</sub> O-CO <sub>2</sub> system, t = 25°C, pH = 4-10, continuous fluidized bed reactor	-3.92	-7.40	-10.00	-1.78

log k<sub>i</sub> are given in mol.s<sup>-1</sup>.cm<sup>-2</sup>



**Table 4a - Values of *a* and *b* constants needed to calculate the temperature dependence between 0 and 45°C of the dissolution rate constants.**

Rate constants	Sedimentary Dolomite a	Dolomite b	Hydrothermal Dolomite a	Dolomite b
Log k <sub>1</sub>	-1880	-0.88	-2960	2.17
Log k <sub>2</sub>	-1800	-3.07	-2360	-1.45
Log k <sub>3</sub>	-2700	-2.47	-4970	4.07
Log k <sub>4</sub> *	-2300	0.16	-2300	0.16
Log k <sub>4</sub> **	-3700	4.34	-3709	4.31

**Table 4b - Kinetics of dissolution and backward reaction of dolomite.**

References	Experimental conditions	Log k <sub>1</sub>	Log k <sub>2</sub>	Log k <sub>3</sub>	Log k <sub>4</sub> *	Log k <sub>4</sub> **	n
Busenberg and Plummer (1982) sedimentary dolomites	H <sub>2</sub> O-CO <sub>2</sub> system, t = 25°C, pCO <sub>2</sub> = 0-0.96 atm, pH = 0-10	-7.19	-9.11	-11.53	-7.55	-8.07	0.5
same workers and dolomites	same conditions, t = 45°C	-6.79	-8.73	-10.96	-7.07	-7.29	0.5
Busenberg and Plummer (1982) hydrothermal dolomites	H <sub>2</sub> O-CO <sub>2</sub> system, t = 25°C, pCO <sub>2</sub> = 0-0.96 atm, pH = 0-10	-7.76	-9.37	-12.60	-7.55	-8.07	0.5
same workers and dolomites	same conditions, t = 45°C	-7.13	-8.87	-11.55	-7.07	-7.29	0.5
Chou <i>et al.</i> (1989)	H <sub>2</sub> O-CO <sub>2</sub> system, t = 25°C, pH = 2-10, continuous fluidized bed reactor	-6.58	-8.00	-11.66	-	-	0.75

log k<sub>i</sub> are given in mol.s<sup>-1</sup>.cm<sup>-2</sup>

\* for dolomites with 0.7 or less mole % FeCO<sub>3</sub>

\*\* for dolomites with more than 1.0 mole % FeCO<sub>3</sub>

**Table 5 - Kinetics of magnesite and witherite dissolution and precipitation.**

References	Experimental conditions	Log k <sub>1</sub>	Log k <sub>2</sub>	Log k <sub>3</sub>	Log k <sub>-3</sub>
Chou <i>et al.</i> (1989) magnesite	H <sub>2</sub> O-CO <sub>2</sub> system, t = 25°C, pH = 2-8, continuous fluidized bed reactor	-8.60	-9.22	-13.35	-5.35
Chou <i>et al.</i> (1989) witherite	same conditions	-4.12	-7.52	-10.15	-1.69

log k<sub>i</sub> are given in mol.s<sup>-1</sup>.cm<sup>-2</sup>

**Table 6 - Main experimental data and results from calcite kinetic experiments of Busenberg and Plummer (1985).**

$\Omega$ calcite	$\text{Na}_2\text{SO}_4$ molality $\text{mol kg}^{-1}$ water	pH	Rate $\text{mg min}^{-1} \text{g}^{-1}$	decrease factor
2.5	min. 0.003	7.12	14.8	
2.5	max. 0.05	7.17	1.39	10.65
5.0	0.00625	7.27	16.8	
5.0	0.025	7.30	14.1	1.19
10	min. 0.003	7.42	72.2	
10	max. 0.10	7.51	21.6	3.34
15	0.00625	7.52	86.1	
15	0.025	7.54	68.6	1.25
30	0.00625	7.68	195	
30	0.025	7.70	137	1.42

**Table 7 - Reaction orders and calcite precipitation rate constants calculated from experimental results obtained by Busenberg and Plummer (1985).**

$\text{Na}_2\text{SO}_4$ molality $\text{mol kg}^{-1}$ water	$[\text{SO}_4] / [\text{Ca}]$	n	k $\text{mg min}^{-1} \text{g}^{-1}$	r
0.003	0.3	0.88	10.33	
0.00625	0.625	1.04	5.66	0.985
0.0125	1.25	1.22	3.90	
0.025	2.5	1.30	2.10	0.993
0.05	5.0	1.65	0.71	

**Table 8 - Reaction orders and calcite precipitation rate constants calculated from experimental results obtained by Dromgoole and Walter (1990b).**

T °C	$\text{pCO}_2$ atm	pH range	$[\text{Ca}^{2+}]$ $\text{mol l}^{-1}$	$[\text{Mn}^{2+}]/[\text{Ca}^{2+}]$	n	log k $\text{mol cm}^{-2} \text{s}^{-1}$	$r^2$
10	0.099	6.35-6.79	0.1	0.01	1.750	-11.43	0.97
25	0.097	6.27-6.62	0.1	0.01	1.798	-11.00	0.99
25	0.97	6.18-6.45	0.01	0.01	1.696	-10.35	0.97
25	0.97	5.71-6.05	0.1	0.001	1.336	-9.78	0.97
25	0.97	5.70-6.05	0.1	0.01	1.662	-10.25	0.97
25	0.97	5.82-6.06	0.1	0.05	2.053	-11.27	0.98
50	0.88	5.58-5.93	0.1	0.01	1.684	-9.63	0.98

## **Appendix**

## **Review of thermodynamic data and of numerical models for calculating ionic activity coefficients at high salinity from 25°C to high temperatures in the Na-K-Ca-Mg-H-Cl-SO<sub>4</sub>-OH-HCO<sub>3</sub>-CO<sub>3</sub>-CO<sub>2</sub>-H<sub>2</sub>O System**

This short report is a summary of a review of the main thermodynamic data and numerical models for calculating ionic activity coefficients at high salinity from 25°C to high temperatures in the Na-K-Ca-Mg-H-Cl-SO<sub>4</sub>-OH-HCO<sub>3</sub>-CO<sub>3</sub>-CO<sub>2</sub>-H<sub>2</sub>O system. This work was undertaken as part of the research conducted in the QC-SCALE project (CEC-JOULE programme).

### **Numerical models**

Among available numerical models, only the Pitzer ion-interaction model (Harvie *et al.*, 1984; He, 1992; He and Morse, 1993) has been applied with success over a large range of concentrations (up to 6 m) and temperatures (up to 90°C). Other models (extended Debye-Hückel equation, ion association model, Debye-Hückel/Brønsted-Guggenheim/Uniquac (DH-BG-UNI) model, SIT equation, ion hydration model) apply to much more restricted ranges of concentrations or temperatures. The extended Debye-Hückel equation can be only applied up to an ionic strength of 1 m even if it works at temperatures up to 300°C (Wolery *et al.*, 1990). The ion pairing model has been used at 25°C for solutions with an ionic strength up to 1 m (Millero and Schreiber, 1982). The DH-BG-UNI model (Sander, 1984) becomes inaccurate above 2 m NaCl molality when applied to the calculation of calcite solubility in NaCl solutions at 25°C (Haarberg, 1989) and must be again parameterized for more complex electrolytes than NaCl (seawater, for example). Up to now, the SIT equation (Grenthe and Wanner, 1989) and ion hydration model (Stokes and Robinson, 1948; Wolery and Jackson, 1990) have only been developed at 25°C.

The complexity of the carbonic acid system (presence of hydrolysis equilibria in the system, high vapor pressure for bicarbonate solutions, low concentrations limited by solubility constraints) makes application of Pitzer's equations difficult. This complexity and the rare experimental data for determination of activity coefficients for carbonic acid species in solutions of high ionic strength and at high temperature, largely confined to seawater or NaCl solutions (Ellis and Golding, 1963; Takenouchi and Kennedy, 1965; Malinin and Savelyeva, 1972; Malinin and Kurovskaya, 1975; Drummond, 1981; Patterson *et al.*, 1982, 1984; Enick and Klara, 1990; Estrada, 1991; Rumpf *et al.*, 1994), explain why the Pitzer model was extended to temperatures from -55 to 300°C only in the Na-K-Ca-Mg-Cl-SO<sub>4</sub> system (Pabalan and Pitzer, 1987 a, b; Moller, 1988; Greenberg and Moller, 1989; Spencer *et al.*, 1990). Pitzer and his associates (Peiper and Pitzer, 1982; Roy *et al.*, 1984; Pitzer *et al.*, 1985) have parameterized the Na-K-Ca-Mg-HCO<sub>3</sub>-CO<sub>3</sub>-OH system at 25°C and have also extended part of the system (Na-K-HCO<sub>3</sub>-CO<sub>3</sub>-OH) to the temperature range between 0 and 50°C. Harvie *et al.* (1984) have presented a chemical model for the Na-K-Ca-Mg-H-Cl-HSO<sub>4</sub>-SO<sub>4</sub>-OH-HCO<sub>3</sub>-CO<sub>3</sub>-CO<sub>2</sub> system at 25°C based on Pitzer's equations, which is available in the geochemical code EQ3/6 (Wolery, 1995). If this model has been demonstrated to produce accurate predictions for the solubility of many evaporite minerals, including calcium sulfate and alkali

carbonate minerals, applications to the prediction of  $\text{CaCO}_3$  solubility in salt solutions have been less successful (Clegg and Whitfield, 1991).

He (1992) and He and Morse (1993) have used their own measurements in combination with existing data (Pitzer and Weare group's database; Harned and Bonner, 1945; Yasunishi and Yoshida, 1979; Plummer and Busenberg, 1982; Thurmond and Millero, 1982; Millero and Thurmond, 1983; Patterson *et al.*, 1982; 1984; Holmes *et al.*, 1987) to derive Pitzer parameters for the interaction between carbonate species and other ions. At present, this is the only work that permits to obtain relatively accurate predictions of calcite solubility in brines from 0 to 90°C and at 1 atm (Na-K-Ca-Mg-H-Cl-SO<sub>4</sub>-OH-HCO<sub>3</sub>-CO<sub>3</sub>-CO<sub>2</sub>-H<sub>2</sub>O system). When calculated solubilities for calcite obtained using their Pitzer model are compared with the experimental data of Miller (1952; 0.5 m NaCl solution from 25 to 70°C) or of Wolf *et al.* (1989; NaCl, KCl and CaCl<sub>2</sub> solutions from 0 to 60°C), the agreement is generally good. While the solubility of calcite at infinite dilution is well known (Segnit *et al.*, 1962; Plummer and Busenberg, 1982; Sass *et al.*, 1983), solubility data at high ionic strength have been mainly determined for seawater below 40°C (MacIntyre, 1965; Hawley and Pytkowicz, 1969; Edmond and Gieskes, 1970; Ingle *et al.*, 1973; Ingle, 1975; Millero, 1976, 1979; Plath *et al.*, 1980; Morse *et al.*, 1980; Mucci, 1983; Mucci and Morse, 1984). In other chemical systems or at higher temperatures, these data are rather scarce (Miller, 1952; Shternina and Frolova, 1957; Harvie *et al.*, 1984; Millero *et al.*, 1984; Nagy, 1988; Wolf *et al.*, 1989; Wolf and Rohde, 1992; Estrada, 1991; Estrada *et al.*, 1992). At temperatures above 100°C, the only work we found is that of Ellis (1963) regarding the determination of calcite solubility in NaCl solutions. He and Morse (1993) performed calcite solubility measurements in complex brines initially supersaturated with respect to calcite between 0 and 90°C. They observed an increase in the thermodynamic constant for calcite solubility compared to that given by Plummer and Busenberg (1982). He and Morse (1993) suggested that this increase was probably caused by the incorporation of Na, Mg and SO<sub>4</sub> ions into the calcite lattice. In contrast, the results of undersaturation experiments yielded good agreement between the two sets of data.

The Pitzer model has been incorporated and adjusted in several geochemical codes, including PHRQPITZ (Plummer *et al.*, 1988; Plummer and Parkhurst, 1990), SOLMINEQ.88 (Kharaka *et al.*, 1989), and Haarberg (1989)'s code, allowing to make calculations for complex geochemical systems at high temperatures (and at high pressures for most of them). However, these codes are inappropriate for some applications. In addition, they are not as accurate as the model developed by He and Morse (1993) that has the best predictive ability in the Na-K-Ca-Mg-H-Cl-SO<sub>4</sub>-OH-HCO<sub>3</sub>-CO<sub>3</sub>-CO<sub>2</sub>-H<sub>2</sub>O system between 0 and 90°C and at 1 atm.

## Pressure effect

Pressure effect in the Pitzer model (from 1 to 1000 bar) has only been taken into account by Monnin (1989, 1990) for the Na-Ca-Cl-SO<sub>4</sub>-H<sub>2</sub>O system. Pressure effect is often considered to be small between 1 and 300 bar but can be relatively significant at 62°C and 200 bar. Monnin and Raimboz (1996) indicated that the pressure effect on the anhydrite saturation indices (SI) for Atlantis II brines was approximately 0.2 and practically compensated the SI increase caused by a temperature change from 25 to 62°C. It is very difficult to calculate the effect of pressure on the ionic activity coefficients in high salinity solutions while its influence on the mineral solubility or on the ionic equilibrium constants can be easily evaluated using the established expression:

$$\ln K(T,P) = \ln K(T, 1) - \Delta V_r(T,1) (P-1) + \Delta \kappa_r(T,1) / 2RT (P-1)^2$$

where  $K$  is the solubility product or the ionic equilibrium constant,  $P$  is the applied pressure,  $R$  is the gas constant ( $82.06 \text{ cm}^3 \text{ atm K}^{-1}$ ),  $T$  is the absolute temperature ( $^{\circ}\text{K}$ ),  $\Delta V_r$  and  $\Delta \kappa_r$  are the molal volume and compressibility changes at 1 atm. The latter two parameters are given by:

$$\Delta V_r = \sum V_i (\text{products}) - \sum V_i (\text{reactants})$$

$$\Delta \kappa_r = \sum \kappa_i (\text{products}) - \sum \kappa_i (\text{reactants})$$

$V_i$  and  $\kappa_i$  are the partial molal volume and compressibility of species or mineral  $i$ . Their values can be found in Millero (1982) or in Michard (1983).

## Thermodynamic data

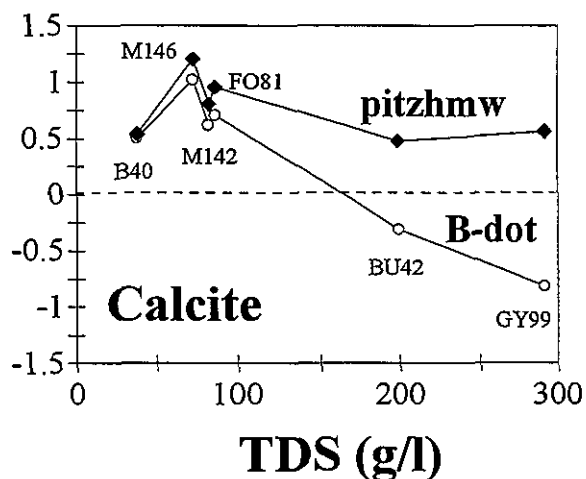
Most of the thermodynamic data commonly used in the Na-K-Ca-Mg-H-Cl-OH-HCO<sub>3</sub>-CO<sub>3</sub>-CO<sub>2</sub>-H<sub>2</sub>O system are compiled in tables 1a, 1b, 1c and 1d. The values of the ionic equilibrium constants and of the equilibrium constants of mineral dissolution-precipitation reaction in this system are given in tables 2 and 3. The selected EQ3/6 database comes mainly from SUPCRT92, an internally consistent database and program created by Johnson, Oelkers and Helgeson (1992) for dealing with thermodynamic data based on the work of Helgeson and his co-workers. Plummer and Busenberg (1982) have critically reviewed the literature for the CO<sub>2</sub>-H<sub>2</sub>O system and they have presented reliable expressions for the corresponding thermodynamic equilibrium constants in the temperature range 0-250°C. The values proposed by Plummer and Busenberg (1982) are those used by He and Morse (1993) in their Pitzer model. In the latter model, the association constants for CaCO<sub>3</sub><sup>°</sup> and MgCO<sub>3</sub><sup>°</sup> are taken from Plummer *et al.* (1988) for the temperature range 0-90°C, which are also derived from Plummer and Busenberg (1982). The values are consistent with those of Harvie *et al.* (1984).

In order to illustrate the need for the use of the Pitzer model in high concentration solutions, calculations of saturation indices for typical oil field brines from the North Sea (table 4) with respect to calcite, aragonite, dolomite and magnesite have been performed at 25°C using the extended Debye-Hückel equation (B-dot equation) and the Pitzer model developed by Harvie *et al.* (1984). These models are available in the geochemical code EQ3NR (Wolery, 1995). Results are presented in figure 1. At very high salinity, the extended Debye-Hückel equation clearly leads to erroneous interpretations.

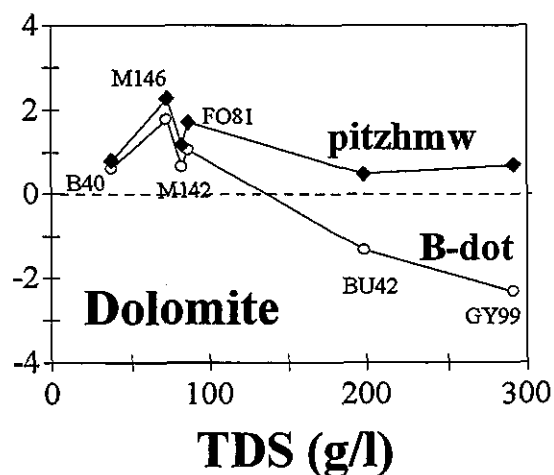
We have found no accurate application of the Pitzer model in the Na-K-Ca-Mg-H-Cl-SO<sub>4</sub>-OH-HCO<sub>3</sub>-CO<sub>3</sub>-CO<sub>2</sub>-H<sub>2</sub>O system extended to organic acids and iron species. In brines from North Sea oil fields, organic acids are commonly present and acetic acid is the dominant component (Barth, 1989). Thermodynamic data on acetic acid, acetate anion and its cation complexes can be found in Shock and Helgeson (1989), Harrison and Thyne (1991), Shock and Koretsky (1993, 1995). Thermodynamic data on iron species and siderite are reported in several EQ3/6 databases (data0.com.R2, for example), Michard (1983), Nordstrom *et al.* (1990), Bruno *et al.* (1992).

**Figure 1 - Calculations of saturation index (SI) for oil field brines from the North Sea with respect to calcite, aragonite, dolomite and magnesite at 25°C using the extended Debye-Hückel equation (B-dot equation) and the Pitzer model developed by Harvie et al. (1984).**

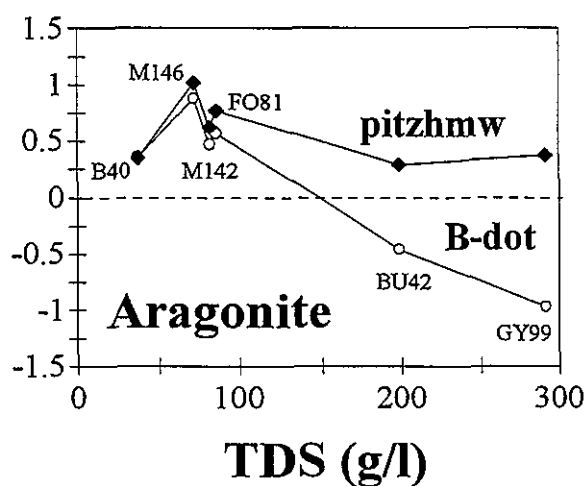
**SI (25°C)**



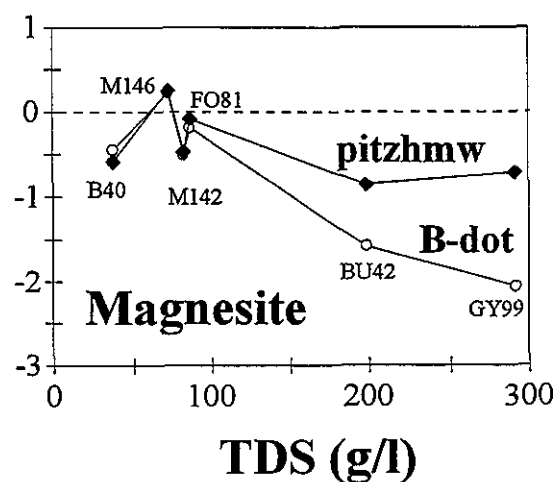
**SI (25°C)**



**SI (25°C)**



**SI (25°C)**



## Carbonate solid-solutions

Carbonate solid-solutions are common minerals at the Earth's surface and have been extensively studied, especially binary systems ( $\text{CaCO}_3\text{-MgCO}_3$ ,  $\text{CaCO}_3\text{-FeCO}_3$ ,  $\text{MgCO}_3\text{-FeCO}_3$ ,  $\text{CaCO}_3\text{-MnCO}_3$ ,  $\text{CaCO}_3\text{-SrCO}_3$ ). An interesting review of the main studies (experiments, investigations and discussions of solid-solution/aqueous-solution theory) was accomplished by Woods and Garrels (1991). These authors present the low-temperature ternary Ca-Mg-Fe phase relations for rhombohedral carbonates as well as phase diagrams at 25 and 150°C. They proposed a method for estimating the composition of an aqueous solution from the composition of the solid-solution carbonate assumed to be in equilibrium with it. Nevertheless, the identification of the variables of the fluid chemistry controlling the composition of the solid-solutions is complex and remains problematic.

The literature on this subject is abundant but frequently marked by controversy. For example, the partitioning of  $\text{Mg}^{2+}$  in natural inorganic calcite, that has been studied far more extensively than any other coprecipitation reaction involving carbonate minerals, may be very different (Burton and Walter, 1991; Hartley and Mucci, 1996). Laboratory-precipitated cements, grown from seawater in controlled experiments at 25°C, contain about 8 mol%  $\text{MgCO}_3$  (Berner, 1975; Mucci and Morse, 1983; Hartley and Mucci, 1996) whereas natural shallow marine calcite cements have a large compositional range from 11 to 18 mol%  $\text{MgCO}_3$ , averaging 12 mol% (Chave, 1954; Videtich, 1985; Mucci, 1987). Numerous experimental studies have determined partition coefficients for  $\text{Mg}^{2+}$  in calcite (Katz, 1973; Mucci and Morse, 1983; Mucci, 1986, 1987; Oomori *et al.*, 1987) but there are large discrepancies between the results of these studies. The variations are likely due to differences in fluid chemistry or in experimental methods.

The incorporation of  $\text{MgCO}_3$  in calcite has been shown to be dependent on several variables, such as  $\text{Mg}^{2+}/\text{Ca}^{2+}$  ratios in fluid (Berner, 1975; Mucci and Morse, 1983; Morse and Bender, 1990), temperature (Katz, 1973; Burton and Walter, 1987a; Mucci, 1987), carbonate ion concentration or saturation state (MacKenzie *et al.*, 1983; Given and Wilkinson, 1985), sulphate concentration (Burton and Walter, 1985, 1987b; Mucci *et al.*, 1989), salinity (Zhong and Mucci, 1989),  $\text{CO}_2$  partial pressure or pH (Burton and Walter, 1991; Oomori *et al.*, 1987), presence of dissolved organic matter (Morse, 1983; Hartley and Mucci, 1996), etc.. However, the influence of some variables, i.e., carbonate ion concentration,  $\text{pCO}_2$ , presence of dissolved organic matter, is questioned (Burton and Walter, 1991; Hartley and Mucci, 1996). Hartley and Mucci (1996) pointed out that only the combined variations of Mg/Ca ratio,  $\text{SO}_4$  and temperature could have a clearly demonstrable influence on magnesium incorporation in naturally occurring marine abiotic calcites. They suggested that other factors or combination of factors such as the surface properties of the substrate (nonequivalent crystallographic sectors of precipitated calcite and role of adsorbed organic matter) had to be considered. They observed that the amount of  $\text{MgCO}_3$  incorporated in calcite precipitated from seawater was independent of  $\text{pCO}_2$  over four orders of magnitude ( $10^{-0.5}$  to  $10^{-4.6}$  atm). These results contrast with those obtained by Burton and Walter (1991) obtained under similar conditions. Contrary to Mg, the partitioning of trace elements, such as Fe and Mn, in calcite is also dependent on the precipitation rate (Mucci and Morse, 1983; Dromgoole and Walter, 1990a, 1990b). Clearly, present knowledge of element partitioning in calcite is insufficient.



**Table 1a - Compilation of standard partial molal thermodynamic data (Gibbs free energy of formation  $\Delta G^\circ_f$ , enthalpy of formation  $\Delta H^\circ_f$ , entropy  $S^\circ$ , heat capacity  $C_p^\circ$  at constant pressure, volume  $V^\circ$  and compressibility  $\kappa^\circ$ ) in the Na, K, Ca, Mg, H, Cl, OH,  $\text{CO}_2$ ,  $\text{HCO}_3$ ,  $\text{CO}_3$ ,  $\text{H}_2\text{O}$  system: Inorganic neutral species.**

Species	Source	$\Delta G^\circ_f{}^a$	$\Delta H^\circ_f{}^a$	$S^\circ{}^b$	$C_p^\circ{}^b$	$V^\circ{}^c$	$\kappa^\circ{}^d$
$\text{H}_2\text{O}$	Michard (1983)	-56.687	-68.315	16.71	18.06	18.10	$-7.96 \cdot 10^{-4}$
$\text{H}_2\text{O}$	Harvie <i>et al.</i> (1984)	-56.688	-68.317	16.71	-	-	-
$\text{H}_2\text{O}$	EQ3/6 data0.com.R2 (1995)	-56.688	-68.317	16.71	-	-	-
$\text{H}_2\text{CO}_3$	Michard (1983)	-148.943	-167.086	45.24	63.00	52.15	$2.40 \cdot 10^{-3}$
$\text{CO}_2$ (aq)	Millero (1983)	-	-	-	-	33.60	-
$\text{CO}_2$ (aq)	Harvie <i>et al.</i> (1984)	-92.238	-	-	-	-	-
$\text{CO}_2$ (aq)	Shock <i>et al.</i> (1989)	-92.250	-98.900	28.10	58.10	32.80	
$\text{CO}_2$ (aq)	EQ3/6 data0.com.R2 (1995)	-92.250	-98.900	28.10	-	-	-

a. kcal mol<sup>-1</sup>

b. cal mol<sup>-1</sup> K<sup>-1</sup>

c. cm<sup>3</sup> mol<sup>-1</sup>

d. cm<sup>3</sup> mol<sup>-1</sup> bar<sup>-1</sup>

**Table 1b - Compilation of standard partial molal thermodynamic data in the Na, K, Ca, Mg, H, Cl, OH, CO<sub>2</sub>, HCO<sub>3</sub>, CO<sub>3</sub>, H<sub>2</sub>O system: Ions.**

Species	Source	$\Delta G^\circ_f^a$	$\Delta H^\circ_f^a$	$S^\circ_b$	$C_p^\circ b$	$V^\circ c$	$\kappa^\circ d$
OH <sup>-</sup>	Millero (1982)	-	-	-	-	-3.98	-3.86 10 <sup>-3</sup>
OH <sup>-</sup>	Michard (1983)	-37.604	-54.977	-2.56	-28.00	-4.11	-3.40 10 <sup>-3</sup>
OH <sup>-</sup>	Harvie <i>et al.</i> (1984)	-37.584	-	-	-	-	-
OH <sup>-</sup>	Shock and Helgeson (1988)	-37.595	-54.977	-2.56	-32.79	-4.18	-3.72 10 <sup>-3</sup>
OH <sup>-</sup>	EQ3/6 data0.com.R2 (1995)	-37.595	-54.977	-2.56	-	-	-
Cl <sup>-</sup>	Millero (1982)	-	-	-	-	17.82	-7.4 10 <sup>-4</sup>
Cl <sup>-</sup>	Michard (1983)	-31.380	-39.933	13.56	-32.55	17.50	-9.0 10 <sup>-4</sup>
Cl <sup>-</sup>	Harvie <i>et al.</i> (1984)	-31.375	-	-	-	-	-
Cl <sup>-</sup>	Shock and Helgeson (1988)	-31.379	-39.933	13.56	-29.44	17.79	4.6 10 <sup>-4</sup>
Cl <sup>-</sup>	EQ3/6 data0.com.R2 (1995)	-31.379	-39.933	13.56	-	-	-
HCO <sub>3</sub> <sup>-</sup>	Millero (1982)	-	-	-	-	24.29	-2.75 10 <sup>-3</sup>
HCO <sub>3</sub> <sup>-</sup>	Michard (1983)	-140.282	-164.898	23.53	-11.12	24.85	-4.0 10 <sup>-4</sup>
HCO <sub>3</sub> <sup>-</sup>	Harvie <i>et al.</i> (1984)	-140.271	-	-	-	-	-
HCO <sub>3</sub> <sup>-</sup>	Shock and Helgeson (1988)	-140.282	-164.898	23.53	-8.46	24.60	-2.75 10 <sup>-3</sup>
HCO <sub>3</sub> <sup>-</sup>	EQ3/6 data0.com.R2 (1995)	-140.282	-164.898	23.53	-	-	-
CO <sub>3</sub> <sup>-</sup>	Millero (1982)	-	-	-	-	-3.78	-7.35 10 <sup>-3</sup>
CO <sub>3</sub> <sup>-</sup>	Michard (1983)	-126.191	-161.386	-11.95	-76.00	-2.30	4.0 10 <sup>-4</sup>
CO <sub>3</sub> <sup>-</sup>	Harvie <i>et al.</i> (1984)	-126.166	-	-	-	-	-
CO <sub>3</sub> <sup>-</sup>	Shock and Helgeson (1988)	-126.191	-161.385	-11.95	-69.50	-5.02	-7.35 10 <sup>-3</sup>
CO <sub>3</sub> <sup>-</sup>	EQ3/6 data0.com.R2 (1995)	-126.191	-161.385	-11.95	-	-	-
Ca <sup>++</sup>	Millero (1982)	-	-	-	-	-17.83	-7.61 10 <sup>-3</sup>
Ca <sup>++</sup>	Michard (1983)	-132.120	-129.800	-13.48	-6.21	-18.70	-6.60 10 <sup>-3</sup>
Ca <sup>++</sup>	Harvie <i>et al.</i> (1984)	-132.302	-	-	-	-	-
Ca <sup>++</sup>	Shock and Helgeson (1988)	-132.120	-129.800	-13.50	-7.53	-18.06	-7.61 10 <sup>-3</sup>
Ca <sup>++</sup>	EQ3/6 data0.com.R2 (1995)	-132.120	-129.800	-13.50	-	-	-
Mg <sup>++</sup>	Millero (1982)	-	-	-	-	-21.15	-8.01 10 <sup>-3</sup>
Mg <sup>++</sup>	Michard (1983)	-108.700	-111.563	-33.00	-3.82	-21.10	-7.60 10 <sup>-3</sup>
Mg <sup>++</sup>	Harvie <i>et al.</i> (1984)	-108.702	-	-	-	-	-
Mg <sup>++</sup>	Shock and Helgeson (1988)	-108.505	-111.367	-33.00	-5.34	-21.55	-7.42 10 <sup>-3</sup>
Mg <sup>++</sup>	EQ3/6 data0.com.R2 (1995)	-108.505	-111.367	-33.00	-	-	-
Na <sup>+</sup>	Millero (1982)	-	-	-	-	-1.21	-3.94 10 <sup>-3</sup>
Na <sup>+</sup>	Michard (1983)	-62.593	-57.428	13.96	9.90	-1.00	-3.80 10 <sup>-3</sup>
Na <sup>+</sup>	Harvie <i>et al.</i> (1984)	-62.596	-	-	-	-	-
Na <sup>+</sup>	Shock and Helgeson (1988)	-62.591	-57.433	13.96	9.06	-1.11	-3.28 10 <sup>-3</sup>
Na <sup>+</sup>	EQ3/6 data0.com.R2 (1995)	-62.591	-57.433	13.96	-	-	-
K <sup>+</sup>	Millero (1982)	-	-	-	-	9.03	-3.37 10 <sup>-3</sup>
K <sup>+</sup>	Michard (1983)	-67.529	-60.250	24.15	2.98	9.10	-3.20 10 <sup>-3</sup>
K <sup>+</sup>	Harvie <i>et al.</i> (1984)	-67.518	-	-	-	-	-
K <sup>+</sup>	Shock and Helgeson (1988)	-67.510	-60.270	24.15	1.98	9.06	-3.30 10 <sup>-3</sup>
K <sup>+</sup>	EQ3/6 data0.com.R2 (1995)	-67.510	-60.270	24.15	-	-	-

**Table 1c - Compilation of standard partial molal thermodynamic data in the Na, K, Ca, Mg, H, Cl, OH, CO<sub>2</sub>, HCO<sub>3</sub>, CO<sub>3</sub>, H<sub>2</sub>O system: Complexes.**

Species	Source	$\Delta G^\circ_f^a$	$\Delta H^\circ_f^a$	$S^\circ_b$	$C_p^\circ_b$	$V^\circ_c$	$\kappa^\circ_d$
NaOH <sup>o</sup>	EQ3/6 data0.com.R2 (1995)	-99.095	-112.927	-	-	-	-
KOH <sup>o</sup>	EQ3/6 data0.com.R2 (1995)	-104.471	-	-	-	-	-
CaOH <sup>+</sup>	EQ3/6 data0.com.R2 (1995)	-171.277	-	-	-	-	-
MgOH <sup>+</sup>	Michard (1983)	-149.320	-165.18	-	-	-	-
MgOH <sup>+</sup>	Harvie <i>et al.</i> (1984)	-149.270	-	-	-	-	-
HCl <sup>o</sup>	EQ3/6 data0.com.R2 (1995)	-30.465	-	-	-	-	-
NaCl <sup>o</sup>	EQ3/6 data0.com.R2 (1995)	-92.910	-96.120	28.00	-	-	-
KCl <sup>o</sup>	EQ3/6 data0.com.R2 (1995)	-96.850	-96.810	42.25	-	-	-
CaCl <sup>+</sup>	EQ3/6 data0.com.R2 (1995)	-162.550	-169.250	-1.50	-	-	-
CaCl <sub>2</sub> <sup>o</sup>	EQ3/6 data0.com.R2 (1995)	-194.000	-211.060	6.00	-	-	-
MgCl <sup>+</sup>	EQ3/6 data0.com.R2 (1995)	-139.70	-151.44	-20.50	-	-	-
NaCO <sub>3</sub> <sup>-</sup>	EQ3/6 data0.com.R2 (1995)	-792.80	-935.92	-49.80	-	-	-
CaHCO <sub>3</sub> <sup>+</sup>	Michard (1983)	-273.750	-289.290	-	7.90	8.10	-7.0 10 <sup>-3</sup>
CaHCO <sub>3</sub> <sup>+</sup>	EQ3/6 data0.com.R2 (1995)	-273.830	-294.350	16.00	-	-	-
CaCO <sub>3</sub> <sup>o</sup>	Michard (1983)	-262.620	-287.161	2.51		- 10.20	-7.0 10 <sup>-3</sup>
CaCO <sub>3</sub> <sup>o</sup>	Harvie <i>et al.</i> (1984)	-262.767	-	-	-	-	-
CaCO <sub>3</sub> <sup>o</sup>	EQ3/6 data0.com.R2 (1995)	-262.850	-287.390	2.50	-	-	-
MgHCO <sub>3</sub> <sup>+</sup>	Michard (1983)	-250.441	-275.269	-0.57	13.06	9.10	-8.0 10 <sup>-3</sup>
MgHCO <sub>3</sub> <sup>+</sup>	EQ3/6 data0.com.R2 (1995)	-250.200	-275.750	-3.00	-	-	-
MgCO <sub>3</sub> <sup>o</sup>	Michard (1983)	-238.966	-270.940	-24.52	-46.80	- 13.40	-8.0 10 <sup>-3</sup>
MgCO <sub>3</sub> <sup>o</sup>	Harvie <i>et al.</i> (1984)	-238.863	-	-	-	-	-
MgCO <sub>3</sub> <sup>o</sup>	EQ3/6 data0.com.R2 (1995)	-238.760	-270.570	-24.00	-	-	-

**Table 1d - Compilation of standard partial molal thermodynamic data in the Na, K, Ca, Mg, H, Cl, OH, CO<sub>2</sub>, HCO<sub>3</sub>, CO<sub>3</sub>, H<sub>2</sub>O system: Minerals.**

Minerals	Source	$\Delta G^\circ_f$ <sup>a</sup>	$\Delta H^\circ_f$ <sup>a</sup>	S <sup>ob</sup>	Cp <sup>ob</sup>	V <sup>oc</sup>
calcite	Naumov <i>et al.</i> (1971)	-269.880	-288.440	-	-	-
calcite	Helgeson <i>et al.</i> (1978)	-270.100	-288.772	22.15	-	-
calcite	Robie <i>et al.</i> (1978)	-269.800	-288.568	21.92	-	-
calcite	Michard (1983)	-269.930	-288.680	21.92	19.57	36.93
calcite	Harvie <i>et al.</i> (1984)	-269.936	-	-	-	-
calcite	EQ3/6 data0.com.R2 (1995)	-269.880	-288.552	22.15	19.57	36.93
aragonite	Naumov <i>et al.</i> (1971)	-269.650	-288.480	-	-	-
aragonite	Helgeson <i>et al.</i> (1978)	-269.875	-288.723	21.56	-	-
aragonite	Robie <i>et al.</i> (1978)	-269.549	-288.583	21.03	-	-
aragonite	Michard (1983)	-269.700	-288.630	21.03	19.43	34.15
aragonite	Harvie <i>et al.</i> (1984)	-269.681	-	-	-	-
aragonite	EQ3/6 data0.com.R2 (1995)	-269.683	-288.531	21.56	19.43	34.15
magnesite	Harvie <i>et al.</i> (1984)	-245.555	-	-	-	-
magnesite	EQ3/6 data0.com.R2 (1995)	-245.658	-265.630	15.70	18.13	28.02
dolomite	Michard (1983)	-517.980	-516.652	37.09	37.70	64.34
dolomite	Harvie <i>et al.</i> (1984)	-516.640	-	-	-	-
dolomite	EQ3/6 data0.com.R2 (1995)	-517.760	-556.631	37.09	37.58	64.37
disord. dolomite	Michard (1983)	-516.652	-555.564	37.09	37.70	64.34
disord. dolomite	EQ3/6 data0.com.R2 (1995)	-515.653	-553.704	39.84	37.70	64.39

Table 2 - Values commonly used for ionic equilibrium constants in the Na, K, Ca, Mg, H, Cl, OH, CO<sub>2</sub>, HCO<sub>3</sub><sup>-</sup>, CO<sub>3</sub><sup>2-</sup>, H<sub>2</sub>O system.

Reaction	Source	Log K (25°C)	50°C	60°C	100°C	150°C	200°C
H <sub>2</sub> O = OH <sup>-</sup> + H <sup>+</sup>	(1)	-13.992	-	-	-	-	-
H <sub>2</sub> O = OH <sup>-</sup> + H <sup>+</sup>	(2)	-13.99	-13.27	-	-12.26	-11.65	-11.30
at P = 500 bar	(2)	-13.81	-13.11	-	-12.10	-11.46	-11.05
H <sub>2</sub> O = OH <sup>-</sup> + H <sup>+</sup>	(3)	-13.9967	-	-	-	-	-
H <sub>2</sub> O = OH <sup>-</sup> + H <sup>+</sup>	(5)	-13.9951	-	-13.0272	-12.2551	-11.6308	-11.2836
CO <sub>2</sub> (g) = CO <sub>2</sub> (aq)	(1)	-1.468	-1.711	-1.784	-1.979	-2.074	-2.063
CO <sub>2</sub> (g) = CO <sub>2</sub> (aq)	(3)	-1.4818	-	-	-	-	-
CO <sub>2</sub> (g) = CO <sub>2</sub> (aq)	(5)	-1.4689	-	-1.7843	-1.9692	-2.0457	-2.0196
CO <sub>2</sub> (g) = CO <sub>2</sub> (aq)	(6)	-1.47	-	-	-1.91 (100 bar)	-	-
CO <sub>2</sub> (aq) = HCO <sub>3</sub> <sup>-</sup> + H <sup>+</sup>	(1)	-6.352	-6.286	-6.290	-6.427	-6.769	-7.232
CO <sub>2</sub> (aq) = HCO <sub>3</sub> <sup>-</sup> + H <sup>+</sup>	(2)	-6.35	-6.28	-	-6.41	-6.76	-7.24
at P = 500 bar	(2)	-6.14	-6.06	-	-6.18	-6.50	-6.92
CO <sub>2</sub> (aq) = HCO <sub>3</sub> <sup>-</sup> + H <sup>+</sup>	(3)	-6.3374	-	-	-	-	-
CO <sub>2</sub> (aq) = HCO <sub>3</sub> <sup>-</sup> + H <sup>+</sup>	(5)	-6.3447	-	-6.2684	-6.3882	-6.7235	-7.1969
CO <sub>2</sub> (aq) = HCO <sub>3</sub> <sup>-</sup> + H <sup>+</sup>	(6)	-6.35	-	-	-6.38 (100 bar)	-	-
HCO <sub>3</sub> <sup>-</sup> = CO <sub>3</sub> <sup>2-</sup> + H <sup>+</sup>	(1)	-10.329	-10.174	-10.144	-10.155	-10.387	-10.782
HCO <sub>3</sub> <sup>-</sup> = CO <sub>3</sub> <sup>2-</sup> + H <sup>+</sup>	(2)	-10.33	-10.18	-	-10.17	-10.35	-10.68
at P = 500 bar	(2)	-10.09	-9.95	-	-9.93	-10.12	-10.41
CO <sub>2</sub> (aq) = HCO <sub>3</sub> <sup>-</sup> + H <sup>+</sup>	(3)	-10.3393	-	-	-	-	-
CO <sub>2</sub> (aq) = HCO <sub>3</sub> <sup>-</sup> + H <sup>+</sup>	(5)	-10.3288	-	-10.1304	-10.0836	-10.2003	-10.4648
CO <sub>2</sub> (aq) = HCO <sub>3</sub> <sup>-</sup> + H <sup>+</sup>	(6)	-10.33	-	-	-10.11 (100 bar)	-	-
NaCO <sub>3</sub> <sup>-</sup> + H <sup>+</sup> = Na <sup>+</sup> + HCO <sub>3</sub> <sup>-</sup>	(5)	-9.8144	-	9.7833	9.6347	9.4995	9.3762
Ca <sup>++</sup> + HCO <sub>3</sub> <sup>-</sup> = CaHCO <sub>3</sub> <sup>+</sup>	(1)	-1.11	1.21	1.23	-1.36	-	-
Ca <sup>++</sup> + HCO <sub>3</sub> <sup>-</sup> = CaHCO <sub>3</sub> <sup>+</sup>	(2)	1.22	1.33	-	-1.65	2.02	2.43
at P = 500 bar	(2)	1.20	1.30	-	1.57	1.89	2.23
Ca <sup>++</sup> + HCO <sub>3</sub> <sup>-</sup> = CaHCO <sub>3</sub> <sup>+</sup>	(5)	1.0467	-	1.1592	1.4181	1.8587	2.4000
Ca <sup>++</sup> + HCO <sub>3</sub> <sup>-</sup> = CaHCO <sub>3</sub> <sup>+</sup>	(6)	1.11	-	-	1.00*	1.00*	-

(1) Plummer and Busenberg (1982)

(2) Michard (1983)

(3) Harvie *et al.* (1984)(4) Nordstrom *et al.* (1990)

(5) EQ3/6 data0.com.R2 (1995)

(6) Shiraki and Brantley (1995)

Table 2 - continuation

Reaction	Source	Log K (25°C)	50°C	60°C	100°C	150°C	200°C
$\text{Ca}^{++} + \text{CO}_3^{--} = \text{CaCO}_3^{\circ}$	(1)	3.22	3.51	3.65	4.17	-	-
$\text{Ca}^{++} + \text{CO}_3^{--} = \text{CaCO}_3^{\circ}$	(2)	3.16	3.39	-	3.75	4.03	4.25
at P = 500 bar	(2)	3.07	3.29	-	3.60	3.79	3.82
$\text{Ca}^{++} + \text{CO}_3^{--} = \text{CaCO}_3^{\circ}$	(3)	3.1513	-	-	-	-	-
$\text{Ca}^{++} + \text{CO}_3^{--} = \text{CaCO}_3^{\circ}$	(5)	3.3271	-	3.6788	4.120	4.7320	5.4463
$\text{Ca}^{++} + \text{CO}_3^{--} = \text{CaCO}_3^{\circ}$	(6)	3.22	-	-	4.17*	4.67*	-
$\text{Mg}^{++} + \text{HCO}_3^{-} = \text{MgHCO}_3^{+}$	(2)	1.07	1.15	-	1.39	1.66	1.95
at P = 500 bar	(2)	1.02	1.10	-	1.31	1.53	1.72
$\text{Mg}^{++} + \text{HCO}_3^{-} = \text{MgHCO}_3^{+}$	(4)	1.068	0.856	0.764	0.089	-	-
$\text{Mg}^{++} + \text{HCO}_3^{-} = \text{MgHCO}_3^{+}$	(5)	1.0357	-	1.1638	1.4355	1.8804	2.4146
$\text{Mg}^{++} + \text{CO}_3^{--} = \text{MgCO}_3^{\circ}$	(2)	2.99	3.13	-	3.46	3.82	4.20
at P = 500 bar	(2)	2.90	3.03	-	3.32	3.60	3.80
$\text{Mg}^{++} + \text{CO}_3^{--} = \text{MgCO}_3^{\circ}$	(3)	2.9285	-	-	-	-	-
$\text{Mg}^{++} + \text{CO}_3^{--} = \text{MgCO}_3^{\circ}$	(4)	2.980	3.080	3.113	3.146	-	-
$\text{Mg}^{++} + \text{CO}_3^{--} = \text{MgCO}_3^{\circ}$	(5)	2.9789	-	3.2042	3.5204	3.9958	4.5923
$\text{NaOH}^{\circ} + \text{H}^{+} = \text{Na}^{+} + \text{H}_2\text{O}$	(4)	14.18	-	-	-	-	-
$\text{NaOH}^{\circ} + \text{H}^{+} = \text{Na}^{+} + \text{H}_2\text{O}$	(5)	14.7948	-	13.8004	12.8848	11.9708	11.2215
$\text{KOH}^{\circ} + \text{H}^{+} = \text{K}^{+} + \text{H}_2\text{O}$	(4)	14.46	-	-	-	-	-
$\text{KOH}^{\circ} + \text{H}^{+} = \text{K}^{+} + \text{H}_2\text{O}$	(5)	14.4600	-	-	-	-	-
$\text{CaOH}^{+} + \text{H}^{+} = \text{Ca}^{++} + \text{H}_2\text{O}$	(1)	12.692	-	-	-	-	-
$\text{CaOH}^{+} + \text{H}^{+} = \text{Ca}^{++} + \text{H}_2\text{O}$	(4)	12.78	-	-	-	-	-
$\text{CaOH}^{+} + \text{H}^{+} = \text{Ca}^{++} + \text{H}_2\text{O}$	(5)	12.8500	-	-	-	-	-
$\text{MgOH}^{+} + \text{H}^{+} = \text{Mg}^{++} + \text{H}_2\text{O}$	(2)	11.78	10.95	-	9.66	8.69	7.96
$\text{MgOH}^{+} + \text{H}^{+} = \text{Mg}^{++} + \text{H}_2\text{O}$	(3)	11.8091	-	-	-	-	-
$\text{MgOH}^{+} + \text{H}^{+} = \text{Mg}^{++} + \text{H}_2\text{O}$	(4)	11.44	-	-	-	-	-
$\text{Mg}_4(\text{OH})_4^{4+} + 4\text{H}^{+} = 4\text{Mg}^{++} + 4\text{H}_2\text{O}$	(5)	39.7500	-	-	-	-	-
$\text{NaCl}^{\circ} = \text{H}^{+} + \text{Cl}^{-}$	(5)	0.7770	-	0.6509	0.4730	0.2140	-0.0933
$\text{KCl}^{\circ} = \text{H}^{+} + \text{Cl}^{-}$	(5)	1.4946	-	1.2163	0.9240	0.5747	0.2148
$\text{CaCl}^{+} = \text{Ca}^{++} + \text{Cl}^{-}$	(5)	0.6956	-	0.5886	0.3566	-0.0399	-0.5332
$\text{CaCl}_2^{\circ} = \text{Ca}^{++} + 2\text{Cl}^{-}$	(5)	0.6436	-	0.6288	0.3811	-0.1593	-0.9109
$\text{MgCl}^{+} = \text{Mg}^{++} + \text{Cl}^{-}$	(5)	0.1349	-	0.0548	-0.1820	-0.6068	-1.1389

(1) Plummer and Busenberg (1982)

(2) Michard (1983)

(3) Harvie *et al.* (1984)(4) Nordstrom *et al.* (1990)

(5) EQ3/6 data0.com.R2 (1995)

(6) Shiraki and Brantley (1995)

**Table 3 - Values commonly used for the equilibrium constants of mineral dissolution-precipitation reaction in the Na, K, Ca, Mg, H, Cl, OH, CO<sub>2</sub>, HCO<sub>3</sub>, CO<sub>3</sub>, H<sub>2</sub>O system.**

Reaction	Source	Log K (25°C)	50°C	60°C	100°C	150°C	200°C
$\text{CaCO}_3 (\text{a}) + \text{H}^+ = \text{Ca}^{++} + \text{HCO}_3^-$	(1)	1.9928	1.6388	1.5062	0.9893	-	-
$\text{CaCO}_3 (\text{a}) + \text{H}^+ = \text{Ca}^{++} + \text{HCO}_3^-$	(2)	1.98	1.61	-	0.89	0.21	-0.44
at P = 500 bar	(2)	2.25	1.86	-	1.12	0.49	-0.07
$\text{CaCO}_3 (\text{a}) + \text{H}^+ = \text{Ca}^{++} + \text{HCO}_3^-$	(3)	2.1198	-	-	-	-	-
$\text{CaCO}_3 (\text{a}) + \text{H}^+ = \text{Ca}^{++} + \text{HCO}_3^-$	(5)	1.9931	-	1.4762	0.9179	0.2467	-0.4315
$\text{CaCO}_3 (\text{c}) + \text{H}^+ = \text{Ca}^{++} + \text{HCO}_3^-$	(1)	1.8491	1.5116	1.3850	0.8887	-	-
$\text{CaCO}_3 (\text{c}) + \text{H}^+ = \text{Ca}^{++} + \text{HCO}_3^-$	(2)	1.81	1.45	-	0.73	0.05	-0.60
at P = 500 bar	(2)	2.12	1.70	-	0.99	0.36	-0.21
$\text{CaCO}_3 (\text{c}) + \text{H}^+ = \text{Ca}^{++} + \text{HCO}_3^-$	(3)	1.9330	-	-	-	-	-
$\text{CaCO}_3 (\text{c}) + \text{H}^+ = \text{Ca}^{++} + \text{HCO}_3^-$	(5)	1.8487	-	1.3330	0.7743	0.0999	-0.5838
$\text{CaCO}_3 (\text{c}) + \text{H}^+ = \text{Ca}^{++} + \text{HCO}_3^-$	(6)	1.85	-	-	0.94*	-	-
$\text{MgCO}_3 (\text{m}) + \text{H}^+ = \text{Mg}^{++} + \text{HCO}_3^-$	(3)	2.5054	-	-	-	-	-
$\text{MgCO}_3 (\text{m}) + \text{H}^+ = \text{Mg}^{++} + \text{HCO}_3^-$	(5)	2.2936	-	1.4383	0.5875	-0.3520	-1.2275
$\text{dol.} + 2\text{H}^+ = \text{Ca}^{++} + \text{Mg}^{++} + 2\text{HCO}_3^-$	(2)	2.49	1.63	-	0.02	-1.48	-2.87
at P = 500 bar	(2)	3.02	2.09	-	0.46	-0.93	-2.14
$\text{dol.} + 2\text{H}^+ = \text{Ca}^{++} + \text{Mg}^{++} + 2\text{HCO}_3^-$	(2)	3.47	2.54	-	0.80	-0.78	-2.25
$\text{dol.} + 2\text{H}^+ = \text{Ca}^{++} + \text{Mg}^{++} + 2\text{HCO}_3^-$	(3)	3.5960	-	-	-	-	-
$\text{dol.} + 2\text{H}^+ = \text{Ca}^{++} + \text{Mg}^{++} + 2\text{HCO}_3^-$	(4)	3.57	-	-	-	-	-
$\text{dol.} + 2\text{H}^+ = \text{Ca}^{++} + \text{Mg}^{++} + 2\text{HCO}_3^-$	(5)	2.5135	-	1.3314	0.0944	-1.3493	-2.7744
$\text{d.dol.} + 2\text{H}^+ = \text{Ca}^{++} + \text{Mg}^{++} + 2\text{HCO}_3^-$	(4)	4.12	-	-	-	-	-
$\text{d.dol.} + 2\text{H}^+ = \text{Ca}^{++} + \text{Mg}^{++} + 2\text{HCO}_3^-$	(5)	4.0579	-	2.6502	1.2070	-0.4400	-2.0253

(1) Plummer and Busenberg (1982)

(2) Michard (1983)

(3) Harvie *et al.* (1984)

(4) Nordstrom *et al.* (1990)

(5) EQ3/6 data0.com.R2 (1995)

(6) Shiraki and Brantley (1995)

(\*) at 100 bar

**Table 4 - Chemical composition of oil field brines from the North Sea (Warren and Smalley, 1994; Ziegler and Coleman, 1995; Sanjuan et al., 1995).**

Name	B40	M142	M146	FO81	BU42	GY99
field	Oseberg	Miller	Miller	Forties	Buchan	Gyda
depth (m)	2700	4159	3980	2180	2926	4225
lithology	sandstone	sandstone	sandstone	sandstone	sandstone	sandstone
temperature (T°C)	108	120	120	96	105	154
pressure (bar)	300	504	500	172	400	-
density (g/cm <sup>3</sup> )	1.027	1.058	1.052	1.074	1.148	1.205
pH	6.95	6.70	7.66	7.00	5.80	5.40
Na (mg/l)	13656	28800	26740	29364	56700	68724
K (mg/l)	259	1820	865	372	1525	6248
Ca (mg/l)	766	1060	505	2809	16075	33200
Mg (mg/l)	123	115	115	504	1250	2550
Cl (mg/l)	22311	47680	43140	52361	121600	178420
HCO <sub>3</sub> (mg/l)	842	2070	1040	496	200	130
SO <sub>4</sub> (mg/l)	9	7	3	11	220	0.1
Total dissolved salts (TDS in mg/l)	38000	82690	73100	86758	198631	291885



## References

- Barth, T., 1991. Organic acids and inorganic ions in waters from petroleum reservoirs, norwegian continental shelf: A multivariate statistical analysis and comparison with American reservoir formation waters. *Appl. Geochem.*, 6, 1-15.
- Berner, R.A., 1975. The role of magnesium in the crystal growth of calcite and aragonite from seawater. *Geochim. Cosmochim. Acta*, 39, 489-504.
- Burton, E.A., and Walter, L.M., 1985. Relative growth rates and compositions of aragonite and Mg-calcite cements in seawater: effects of temperature and sulfate. *Geol. Soc. Amer. Abstr. Prog.*, 17, 536.
- Burton, E.A., and Walter, L.M., 1987a. Relative precipitation rates of aragonite and Mg calcite from seawater: temperature or carbonate ion control? *Geology*, 15, 111-114.
- Burton, E.A., and Walter, L.M., 1987b. Influence of seawater chemistry on calcite cement mineralogy: effects of pCO<sub>2</sub> and sulfate. *Geol. Soc. Amer. Abstr. Prog.*, 607.
- Burton, E.A., and Walter, L.M., 1991. The effects of pCO<sub>2</sub> and temperature on magnesium incorporation in calcite in seawater and MgCl<sub>2</sub>-CaCl<sub>2</sub> solutions. *Geochim. Cosmochim. Acta*, 55, 777-785.
- Clegg, S.L., and Whitfield, M., 1991. Activity coefficients in natural waters. In "Activity Coefficients in Electrolyte Solutions", 2nd Edn. (Ed. K.S. Pitzer), CRC Press, 279-434.
- Dromgoole, E.L., and Walter, L.M., 1990a. Iron and manganese incorporation into calcite: Effects of precipitation rate, temperature, and solution composition. *Chem. Geol.*, 81, 311-336.
- Dromgoole, E.L., and Walter, L.M., 1990b. Inhibition of calcite growth rates by Mn<sup>2+</sup> in CaCl<sub>2</sub> solutions at 10, 25, and 50°C. *Geochim. Cosmochim. Acta*, 54, 2991-3000.
- Drummond, S.E., 1981. Boiling and mixing of hydrothermal fluids: chemical effects on mineral precipitation. Ph.D Thesis, Pennsylvania State University, 380 p.
- Edmond, J.M., and Gieskes, J.M.T.M., 1970. On the calculation of the degree of saturation of seawater with respect to calcium carbonate under in situ conditions. *Geochim. Cosmochim. Acta*, 34, 1261-1291.
- Ellis, A.J., 1963. The solubility of calcite in sodium chloride solutions at high temperatures. *Amer. J. Sci.*, 261, 259-267.
- Ellis, A.J., and Golding, R.M., 1963. The solubility of carbon dioxide above 100°C in water and in sodium chloride solutions. *Amer. J. Sci.*, 261, 47-60.
- Enick, R.M., and Klara, S.M., 1990. CO<sub>2</sub> solubility in water and brine under reservoir conditions. *Chem. Eng. Comm.*, 90, 23-33.
- Estrada Maldonado, C.F., 1991. Contribution à l'étude du système Ca-Mg-CO<sub>2</sub>-H<sub>2</sub>O: Dissolution de la calcite et de la dolomite dans l'eau de mer et dans des solutions de NaCl de 0 à 300°C. Thèse de doctorat, Université de Toulouse, 196 p.
- Estrada Maldonado, C.F., Giroir, G., Dandurand, J.L., and Schott, J., 1992. The dissolution of calcite in seawater from 40° to 90°C at atmospheric pressure and 35‰ salinity. *Chem. Geol.*, 97, 113-123.

- Given, R.K., and Wilkinson, B.H., 1985. Kinetic control of morphology, composition, and mineralogy of abiotic sedimentary carbonates. *J. Sediment. Petrol.*, 55, 109-119.
- Greenberg, J.P., and Moller, N., 1989. The prediction of minerals solubilities in natural waters: A chemical equilibrium model for the Na-K-Ca-Cl-SO<sub>4</sub>-H<sub>2</sub>O system to high concentration from 0 to 250°C. *Geochim. Cosmochim. Acta*, 53, 2503-2518.
- Grenthe, I., and Wanner, H., 1989. Guidelines for the extrapolation to zero ionic strength. NEA-TDB, TDB-2.1.
- Haarberg, T., 1989. Mineral deposition during oil recovery. An equilibrium model. Ph.D. dissertation, Trondheim University, Trondheim, Norway, 150 p.
- Harned, H.S., and Bonner, F.T., 1945. The first ionization of carbonic acid in aqueous solutions of NaCl. *J. Amer. Chem. Soc.*, 67, 1026-1031.
- Harrison, W.J., and Thyne, G.D., 1991. Predictions of diagenetic reactions in the presence of organic acids. *Geochim. Cosmochim. Acta*, 56, 565-586.
- Hartley, G., and Mucci, A., 1996. The influence of pCO<sub>2</sub> on the partitioning of magnesium in calcite overgrowths precipitated from artificial seawater at 25°C and 1 atm total pressure. *Geochim. Cosmochim. Acta*, 60, 315-324.
- Harvie, C.E., Moller, N., and Weare, J.H., 1984. The prediction of minerals solubilities in natural waters: The Na-K-Mg-Ca-H-Cl-SO<sub>4</sub>-OH-HCO<sub>3</sub>-CO<sub>3</sub>-CO<sub>2</sub>-H<sub>2</sub>O system to high ionic strengths at 25°C. *Geochim. Cosmochim. Acta*, 48, 723-751.
- Hawley, J., and Pytkowicz, R.M., 1969. Solubility of calcium carbonate in seawater at high pressures and 2°C. *Geochim. Cosmochim. Acta*, 33, 1557-1561.
- He, S., 1992. Effects of solution composition, temperature, and pressure on the carbonic acid system and calcite solubility in the system Na-K-Mg-Ca-H-Cl-SO<sub>4</sub>-OH-HCO<sub>3</sub>-CO<sub>3</sub>-CO<sub>2</sub>-H<sub>2</sub>O. Ph.D. Dissertation, Texas A&M University, College Station, Texas, USA.
- He, S., and Morse, W., 1993. The carbonic acid system and calcite solubility in aqueous Na-K-Ca-Mg-Cl-SO<sub>4</sub> solutions from 0 to 90°C. *Geochim. Cosmochim. Acta*, 57, 3533-3554.
- Helgeson, H.C., Delany, J., Nesbitt, H.W., and Bird, D.K., 1978. Summary and critique of the thermodynamic properties of rock forming minerals. *Amer. J. Sci.*, 278A, 1-229.
- Holmes, H.F., Baes, C.F., Jr, and Mesmer, R.E., 1987. The enthalpy of dilution of HCl(aq) to 648 K and 40 MPa: Thermodynamic properties. *J. Chem. Thermodyn.*, 19, 863-890.
- Ingle, S.E., 1975. Solubility of calcite in the ocean. *Mar. Chem.*, 3, 301-319.
- Ingle, S.E., Culberson, C.H., Hawley, J.E., and Pytkowicz, R.M., 1973. The solubility of calcite in seawater at atmospheric pressure and 35 ‰ salinity. *Mar. Chem.*, 1, 295-307.
- Johnson, J.W., Oelkers, E.H., and Helgeson, H.C., 1992. SUPCRT92: A software package for calculating the standard molal thermodynamic properties of minerals, gases, aqueous species, and reactions from 1 to 5000 bar and 0° to 1000°C, *Computers and Geosciences*, 18, 899-947.
- Katz, A., 1973. The interaction of magnesium with calcite during crystal growth at 25°-90°C and one atmosphere. *Geochim. Cosmochim. Acta*, 37, 1563-1586.
- Kharaka, Y.K., Gunter, W.D., Aggarwal, P.K., Perkins, E.H., and DeBraal, J.D., 1989. SOLMINEQ.88: A computer program for geochemical modeling of water-rock interactions, U.S. Geol. Survey, 420 p.

- MacIntyre, W.G., 1965. The temperature variation in the solubility product of calcium carbonate in seawater. Manuscript Report Series of The Fisheries Research Board of Canada, 200, 153 p.
- MacKenzie, F.T., Bischoff, W.D., Bishop, F.C., Lojens, M., Schoonmaker, J., and Wollast, R., 1983. Magnesian calcites: Low-temperature occurrence, solubility and solid-solution behavior. In "Carbonates: Mineralogy and Chemistry" (Ed. R.J. Reeder), Reviews in Mineralogy 11, 97-144.
- Malinin, S.D., and Kurovskaya, N.A., 1975. Solubility of CO<sub>2</sub> in chloride solutions at elevated temperatures and CO<sub>2</sub> pressures. *Geochem. Int.*, 12, 199-201.
- Malinin, S.D., and Savelyeva, N.I., 1972. Solubility of CO<sub>2</sub> in NaCl and CaCl<sub>2</sub> solutions at 25, 50 and 75°C and elevated CO<sub>2</sub> pressure. *Geochem. Int.*, 9, 410-418.
- Michard, G., 1983. Recueil des données thermodynamiques concernant les équilibres eaux-minéraux dans les réservoirs hydrothermaux. CCE, report EUR 8590FR, 155 p.
- Miller, J.P., 1952. A portion of the system calcium carbonate-carbon dioxide-water, with geological implications. *Amer. J. Sci.*, 250, 161-203.
- Millero, F.J., 1976. The effect of pressure on the solubility of calcite in seawater at 25°C. *Geochim. Cosmochim. Acta*, 40, 983-985.
- Millero, F.J., 1979. The thermodynamics of the carbonate system in seawater. *Geochim. Cosmochim. Acta*, 43, 1651-1661.
- Millero, F.J., 1982. The effect of pressure on the solubility of minerals in water and seawater. *Geochim. Cosmochim. Acta*, 46, 11-22.
- Millero, F.J., and Schreiber, D.R., 1982. Use of the ion pairing model to estimate activity coefficients of the ionic components of natural waters. *Amer. J. Sci.*, 282, 1508-1540.
- Millero, F.J., and Thurmond, V.L., 1983. The ionization of carbonic acid in Na-Mg-Cl solutions at 25°C. *J. Soln. Chem.*, 10, 401-412.
- Millero, F.J., Milne, P.J., and Thurmond, V.L., 1984. The solubility of calcite, strontianite and witherite in NaCl solutions at 25°C. *Geochim. Cosmochim. Acta*, 48, 1141-1143.
- Moller, N., 1988. The prediction of mineral solubilities in natural waters: A chemical model for the Na-Ca-Cl-SO<sub>4</sub>-H<sub>2</sub>O system to high temperatures and concentrations. *Geochim. Cosmochim. Acta*, 52, 821-837.
- Monnin, C., 1989. An ion interaction model for the volumetric properties of natural waters: density of the solution and partial molal volumes of electrolytes to high concentration at 25°C. *Geochim. Cosmochim. Acta*, 54, 3265-3282.
- Monnin, C., 1990. The influence of pressure on the activity coefficients of the solutes and on the solubility of minerals in the system Na-Ca-Cl-SO<sub>4</sub>-H<sub>2</sub>O to 200°C and 1 kbar, and to high NaCl concentration. *Geochim. Cosmochim. Acta*, 54, 3265-3282.
- Monnin, C., and Raimboz, C., 1996. The anhydrite saturation index of the ponded brines and sediment pore waters of the Red Sea deeps. *Chem. Geol.*, 127, 141-159.
- Morse, J.W., 1983. The kinetics of calcium carbonate dissolution and precipitation. In "Carbonates: Mineralogy and Chemistry" (ed. R.J. Reeder); *Rev. Mineral.*, 11, 227-264.

- Morse, J.W., and Bender, M.L., 1990. Partition coefficients in calcite: Examination of factors influencing the validity of experimental results and their application to natural systems. *Chem. Geol.*, 82, 265-277.
- Morse, J.W., Mucci, A., and Millero, F.J., 1980. The solubility of calcite and aragonite in seawater of 35 ‰ salinity at 25°C and atmospheric pressure. *Geochim. Cosmochim. Acta*, 44, 85-94.
- Mucci, A., 1983. The solubility of calcite and aragonite in seawater at various salinities, temperatures, and one atmosphere total pressure. *Amer. J. Sci.*, 283, 780-799.
- Mucci, A., 1986. Growth kinetics and composition of magnesian calcite overgrowths precipitated from seawater: Quantitative influence of orthophosphate ions. *Geochim. Cosmochim. Acta*, 50, 2255-2265.
- Mucci, A., 1987. Influence of temperature on the composition of magnesian calcite overgrowths precipitated from seawater. *Geochim. Cosmochim. Acta*, 51, 1977-1984.
- Mucci, A., and Morse, J.W., 1983. The incorporation of  $Mg^{2+}$  and  $Sr^{2+}$  into calcite overgrowths: Influences of growth rate and solution composition. *Geochim. Cosmochim. Acta*, 47, 217-233.
- Mucci, A., and Morse, J.W., 1984. The solubility of calcite in seawater solutions of various magnesium concentrations,  $I_t = 0.697$  m at 25°C and one atmosphere total pressure. *Geochim. Cosmochim. Acta*, 48, 815-823.
- Mucci, A., Canuel, R., and Zhong, S., 1989. The solubility of calcite and aragonite in sulfate-free seawater and seeded growth kinetics and composition of precipitates at 25°C. *Chem. Geol.*, 74, 309-329.
- Nagy, K.L., 1988. The solubility of calcite in sodium-chloride and sodium-calcium-chloride brines. Ph.D Thesis, Graduate College of Texas A&M University, College Station, Texas, 246 p.
- Naumov, G.B., Ryzhenko, B.N., and Khodakhovsky, I.L., 1971. Handbook of thermodynamic quantities for geology. Moscow, Atomizdat. Trad.
- Nordstrom, D.K., Plummer, L.N., Langmuir, D., Busenberg, E., May, H.M., Jones, B.F., and Parkhurst, D.L., 1990. Revised chemical equilibrium data for major water-mineral reactions and their limitations. In "Chemical Modeling of aqueous systems II" (eds D.C. Melchor and R.L. Bassett), American Chemical Society, chapter 31, 399-413.
- Oomori, T., Kaneshima, H., Maezato, Y., and Kitano, Y., 1987. Distribution coefficient of  $Mg^{2+}$  ions between calcite and solution at 10-50°C. *Mar. Chem.*, 20, 327-336.
- Pabalan, R.T., and Pitzer, K.S., 1987a. Thermodynamics of NaOH(aq) in hydrothermal solutions. *Geochim. Cosmochim. Acta*, 51, 829-837.
- Pabalan, R.T., and Pitzer, K.S., 1987b. Thermodynamics of concentrated electrolyte mixtures and the prediction of mineral solubilities to high temperatures for mixtures in the system Na-K-Mg-Cl-SO<sub>4</sub>-OH-H<sub>2</sub>O. *Geochim. Cosmochim. Acta*, 51, 2429-2443.
- Patterson, C.S., Slocum, G.H., Busey, R.H., and Mesmer, R.E., 1982. Carbonate equilibria in hydrothermal systems: first ionization of carbonic acid in NaCl media to 300°C. *Geochim. Cosmochim. Acta*, 46, 1653-1663.
- Patterson, C.S., Busey, R.H., and Mesmer, R.E., 1984. Second ionization of carbonic acid in NaCl media to 250°C. *J. Solution Chem.*, 13, n° 9, 647-660.

- Peiper, J.C., and Pitzer, K.S., 1982. Thermodynamics of aqueous carbonate solutions including mixtures of sodium carbonate, bicarbonate, and chloride electrolytes. *J. Chem. Thermodyn.*, 14, 613-638.
- Pitzer, K.S., Olsen, J., Simonson, J.M., Roy, R.N., Gibbons, J., and Rowe, L., 1985. Thermodynamics of aqueous magnesium and calcium bicarbonates and mixtures with chloride. *J. Chem. Eng. Data*, 13, 1-102.
- Plath, D.C., Johnson, K.S., and Pytkowicz, R.M., 1980. The solubility of calcite - probably containing magnesium - in seawater. *Mar. Chem.*, 10, 9-29.
- Plummer, L.N., and Busenberg, E., 1982. The solubility of calcite, aragonite and vaterite in  $\text{CO}_2$ - $\text{H}_2\text{O}$  solutions between 0 and 90°C, and an evaluation of the aqueous model for the system  $\text{CaCO}_3$ - $\text{CO}_2$ - $\text{H}_2\text{O}$ . *Geochim. Cosmochim. Acta*, 46, 1011-1040.
- Plummer, L.N., and Parkhurst, D.L., 1990. Application of the Pitzer Equations to the PHREEQUE geochemical model. In "Chemical Modeling of Aqueous Systems II" (Eds D.C. Melchior and R.L. Bassett), Amer. Chem. Soc. Symposium Ser., Washington D.C., 416, 128-137.
- Plummer, L.N., Parkhurst, D.L., Fleming, G.W., and Dunkle, S.A., 1988. A computer Program Incorporating Pitzer's Equations for Calculation of Geochemical Reactions in Brines. U.S. Geol. Survey, Water-Resources Investigations Report, 88-4153.
- Robie, R.A., Hemingway, B.S., and Fisher, J.R., 1978. Thermodynamic properties of minerals and related substances at 298.15°K and 1 bar pressure and at higher temperatures. U.S. Geol. Survey Bull., 1452.
- Roy, R.N., Gibbons, J.J., Williams, R., Godwin, L., Baker, G., Simonson, J.M., and Pitzer, K.S., 1984. The Thermodynamics of aqueous carbonate solutions. II. Mixtures of potassium carbonate, bicarbonate, and chloride. *J. Chem. Thermodyn.*, 16, 303-315.
- Rumpf, B., Nicolaisen, H., Ocal, C., and Maurer, G., 1993. Solubility of carbon dioxide in aqueous solutions of sodium chloride: Experimental results and correlation. *J. Solution Chem.*, 23, n° 3, 431-448.
- Sander, B., 1984. Extended UNIFAC/UNIQUAC models for gas solubility calculations and electrolyte solutions. Ph.D. Thesis, Inst. for kemiteknik, DTH, Lyngby, Denmark.
- Sanjuan, B., Girard, J.P., and Czernichowski, I., 1995. Geochemical modelling of the main diagenetic processes in the Oseberg sandstone reservoir, Oseberg Field, northern North Sea. BRGM report R38599, CEC Joule II - Reservoir Engineering Project, 165 p.
- Sass, E., Morse, J.W., and Millero, F.J., 1983. Dependence of the calcite and aragonite thermodynamic solubility products on ionic models. *Amer. J. Sci.*, 283, 218-229.
- Segnit, E., Holland, H.D., and Biscardi, C.J., 1962. The solubility of calcite in aqueous solutions: I. The solubility of calcite in water between 75 and 200°C at  $\text{CO}_2$  pressures up to 60 atm. *Geochim. Cosmochim. Acta*, 26, 1301-1331.
- Shock, E.L., and Helgeson, H.C., 1988. Calculation of the thermodynamic and transport properties of aqueous species at high pressures and temperatures: Correlation algorithms for ionic species and equation of state predictions to 5 kb and 1000°C. *Geochim. Cosmochim. Acta*, 52, 2009-2036.

- Shock, E.L., and Helgeson, H.C., 1989. Calculation of the thermodynamic and transport properties of aqueous species at high pressures and temperatures: Standard partial molal properties of organic species. *Geochim. Cosmochim. Acta*, 54, 915-945.
- Shock, E.L., and Koretsky, C.M., 1993. Metal organic complexes in geochemical processes: Calculation of standard partial molal thermodynamic properties of aqueous acetate complexes at high pressures and temperatures. *Geochim. Cosmochim. Acta*, 57, 4899-4922.
- Shock, E.L., and Koretsky, C.M., 1995. Metal organic complexes in geochemical processes: Estimation of standard partial molal thermodynamic properties of aqueous complexes between metal cations and monovalent organic acid ligands at high pressures and temperatures. *Geochim. Cosmochim. Acta*, 59, 1497-1532.
- Shock, E.L., Helgeson, H.C., and Sverjensky, D.A., 1989. Calculation of the thermodynamic and transport properties of aqueous species at high pressures and temperatures: Standard partial molal properties of inorganic neutral species. *Geochim. Cosmochim. Acta*, 53, 2157-2183.
- Shternina, E.B., and Frolova, E.V., 1957. Solubility in the system  $\text{CaCO}_3\text{-CaSO}_4\text{-NaCl-CO}_2\text{-H}_2\text{O}$ . *Zh. Neorg. Khim.*, 2, 1649-1654.
- Stokes, R.H., and Robinson, R.A., 1948. Ionic hydration and activity in electrolyte solutions. *J. Amer. Chem. Soc.*, 70, 1870-1878.
- Spencer, R.J., Moller, N., and Weare, J.H., 1990. The prediction of mineral solubilities in natural waters: A chemical equilibrium model for the system  $\text{Na-K-Ca-Cl-SO}_4\text{-H}_2\text{O}$  at temperature below 25°C. *Geochim. Cosmochim. Acta*, 54, 575-590.
- Takenouchi, S., and Kennedy, G.C., 1965. The solubility of carbon dioxide in NaCl solutions at high temperatures and pressures. *Amer. J. Sci.*, 263, 445-454.
- Thurmond, V.L., and Millero, J.F., 1982. Ionization of carbonic acid in sodium chloride solutions at 25°C. *J. Soln. Chem.*, 11, 447-456.
- Warren, E.A., and Smalley, P.C. (Eds.), 1994. North Sea Formation Water Atlas. Geological Society Memoir 15, London, 208 p.
- Wolery, T.J., 1995. EQ3NR, A computer program for geochemical aqueous speciation-solubility calculations: theoretical manual, user's guide and related documentation (Version 7.2b) UCRL-MA-110662-PT-I, Lawrence Livermore National Laboratory, Livermore, California.
- Wolery, T.J., and Jackson, K.J., 1990. Activity Coefficients in Aqueous Salt Solutions. Hydration theory equations. In "Chemical Modeling of Aqueous Systems II" (Eds D.C. Melchior and R.L. Bassett), Amer. Chem. Soc. Symposium Ser., Washington D.C., Chapt. 2, 16-29.
- Wolery, T.J., and Jackson, K.J., Bourcier, W.L., Bruton, C.L., Viani, B.E., Knauss, K.G., and Delany, J.M., 1990. Current Status of the EQ3/6 Software Package for Geochemical Modeling. In "Chemical Modeling of Aqueous Systems II" (Eds D.C. Melchior and R.L. Bassett), Amer. Chem. Soc. Symposium Ser., Washington D.C., Chapt. 8, 104-116.
- Wolf, M., Breitkopf, O., and Puk, R., 1989. Solubility of calcite in different electrolytes at temperatures between 10° and 60°C and at  $\text{CO}_2$  partial pressures of about 1 kPa. *Chem. Geol.*, 76, 291-301.

- Wolf, M., and Rohde, H., 1992. Solubility of calcite in mixed aqueous solutions of NaCl and KCl at 25°C and CO<sub>2</sub> partial pressures of about 1kPa. *Water-Rock Interaction*, Kharaka & Maest (eds), Balkema, 195-198.
- Woods, T.L., and Garrels, R.M., 1992. Calculated aqueous-solution-solid-solution relations in the low-temperature system CaO-MgO-FeO-CO<sub>2</sub>-H<sub>2</sub>O. *Geochim. Cosmochim. Acta*, 56, 3031-3043.
- Yanushi, A., and Yoshida, F., 1979. Solubility of CO<sub>2</sub> in aqueous electrolyte solutions. *J. Chem. Eng. Data*, 24, 11-14.
- Zhong, S., and Mucci, A., 1989. Calcite and aragonite precipitation from seawater solutions of various salinities: Precipitation rates and overgrowth compositions. *Chem. Geol.*, 78, 283-299.
- Ziegler, K., and Coleman, M.L., 1995. Geochemistry of formation waters from the Oseberg Field. Final CEC report, Joule II - Reservoir Engineering Project, 84 p.

**BRGM**  
**DIRECTION DE LA RECHERCHE**  
**Département Hydrologie, Géochimie et Transfert**  
BP 6009 - 45060 ORLEANS Cedex 2 - France - Tél. : (33) 38.64.34.34